CHARACTERIZATION OF BLAST FURNACE SLAG

A Thesis Submitted to

National Institute of Technology, Rourkela

For the Degree of Doctor of Philosophy

In the Faculty of Engineering

Jai Narain Tiwari

Roll No. **510MM904**

Metallurgical & Materials Engg. Dept.

National Institute of Technology

Rourkela-769 008, Odisha, India

2014

If I have seen any further…….
It is by standing on the shoulders
Of Giants

……. Sir Isaac Newton

Dedicated to my parents
My mother Mrs Rajkeshwari Devi, 88
My Father Mr Uma Shanker Tiwari, 93

Certificate

This is to certify that the thesis entitled 'Characterization of Blast Furnace Slag' submitted by Sri J.N.Tiwari, Executive Director, OCL India Limited(Refractory Division), Rajagangpur, Odisha, for the Ph.D. degree of NIT Rourkela has been carried out under our supervision & has not been submitted elsewhere for the award of any degree.

Dr S Sarkar:
Associate professor,
Dept. Of Metallurgical &Materials Engg.
National Institute of Technology
Rourkela-769008
Odisha

Dr U K Mohanty
Professor,
Dept. of Metallurgical &Materials Engg
National Institute of Technology
Rourkela- 769008
Odisha

Acknowledgement

The work of this magnitude cannot be done alone. Support from all and devotion to work has to be at its zenith to achieve the goal.

I sincerely thank Dr.U.K.Mohanty for his continuous guidance and hand holding during these tumultuous years. He ensured that I remain a devoted student. Dr. S. Sarkar made many concepts clear, whereas Dr. B. Mishra of DISIR helped analyzing data and fixing test equipment parameters.

I acknowledge with gratitude the knowledge imparted by Dr.S.C.Mishra, Dr.S.K.Karak, Dr.D.Chihara, Dr.S.K.Sahoo, Dr.B.B.Verma, Dr.B.C.Roy of NIT Rourkela from my days of initial study to completion of this thesis.

Special mention is essential for Mr.A.K.Sahu, Mr.U.Sahoo, Mr.S.Dasgupta, Mr.R.Achari, Mr.A.Chakraborty and Ms.Smriti Satpathy who have helped in experimentation and checking, correcting the manuscript many times over critically with extreme patience.

Department of Science and Technology, Govt. Of India sanctioned the purchase of Viscometer. I am thankful to them for this investment.

Mr.R.H.Dalmia, President, OCL India Limited was kind enough to accord permission and have always encouraged me by taking progress reports.

My family has supported me in my endeavor wholeheartedly, especially my wife, Mrs. Kumud Tiwari, who tolerated my avoidance of domestic chores.

J. N. Tiwari

Abbreviations Used

Abbreviations	Meaning
kCal/Mole	Kilo Calories/Moles
PaS	Pascal-Second
K	Kelvin
mm	Millimeter
V	Volt
W	Watt
dPaS	Deci Pascal second
hr	Hour
min	Minute
cm	Centimeters
rpm	Rotations per minute
gm	Gram
kg	Kilogram

*****

------xoxoxoxo----

LIST OF TABLES

LIST OF FIGURES

Abstract

Viscosity & flow characteristics of the Blast Furnace slag constitute two very Important parameters for ensuring the smooth operation of the Blast Furnace producing pig iron.

Ideally, the Blast Furnace slag should neither be very viscous nor very fluid. A Viscous slag interferes with efficient slag- metal separation; while a slag with very low viscosity is more likely to interfere with the thermal balance of the Furnace & affect the retention time of the metal droplets in the slag affecting the slag-metal reactions/ exchanges.

Flow characteristics in the Blast Furnace slag can provide a fair knowledge about the location & extent of the cohesive zone in the Furnace. The cohesive zone in the Furnace acts as a gas distributor & its place lower down the Furnace would create less probability for the softened slag for choking the Furnace. Also a cohesive zone lower down the Furnace would result in less Si pick up in the hot metal.

The present work aims at characterizing the Blast Furnace slag on the basis of its viscosity and flow characteristics. Empirical equations are developed to predict the flow characteristics of Blast Furnace slag and the same was validated through further experimentation. The viscosity of the Blast Furnace slag (synthetic one prepared in laboratory in line with the compositional details as encountered in the industry) is determined for C/S (CaO/SiO_2) variation, MgO content variation and TiO_2 variation and along with that to the simultaneous variation of C/S ratio & MgO content. The compositional dependence of the slag viscosity is discussed at length.

Relevance of the present work

The present work has definite relevance in the process of iron making in the Blast Furnace route. It is based on characterizing high alumina Blast Furnace slag on the basis of its 'flow characteristic' and 'viscosity' in order that a smooth process is ensured. Both the parameters mentioned above must be favorable under the operating conditions of the Blast Furnace.

Selection of slag composition

Viscosity and Flow Characteristics, both are determined as a function of chemical composition of slag. Therefore, for the purpose of characterization, synthetic slag prepared in laboratory in line with the chemical composition in the related industry is considered.

Flow Characteristics of Blast Furnace Slag

The flow characteristics of slag analyzed on the basis of 3 of the 4 characteristics temperature viz. the ST, the HT, & the FT establish dependence of the specific characteristics temperatures on the chemical composition of slag. It is found that a combination of high CaO, & high MgO in the slag results in the formation a 'short –slag' which flows soon after its melting without the requirement of higher extents of additional heat & thus is beneficial for the Blast Furnace process of iron making. Empirical equations are developed using Factorial Design technique to predict these specific temperatures in terms of the chemical composition of the slag. These equations are validated through experiments and can be used fairly accurately to predict the characteristic temperatures of the slag from its chemical composition. It is also established that, CaO, MgO, & TiO_2 collectively influence the characteristic temperature and that any attempt at evaluating the effect of any of these components independent of the other two will be futile. Ideally, the blast furnace slag should neither be very viscous nor very fluid.

Viscosity of Blast Furnace Slag

Viscosity is determined separately for four groups of the slag samples, each group containing 5 numbers of samples. In the first group, CaO/SiO_2 (C/S) ratio, is varied from 0.9 to 1.1 in steps of 0.05; in the Second Group MgO is varied from 4% to 12% in steps of 2%; in the third group TiO_2 is varied from 0.2% to 1% in steps of 0.2% with varied C/S ratio and MgO content, and in the fourth group both C/S ratio & MgO contents simultaneously vary from 0.9 to 1.1 and 4% to 12% respectively. The alumina content in all these slag samples is kept high at 20%. It is established by analyzing the results that viscosity also, is a function of chemical composition of slag & that the chemical composition of the resultant slag emanating from the Blast Furnace can be altered as per requirements to influence the viscosity for a smooth Blast Furnace operation.

Chapter 1

INTRODUCTION AND LITERATURE SURVEY

1.1 INTRODUCTION

The quantity and type of oxides that combine to form the slag in a blast furnace greatly influence the characteristic properties of the slag and hence the smooth operation of the blast furnace. Out of the three major products of the blast furnace viz the BF gas, the BF hot metal and the BF slag, it is the slag which constitutes one of the most important products. The generation of the slag not only affects the productivity of the furnace, it spells out the quality of the metal to be produced by reacting with and retaining the gangue material in the burden. The actual transfer of constituents takes place at the slag metal interface. The extent and nature of the transfer are greatly dependent on the volume and the nature of the slag which in turn depends on the extent and types of oxides which form it. Therefore, it is only pertinent to dig into the details of slag formation with respect to its constituents and its various characteristic properties such as viscosity, activation energy, flow characteristics, chemical affinity, etc. as a function of its chemical composition as derived from the type and composition of the burden material to ensure conditions that would result in the smooth operation of the BF with an enhanced production of the metal of choice.

The iron making blast furnace is a complex, high temperature, counter current reactor in which the softening and melting of the burden greatly affects the permeability of the bed. This softening-melting characteristics of the burden material regulates the gas flow in the furnace playing a significant role in the aerodynamics, the heat and mass transfer in the furnace. The above mentioned phenomena actually regulates the process of iron making. The BF slag should be a short slag, a slag with a small difference between the softening temperature and the flow temperature. Such a slag, soon after its melting, acquires liquid mobility and trickles down the furnace away from the site where it starts distorting plastically, without the necessity of higher additional heat input. This results in the faster creation of fresh reaction sites, enhancing slag-metal reaction rate, influencing blast furnace operation and the quality of hot metal produced. It is, thus, important to estimate the softening-melting characteristics of the BF slag which involves the measurement of characteristic temperatures of the slag defined by the softening-temperature, melting temperature and the flow temperature. The flow

characteristics of the slag depend on the composition and the quantity and quality of the associated gangue.

The C/S [CaO/SiO_2] ratio and MgO content of the slag greatly influence its softening-melting characteristics [1]. Considering the importance of MgO in influencing the flow characteristic of BF slag it is proposed [2] to introduce MgO through the tuyers to make it available later in the process when the burden reaches the tuyer level. It is reported [3] that the flow temperature decreases with the increase in the C/S ratio and that the rate of decrease of flow temperature decreases with an increase in the C/S ratio in the slag [4]. It is also reported that a combination of high C/S ratio and high MgO content result in the formation of a short slag [5, 6].

The viscosity of the slag in the BF has a greater say about the productivity and the quality of hot metal produced. It directly affects mass and heat transfer as well as the chemical reactions between the slag and the metal. The slag must be a free flowing with affinity for the gangue constituents for their separation from the metal and retained in the slag under the operating conditions of the Blast Furnace. The flow Patten of the molten slag significantly influences the gas permeability and the heat transfer in the furnace from the ascending hot-gasses to the descending burden material.

The diffusion of the ions through the liquid slag to and from the slag metal interface governs the slag-metal reaction exchanges in the furnace. It is a direct function of the viscosity of the slag which is structure oriented, strongly depending on its composition under the operating conditions [7]. Three factors, number of non-bridging oxygen per tetragonally bonded oxygen (NBO/T), Optical basicity and a factor 'Q' which is a measure of the polymerization {Q=4-(NBO/T)} of the slag [8] provide a measure of polymerization/de-polymerization of the slag influencing the structure of the slag and hence its viscosity. All of these three factors are direct functions of the composition of the slag establishing compositional dependence of viscosity strongly. Various workers [8, 9] have reported the complicated nature of variation of BF slag viscosity with composition.

It is observed that SiO_2 and Al_2O_3 are highly covalent and increase the viscosity of the BF slag whereas monoxides like CaO and MgO exhibit an ionic behavior, destroy the silicate network and lower the viscosity. However, higher activities of the

monoxides results in the precipitation of the solid phases, increasing the overall viscosity in case their concentration in the melt exceeds some initial value [10, 11]. It is agreed, based on the findings, that higher MgO content needs lower CaO/SiO_2 ratios for an optimum viscosity; combinations of high MgO and high CaO/SiO_2 results in a short slog. High alumina (20-34%) containing BF slag show erratic viscosity variations. Lee et al [12] have shown the combined effect of degree of de-polymerization and liquidus temperature of the slag on the slag viscosity. Conversely, when the prevailing experimental temperature approaches the liquidus temp, it is the liquid temp which affects the viscosity more.

The activation energy of viscous flow is highly temperature dependent [13] as dictated by the structural changes occurring in the system. It is the function of prevailing temp and the composition of the melt. These structural changes may include a process of depolymerization or simply a loosening effect on the bond between the cations and the anions. Activation energy Eμ of viscous flow is related to the energy requirement to move one silicate group with respect to another; higher the energy requirement; more difficult it is to move the silicate group and higher is the viscosity of the melt. The reverse is also true. A reduced viscosity indicates a lowering down of the activation energy of viscous flow. It is proposed [14, 15] that the energy of activation-composition relationship is best explained by a structure that contains discrete silicate ions. An increase in the SiO_2 content results in the formation of discrete silicate chain ions of higher order, increasing the size of the flow unit with a consequent increase in the Eμ value. The structure of the silicate melts is affected by the network breaking cation (e.g. $Ca^{2+,}$ Mg^{2+}), the fitting of certain cation (e.g. Al^{3+}, Ti^{4+}) into the silicate network and the degree of polymerization of the silicate melt [16]. The effect of monovalent metal oxides on Eμ (is more pronounced than divalent ones since at equimolar compositions there are twice as many monovalent cations as divalent one and that the divalent cations maintain the continuous bonding of the lattice by bridging the oxygen atoms. To summarize, it is interesting to note that the activation energy of viscous flow, Eμ (, is an important parameter to judge the viscosity variations of the BF slag with temperature and constituents that finally affect the structure of the slag and

thus it is worthwhile to evaluate Eμ (and to study its variation at varied values of the operating parameters.

Keeping the above in mind the present work attempts to measure the viscosity of BF slag synthetically prepared in the laboratory in total agreement with compositional details of their industrial counterpart and analyses the results on the basis of the prevailing temperature and compositional details. The flow characteristics of the slag are also measured using a hot-stage-microscope and analyzed thoroughly to co-relate the measured values with the composition of the slag. Lastly the activation energy of viscous flow is estimated from the viscosity plots and thoroughly analyzed to comment on the structural objects of the Blast Furnace slag.

Chapter 1 of the thesis houses a thorough introduction to the thesis so that the reader can appreciate the basis on which the present work is performed.

This chapter is also devoted to Literature Review. In this chapter, which is based on the work of several experimenters, an attempt is made to systematically analyze the previous work done on the subject. It is devoted to a study of structural details of binary silicate melts & role of basic oxides on the structure of molten silicate slag. Special mentions of role of alumina on the silicate structures is discussed at length depending on the work of several experimenters. Various models used by different experimenters for predicting the slag viscosity are also given in this chapter.

Chapter 2 deals with the experimental details, including analysis of chemical composition of industrial BF slag; preparation of synthetic slag. It also mentions about the experimental details adopted for the measurement of flow characteristics as well as viscosity.

Chapter 3 discusses about the flow characteristic of the samples, including deviation of the equations to calculate the characteristic temperatures.

Chapter 4 discusses the viscosity of various compositions at different temperatures.

Finally, Chapter 5 gives the findings & conclusion by the author.

At the end, a detail bibliography is presented which mentions the details of literature that have been cited in the thesis.

1.1.1 Structural aspects of liquid slag

The structure of liquid slag dictates various characteristic properties of the slag melt such as its viscosity, electrical conductivity, density, flow characteristics, etc. Also it is possible to predict the structure of the slag concerned from a measurement of its various properties. The different structure dependent characteristic properties of the slag greatly influence the process variables and thus the process itself. For an example, it can be said with emphasis that the viscosity of the BF slag governs the reaction rates in the furnace by regulating the diffusion of ions through the liquid slag at the operating temperatures to and from the slag metal interface. The operational efficiency of the blast furnace is greatly influenced by the flow pattern of the liquid slag which determines the aerodynamics of the furnace by significantly influencing the gas permeability and heat transfer in the furnace.

Studies have been done on different structural aspects of the BF slag, making an attempt, on the basis of the work already done by previous experimenters, to explain different characteristic properties of the molten BF slag. Various factors that influence the structure and hence the characteristic property of slag are also discussed.

The structure of pure silica has been discussed, SiO_2 is the major constituent of molten silicate slag, as found from the majority of the literature.

An exhaustive review of the structural aspects of silicate melts has been made. The structure of binary silicate melts, poly component melts and complex melts has been discussed at length. The role of Al_2O_3, MgO, CaO and FeO in such melts, including that of the minor constituents has been discussed citing references from the literature. Measures of the degree of polymerization which governs the structural aspects of these melts has been also examined. Finally, the structure oriented thermo-physical properties, such as viscosity, flow characteristics have been discussed in detail on the basis of the available literature.

1.1.2 Structure of pure molten silica

Pure solid silica has a 3D continuous network of SiO_4 tetrahedron. Each silicon ion is coordinated with four oxygen ions, while each oxygen is linked to two Si^{4+} ions. Though, there may be a change from long- to short-range ordering during melting, the structure of pure liquid silica is very similar to that of pure solid silica. The very high viscosity of pure fused silica attributed to the associated high activation energy of viscous flow, indicates that the movement of flow units involves breaking of Si-O bonds (heat of dissociation = 104 KCal/mole) [17].

Theoretically, the flow unit is one which requires the least energy of transfer from the initial to the transition state. In the flow of molten silica it is suggested that this is a SiO_2 molecule which moves, since any larger unit would involve a greater number of Si-O bonds during the formation of the activated complex [9]

The high value of viscosity and the activation energy of viscous flow of pure molten silica indicates that, at any instant, only a small fraction of the melt may exist in the form of SiO_2 molecules at a given temperature and that these molecules that take part in the flow process must be formed from the three dimensionally bonded lattices.

1.1.3 Structure of binary silicate melts

With the addition of a basic metal oxide to molten silica, the added oxygen ion enters the network and separates the corners of two tetrahedra, while the added caution remains adjacent to the negative charges breaking the oxygen bridges between groups (**Equations 1.1 and 1.2).**

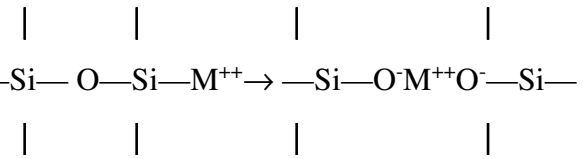

Equation 1.1

$$\begin{array}{cccccccc} | & | & & | & & | & & \\ —Si— & O—Si— & 2M^{+} \rightarrow & —Si— & O^{-}M^{+}O^{-} & —Si— & & \\ | & | & & | & M^{+} & & & \end{array}$$

Equation 1.2

The type of metal oxide added governs the degree of breakdown. While divalent metal cations tend to link the network by bridging two oxygen, monovalent ones do not [18]. Furthermore, a gradual addition of cations (e.g. Na^{+}, Ca^{++}) brings about a progressive breaking of the oxygen bonds with the formation of non-bridging oxygen (NBO), denoted by O^{-} and eventually the formation of free oxygen, O^{2-} ions.

The breaking down of the silicate network results in smaller and smaller silicate groups known as anionic units or flow units. Since smaller and smaller flow units require relatively higher oxygen, the progressive addition of metal oxides is less and less effective in reducing the flow unit size. This explains the decrease in viscosity at a slower rate with the increase in metal oxide percentage [19]. The discrete anion and chain formation concept [9, 18] is probably the most accepted model of silicate melts. Behera et. al [8,20] have discussed the discrete anion theory in detail.

The industrial slag, involved in the actual extraction process, is complex in nature. They contain oxides such as Al_2O_3, CaO, MgO, SiO_2 and many other minor oxides. It is worthwhile to review the effect of these oxides on the structure of the liquid slag.

1.1.3.1 Role Of Alumina on silicate structure

Al_2O_3 in silicate melts acts both as network former and network modifier adopting a fourfold (AlO_4) or sixfold (AlO_6) co-ordinations [4]. This depends on the presence of other cations in the melt that determines whether four or six oxygen ions are required for screening the Al^{3+} ion. For instance, the presence of ions such as K^{+}, Na^{+}, having weaker potential fields, allow the polarization of O^{2-} ions and thus encourage the formation of AlO_4 groups, whereas lithium, with a strong potential field, tightens the

O^- ions to such an extent that more than four O^- ions are required to screen the potential field of Al^{3+} ions, and AlO_6 group formation is favored.

Machin and Hanna [21] suggested that when sufficient basic oxide is present in the melt (molar ratio of Al_2O_3/CaO is less than one), Al adopts a fourfold coordination, and the melt contains $SiO_4^{4-}$and AlO_4^{5-} ions. However, when sufficient oxygen is not available for the formation of the Al and Si tetrahedra as aforementioned, Al adopts a sixfold coordination with oxygen and enters the interstices in the structure [6], thus, when basic oxides present are less than enough to provide for the required oxygen, polymeric ions as in **Equations 1.3 and 1.4** will be formed.

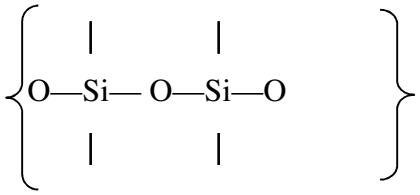

Equation 1. 3

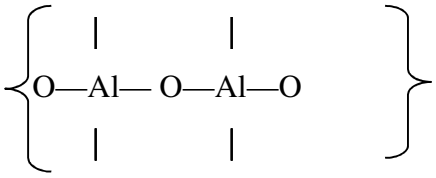

Equation 1. 4

In neutral and basic slag (Al_2O_3/CaO is less than or equal to unity), both Al_2O_3 and SiO_2 behave similarly. This means, in such slag, both Al and Si will occupy similar sites in the lattice, and the total network forming ions will be (Al + Si). However, at high Al_2O_3/CaO ratios and high silica contents, Al_2O_3 would decrease the viscosity acting as network breaker. This is consistent with the generally accepted view that alumina is amphoteric in nature.

Al-nuclear resonance studies on CaO-SiO_2-Al_2O_3 glasses [22] indicate that the oxygen coordination sphere of Al is more or less distorted. This supports the prediction of a variable coordination number of Al^{3+} ions in the melt. It can thus be appreciated

that, in melts containing Al-Si, Al^{3+}-O^{-}-type interactions are also present, besides Ca^{2+}-O^{-} and O^{-}–O^{-}-type interactions. This Al^{3+}-O^{-} interactions in the melt may be high or low depending on the Al_2O_3/SiO_2 ratio, which is, the Al / (Al + Si) ratio and would increase the activation energy of viscous flow, increasing the viscosity of silicate melt.

1.1.3.2 Role of Basic oxides on structure of molten silicate

Increase in percentages of CaO and/or MgO increases the percentage of these polymeric ions in the melt, while the increase in Al_2O_3 or SiO_2 decreases the same. Both CaO & MgO provide metal cations randomly distributed throughout the lattice of the silicate network, introducing weak points in the network. These cations, in general, weaken the Si-O bonds rendering the slag more fluid [20, 23]. The overall effect of these alkali metal oxides is thus to lower the flow temp of the slag by depolymerization of the silicate structure.

The degree of polymerization is represented in **Equation 1.5.**

$$R = (4 - N)/2(N - 2) \qquad \textbf{Equation 1. 5}$$

Here ‘R’ is the degree of polymerization, ‘N’ is the O/Si ratio (the number of oxygen atoms/the number of Si atoms) present in the unit.

1.1.3.3 Role of iron oxide on structure of silicate melts

Data pertaining to viscosity measurement of $FeO\text{-}SiO_2$, $FeO\text{-}CaO\text{-}SiO_2$ and $FeO\text{-}MgO\text{-}SiO_2$ show that [24] the addition of MgO or CaO results in a small decrease in the viscosity, whereas replacing MgO or CaO by Fe, the viscosity can be decreased substantially. The experimenters explained that CaO, in these slag, acts primarily as a diluent for silicate anions and less as a -Si-O-Si- bridge breaker. Furthermore, they suggested that, even when CaO breaks the -Si-O-Si- Bridge, the Ca^{2+} cations raise the potential barriers of the silicate anions and thus increase their contributions to the viscosity. The net result is a small decrease in viscosity with CaO addition. MgO additions lower the viscosity, but as the addition raises the liquidus temperature of the slag, the viscosity measurements are limited to a NMgO/NSiO2 ratio of 0·2 only.

Waseda et al. [25] opine that, at a constant Fe/Si ratio and temperature, the slag system $FeO\text{-}SiO_2$, show a slight rise in viscosity in the region close to the faylite composition. This rise in viscosity is attributed to the bridging of Fe^{2+} cation to SiO^{4-} tetrahedra as presented in **Equation 1.6.**

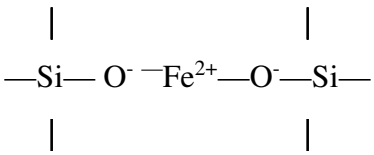

Equation 1. 6

However, at higher temperatures, this structure is easily broken and viscosity is lowered as the ions acquire more energy. This finding leads to the conclusion that, within the range of compositions examined, MgO and CaO act primarily as diluents and less as slag modifiers, whereas FeO acts as a stronger modifier compared to both CaO and MgO.

Dietzel [26] suggests that the cation–oxygen attraction is in the order $Si^{4+} > Mg^{2+} > Fe^{2+} > Ca^{2+}$, on the basis that the effect of a particular cation on silicate anions depends on its attraction for oxygen. This is not in line with the suggestions made by Kucharski et al [24]. They suggested the order to be $Si^{4+} > Mg^{2+} > Ca^{2+} > Fe^{2+}$. This difference in opinion is probably due to the fact that these experimenters did not consider the fact that the cation–oxygen interactions also depend on their surrounding neighbors.

Ferric ion, Fe^{3+}, can adopt both fourfold and six fold coordination [1, 27]. For slag containing 10% Fe_2O_3, Fe^{3+} adopts a fourfold coordination and works as a network former when the $Fe^{3+}/ (Fe^{3+} + Fe^{2+})$ ratio is greater than 0·5. The reverse happens when the ratio is less than 0·3.

According to the reactions given in **Equation 1.7 and Equation 1.8**, iron oxide added to silicate melts can break the silicate anions by providing free oxygen ions [28].

$$FeO = Fe^{2+} + O^{2-} \qquad \textbf{Equation 1.7}$$

$$Fe_2O_3 = 2FeO^{2+} + O^{2-} \qquad \textbf{Equation 1. 8}$$

The iron oxide decreases the viscosity of acid slag to a greater extent compared with that in basic slag. This is because, in basic slag, the trivalent ion exists in the form of ferrite anions to a greater extent, and these ions are not able to provide free oxygen ions. Moreover, in basic slag, though the iron oxide content is low, the silicate union is of smaller size, and hence the viscosity has been already low. Consequently, in basic slag, addition of iron oxide has little effect in lowering the viscosity.

1.1.4 Structure of poly component and complex silicate melts

A ternary melt containing cations of different groups may be viewed as an ideal mixture of two binary melts, provided that the total molar concentration of metal oxides remains the same. The structure of these poly component silicate melts is deduced by measurement of their activation energy (Eμ). It can be determined from the relationship as presented in **Equation 1.9**[29]

$$E_\mu = \eta_A(E_A)_x + \eta_B(E_B)_x \qquad \textbf{Equation 1. 9}$$

where, n_A and n_B are the mole fractions of the two oxides, and $(E_A)_x$ and $(E_B)_x$ are the activation energies for the two groups at the total metal oxide concentrations.

E_μ, calculated using **Equation 1.9**, agrees with the E_μ value experimentally evaluated for poly component systems. Therefore, it has been concluded that the discrete ion theory, based on binary systems, is also applicable to poly component melts. Thus, it has been further concluded that the mechanism of flow in binary and poly component silicate melts is identical at the same molar concentration of SiO_2.

1.2 Parameters used to represent the structure

1.2.1 Discrete Ion Theory

The viscous flow of the slag has been structurally attributed to the polymerization intensity [29] which is not only dependent on the silica network but also on the melting point of the slag.

It has been established that viscous flow in pure silicate melt is because of the single SiO2 structure as a flow unit. In any other liquid under flow, which has the metallic oxide between 10-50% in a silicate melt, the unit of flow is a set of discrete silica ions. These silica ions would arise out of reaction between SiO_2 and MO and would have discrete ions starting with $(Si_3O_9)^{6-}$ to $(Si_{34}O_{51})^{-6}$ with various chain lengths. These discrete ions will have to be balanced with respect to electro-neutrality and stochiometrical consideration [3] .It has also been stated that in binary alkali and alkine earth systems, the flow is largely governed by larger anionic chains. Ternary systems are considered to be ideal mixtures of two binary systems where no intermolecular potential occurs like other ideal solutions. Therefore, in the ternary system also the discrete anionic chains are responsible for viscous flow. [3].

Toop & Semis [11, 30, and 31] have suggested a model explaining the shortcomings of the discrete ion theory. This aspect has been thoroughly explained by Tiwari et al [7].

The discrete anion and chain formation concept of viscous flow of silicate melts is the most accepted structure model of silicate melts [9]. This explanation also defines the changes on physical properties of the melts like miscibility gaps of liquid, their expansivity etc.

Many researchers have tried to define this discrete ion formation mechanism [1, 25, and 30]. The co-ordination no of silicate melts is studied [25] and it is found that in discrete ions of ring type e.g. $Si_3O_9^{-6}$ the number of oxygen surrounding the silicate within the nearest neighbor should be 4. As the addition of alkaline earth metal oxides increases, the discrete anions become smaller as the Si-O-Si bond breaks [25]. This ensures the flowabilty of the silicate melt.

Resonance studies on the CaO-SiO2-Al2O3 system [22] indicates that the oxygen co-ordination sphere of Al is more or less distorted. This supports a variable coordination number of Al^{3+} ions in the melt.

1.2.2 Type of Oxygen Bonding

1.2.2 (a) NBO/T Ratio

State of oxygen in bonding the silica tetrahedra and the metallic ion has been studied by several [1, 30, 32] authors.

In the melt as a consequence of MO additions, O is in one or all the states of oxygen available as state of oxygen - defined as double bonded oxygen, singly bonded oxygen and free oxygen ion (O^o, O^- and O^{2-}).

The discrete anion theory has a limitation that it ignores the formation of free oxygen ions completely.

Troops & Semis [11, 30, and 31] have explained in details taking the example of polymerization of two silicate ions as mentioned below:

$2SiO_4^{4-} = Si_2O_7^{6-} + O^{2-}$

$8O^- = O^0 + 6O^- + O^{2-}$

Or, $2O^- = O^0 + O^{2-}$ **Equation 1.10**

& also, $SiO_4^{4-} + Si_2O_7^{6-} = Si_3 + O_{10}^{8-} + O^{2-}$

$10O^- + O^0 = 8O^- + 2O^0 + O^{2-}$

$2O^- = O^0 + O^{2-}$ **Equation 1.11**

It shows that when two silicate anions polymerize the resultant reaction liberates oxygen ions as singly bonded, doubly bonded & free oxygen as given in **Equation 1.10** or **Equation 1.11**

The equilibrium constant for this reaction is given by:

$$K = \frac{[O^o]\,[O^{2-}]}{[O^-]^2} \qquad \textbf{Equation 1.12}$$

The K value cannot be found easily for a given silicate melt at a given temperature. The value has to be assumed & then has to be seen if the calculated O^{2-} values coincide with the activity values of metal oxides as observed. The above oxygen status defined as N^o (Bridging i.e. doubly bonded) N^{o-} (non-bridging i.e. singly bonded oxygen) and N^{o2-} (free oxygen ions). [33] Expresses the degree of polymerization. De-

polymerization of the silicate melts is defined by term NBO/T i.e. ratio of non-bridging O atoms to total O atoms in tetragonal co-ordination. It is possible to calculate the (NBO/T) corr. as per following equation. The term (NBO/T) corr. has been considered because the cations which will be on the charge balancing role cannot be used as network breaker i.e. Na^{+} is to be placed near Al^{3+} for charge balancing in silica network.

In the calculation first YNB is calculated as per **Equation 1.13** given below, followed by calculation of XT as per **Equation 1.14** and lastly (NBO/T) corr is calculated as per **Equation 1.15.**

$$YNB = \Sigma 2\ [XCaO + XMgO + XFeO + XMnO + 2XTiO_2 + XNaO + XK_2O + 3f \times Fe_2O_3 - 2 \times Al_2O_3 - 2(1-f) \times Fe_2O_3] \quad \textbf{Equation 1.13}$$

$$XT = \Sigma \times SiO_2 + 2 \times Al_2O_3 + 2f \times Fe_2O_3 + \ldots\ldots. \quad \textbf{Equation 1.14}$$

$$(NBo/T)\ corr = YNB/XT \quad \textbf{Equation 1.15}$$

Here f = fraction of Fe^{3+} ion acting as a network breaker and X stands for the mole fraction of respective oxides

The empirical formulae as given in the **Table 1.1** [24] for discrete silicate ions [9] has been given at Si/O molar ratio of 0.25 to 0.33. This corresponds to mass percentage of metal oxides from 66 percent to 50 percent.

Table 1.1 – Empirical Formula of Discrete Silicate Ions

Si: O	$CaO:SiO_2$	% molar oxide	Length of chain	Empirical formula
1:4	$2CaO:SiO_2$	66	1	SiO_4^{4-}
2:7	$3CaO:2SiO_2$	60	2	$Si_2O_7^{6-}$
3:10	$4CaO:3SiO_2$	57	3	$Si_3O_{10}^{8-}$
4:13	$5CaO:4SiO_2$	55	4	$Si_4O_{13}^{10-}$
5:16	$6CaO:6SiO_2$	54	6	$Si_5O_{16}^{12-}$
10:31	$11CaO:10SiO_2$	52	10	$Si_{10}O_{31}^{22-}$
1:3	$CaO:SiO_2$	50	∞	$Si_nO_{3n}^{2n-}$

The addition of SiO_2 gives the chain length of high order which keep increasing till the molar ratio of MO/SiO_2 becomes unity, i.e. SiO_2 males are 50% of the total. The increase in chain length increases the heat of activation.

The requirement of electrical neutrality of the structure led to propagation of $Si3O96^-$ planer rings and $Si_4O_{10}^{4-}$ tetrahedra of silica between 33 mole percent to 50 of CaO.

1.2.2 (b) NBO/Si Ratio

The NBO/Si value is also considered and it gives structures for different ranges of NBO/Si. It is suggested [1] that with increasing NBO/Si ratio, the dimer structure becomes unstable and diminishes, consequently sheet and chain structure appears. It has also been suggested that monomer is the most abundant structures near ortho-silicate but diminishes as NBO/Si ratio reduces.

Based on the stability of monomer, dimer structures and also based on NBO/Si, following equations for equilibrium, relating to anionic structures in a silicate melt are suggested:

For 4> NBO/Si > 2

$$2Si_2O_7^{6-} \rightleftharpoons 2SiO_4^{4-} + Si_2O_6^{4-} \qquad \textbf{Equation 1.16}$$

For 2> NBO/Si > 1

$$3Si_2O_6^{-4} \rightleftharpoons 2SiO_4^{4-} + 2Si_2O_5^{2-} \qquad \textbf{Equation 1.17}$$

And for 1> NBO/Si > 0.1

$$2Si_2O_5^{2-} \rightleftharpoons Si_2O_6^{4-} + 2SiO_2 \qquad \textbf{Equation 1.18}$$

1.2.2 (c) Optical Basicity

The optical basicity concept is first developed by Duffy. Magnitude of negative charge borne by the oxygen atom or ion in a system containing basic oxides which are generally network breakers and are ionic; SiO_2, Al_2O_3 which are network formers and are covalent ;decide the acidity or basicity of a system. This negative charge is

represented by 'Λ', termed as optical basicity [35]. It is obtained by frequency shift of absorption band in the 6s-6s transaction observed in the ultraviolet optical region of the spectrum [35]

It is a scale and the calculation is given by following equation:

Λ= Electron donor power of slag /Electron Donor power of CaO

Equation 1.19

Optical basicity of a slag can be calculated from the optical basicity of the individual oxide present in the slag using following equation.[35]

(a) $\Lambda = \Sigma (X1n1\ \Lambda1 + X2n2\ \Lambda2 + \ldots\ldots\ldots) / \Sigma (X1n1 + X2n2 + X3n3 + \ldots\ldots\ldots\ldots\ldots\ldots)$

Equation 1. 20

Where n = number of oxygen in oxide e.g. n = 2 for SiO_2 and n = 3 for Al_2O_3

(b) Λcorr. is calculated by deducting the mole fraction of cation required for charge balancing the Al^{3+} in the chain. For poly cation system this is manually deducted from the largest cation present i.e. Ba^{2+} thus $X^{corr}_{BaO} = (X_{BaO} - X_{Al2O3})$

Optical basicity (Λ) has been used for interpreting data to examine the effect of composition and ionic structure on the viscosity (Ghosh) [35]

1.2.2 (d) Q Ratio

Another measurement system has been designated by letter Q which is a measure of polymerization and is defined as [32, 33]

$Q = 4-(NBO/T)$ **Equation 1. 21**

For 0, 1, 2, 3, 4 NBO/T ratio the corresponding values of Q will be 4, 3, 2, 1, 0 respectively.

1.3 Viscosity

1.3.1. Viscosity of slag melt

Liquid generation in the slag-forming oxides start developing at the conditions of blast furnace operation, when reaction among the constituents CaO, SiO_2, Al_2O_3, Fe bearing materials etc. starts taking place. In addition to the reaction of these, the softening of liquid phases already formed during a sintering / palletizing process is initiated. The liquid slag thus formed is highly siliceous and its viscous characteristic governs the operation of the blast furnace. At primary stage it affects the reaction of gangue materials and reduction of ferruginous materials. At the beginning and end of cohesive zone it has an impact on the gas flow, slag metal separation conditions. At bosh it impacts the direct reduction, dissolution of ash of the combusted coke, metal exchange and finally at hearth it facilitates the metal separation before flowing out. Therefore, it is important to study the slag viscosity at various stages of iron making in blast furnace but it is not possible to collect the samples of slag from different stages of operation. Efforts are made to draw correlations based on study of finished slag or synthetic slag of various compositions.

The viscosity of silica slag formed as above, is highly non-linear with respect to composition [36]. Each metallic oxide constituent of slag has a specific role to play singly or in combination with other oxides. The content of the oxides, on a given temperature, will change the viscosity based on whether it is a network former or breaker. The constituents not only decide the extent viscosity values at a given temp, these also controls the rate of change in viscosity so as to make it a short or a long slag. It is also reported [37] that the size of the cations has a role in changing the slag viscosity.

While all cations, part of a slag constituent, reduce the viscosity of the original silicate melt, Alumina behaves differently at different cations/anion ratios. Therefore, it becomes far more essential to study the role of Alumina at different composition levels because Al_2O_3 content of the slag in Indian iron making blast furnace ranges around 20%. This is much higher than those referred to in literature.

The impact of composition is evident on the viscosities of various melts. It has been found [37] that at the melting point the viscosity of various compositions are in the following order:

Alumino Silicate > Silicate > Phosphate > Boro Silicate > Aluminate >Borates >Ferrites

Thus an extensive literature review has been done to understand the effect of composition on viscosity of blast furnace slag.

1.3.2 Effect of various constituents on Viscosity

The oxide constituents of the slag react and form compounds which have different behavior in given thermal, mechanical, chemical and environmental conditions. Simultaneous occurrences of various activities makes it a complex system. Various constituents present in slag have effect on phases formed, affecting liquidus and solidus temperatures and finally the viscous flow.

The major constituents of a blast furnace slag are SiO_2, Al_2O_3 CaO, and MgO along with minor constituents of TiO_2, MnO, P_2O_5, etc. The network formers, network breakers and Alumina in a dual role, have been studied in various combinations and conditions in laboratory by many researchers [29, 38].

1.3.2.1 Role of CaO/SiO_2 (C/S) ratio on viscosity

Many researchers have studied the impact of the CaO/SiO_2 ratio of ≥ 1. This includes slag [12] with a C/S ratio of 1.15 – 1.6, Al_2O_3 ranging between 10-15%, MgO 5-10% and FeO 5-20% at 1723K. In $CaO\text{-}SiO_2\text{-}Al_2O_3\text{-}MgO\text{-}FeO$ system impact of FeO appears to be more dominant. The melting point of slag reduces with increasing the, so also the viscosity. The addition of MgO does not affect the viscosity of the slag if FeO is >7.5%. Minimum viscosity value is observed at 7% MgO and 5% FeO at CaO/SiO_2 ratio of 1.15 to 1.6. [29] In general, in slag with C/S ratios up to 1.3, the viscosity value increases because of polymerization of silicate structures leading to discrete anionic groups [29]. The polymerization effect of silica network is more if the temperature at which viscosity is measured is higher than the melting point. Thus melting point in

addition to CaO/SiO_2 ratio also affects the viscosity of the slag. Viscosity of slag at 1773 K decreases with increasing basicity but the rate of decrease of viscosity above CaO/SiO_2 ratio 1.3 decreases [29].

1.3.2.2 Role of MgO on viscosity

The role of MgO in flow characteristic of slag has led to many studies in different conditions. This appears to be temperature based phenomenon because it is found that addition of MgO increases the slag viscosity up to 1723 K followed by a decrease. Nagueira [39] opined that the addition of MgO instead of CaO will not form low melting slag (MgO in general increases the melting point) especially at high MgO/SiO_2 ratio. It establishes the role of CaO in slag flowabilty.

Athappan [40] measured the viscosity of slag containing 20% Al_2O_3 for different MgO contents. It is found that at 1723 K, the viscosity decreases with increase in MgO. However, there is no impact on viscosity if MgO addition exceeds 10% as mentioned above.

MgO, when added to $CaO\text{-}SiO_2$ slag synthetically prepared, decreases the viscosity when the amount of MgO is increased up to 20% (probably due to the absence of minor constituents in the synthetic slag), after that it increases [38]. A similar trend is found in the $CaO\text{-}SiO_2\text{-}Al_2O_3$ system also after addition of MgO. Change in viscosity at constant temperature after MgO addition in these systems is found to be small. It is however necessary that MgO replaces SiO_2 or Al_2O_3 in the system rather than CaO, if decrease in viscosity by the addition of MgO is sought for [38]. This study is in slag with CaO/SiO_2 ratio of ≤ 1.0 and at temperature 1723 K and 1873 K.

The effect of MgO in high alumina slag is found to be pronounced. [41]. As the C/S ratio of 1.2 and 15% Al_2O_3, the viscosity decreases within the MgO range of 2.4 to 5.7%. However, this increases with increasing content of MgO. A similar pattern is found at higher percentages [42] between 4-12% MgO additions. However, at high SiO_2, Al_2O_3 content, the replacement of one with another does not affect viscosity significantly. This observation confirms the postulation that Ca^{2+} are closely associated with the silicate group [29, 31,] Effect of CaO, MgO on viscosity of the high TiO_2 slag is highly temperature dependent [43]

MgO has also been reported to be amphoteric in nature. It is reported that in $CaO-MgO-SiO_2$ system MgO behaves like CaO but in $Na_2O-CaO-SiO_2$ system it acts as in acidic oxide [44].

General observation has been that increase in viscosity after addition of cations of Mg and Ca or Al beyond a certain percentage, increases the viscosity more due to crystallization than the viscous flow of the liquid present [45] At high a CaO/SiO_2 ratio other silicates might be found which increases the viscosity. Similarly the viscosity of slag off CaO/SiO_2 >1.3 at 1723K is affected by solid compounds such as C_2S, Melitite ($C_2MS_2.C_2AS$) and Mervinite (C_3MS_2). [16] The crystallization temperature is shifted to higher temperature with increasing MgO content of the slag because of the formation of some of the high temperature phases for example as spinel $MgO.Al_2O_3$. It is also found that as the temperature decreases the effect of increasing amounts of solid phase on viscosity will be more dominant than the effect of network forming oxides.

1.3.2.3 Role of Alumina on slag viscosity

Silicate slag having $(SiO_4)^{4-}$ tetrahedral form chains bonded by oxygen ions. Addition of alumina effects both ways. The alumina present in the form of $(Al_2O_3)^{5-}$ form polymeric units with $(SiO_4)^{4-}$ and thus it becomes a network former. [35] This substantiates the theory that replacement of SiO_2 by Al_2O_3 does not make substantial change in viscosity of the slag [42]. At higher CaO content when Al_2O_3/CaO ratio is less than 1, Al adopts 4 fold co-ordination and behaves like a network former along with SiO_4 in the melt [21] In case this ratio increases beyond 1 i.e. when sufficient oxygen is not available Al adopts a 6 fold-co-ordination with oxygen and enters with interstices of the structure [6]. In this situation, it behaves like a network breaker.

Poe and McMillan [46] have suggested the importance of formation of five coordinated Al – an intermediate structure on oxygen diffusion and viscosity of $CaO-Al_2O_3$ melts. A relationship between Al and Si has been given by Turkdogan and Bills [47].

In Aluminothermic ferrochrome slag, the reduction in Al_2O_3/CaO ratio reduces the viscosity of slag [20]. At a higher CaO content reduction is less. There is a progressive decrease in viscosity with increase in CaO. Lowering of Al_2O_3 shows that

proportion of AlO_5^{7-} increases and proportion of AlO_4^{5-} decreases because AlO_4^{5-} forms more polymerized units leading to increase in viscosity.

It is found that when both SiO_2 and Al_2O_3 increase, the viscosity and activation energy of the melt increase [42]. The strength of covalent bond is found to be the main reason of increase of the viscosity of SiO_2 and Al_2O_3 melt [48]. At high SiO_2 and Al_2O_3 contents, the replacement of one with another does not affect viscosity significantly. A 'short slag' (sharp drop in viscosity after liquification) is formed at low content of (SiO_2+Al_2O_3 <40 %.). However a value > 40% gives a 'long slag'.

1.3.2.4 Role of Oxides of Fe on viscosity

Fe^{3+} can have both fourfold and sixfold co-ordination and is dependent on the content of Fe_2O_3 and relation of Fe^{3+}/ (Fe^{3+}+Fe^{2+}) ratio. It is network former at the ratio of 0.5 and network breaker if the ratio is <0.3 [1, 27]. It is opined that the breaking of the structure is a result of the availability of free oxygen ions.

1.3.2.5 Role of TiO_2 on viscosity

In all the experiments done [49,50] it has been found that all forms of oxide of Titanium reduce the viscosity added up to 10% TiO_2 level provided Titanium carbide is not formed. It has also been found that Ti_2O_3 is more effective in reducing viscosity that TiO_2 due to its property of modifying the network more severely [43].

1.4 Activation energy

Eμ, the activation energy of viscous flow, is the energy required to move one silicate group or a major part thereof, with respect to the other, enabling the group to move. The effects of monovalent and divalent metal oxides on Eμ are different. Unlike the Group I metal oxide systems, where Eμ is independent of the cationic species at all compositions up to about 35 mole%, in case of Group II metal oxides, the independence is retained till about 55 mole% of metal oxide, indicating that the effect of monovalent metal oxide on Eμ is more pronounced than the divalent ones [35]. This is because, at equimolar compositions, there are twice as many monovalent cations as divalent ones and as pointed out earlier, the divalent cations maintain the continuous bonding of the

lattice by bridging the oxygen atoms. Hence, by addition of Group II metal oxides, the decrease in Eμ will be more gradual. This leads to the fact that in case of the Group II metal oxides, the collapse of the SiO_2 network will occur only when comparatively more metal oxides have been added.

1.4.1 Dependence of Activation Energy (Eμ) on structure

Viscous flow has been attributed to breaking of Si-O bridging and also probably M-O bonds to form an entity in the melt which can move and is called a flow unit during viscous flow. The second consideration may be the concept of requirement of the energy to form a new volume (hole) into which the flow moves. With these considerations the activation energy of viscous flow Eμ will be dependent on the formation and type of discrete ions. Therefore, it depends on the composition, leading to structural configuration of Si-O and M-O hence a slackening of the cation/anion bond with temperature. [43] To a larger extent, if the degree of polymerization is constant, the activation energy will remain constant and therefore a straight line relationship for ln μ vs. 1/T (K) plot is possible.

By this observation, it is obvious that any re-grouping of structure will lead to change in Eμ (activation energy), since in such a case the energy required to move one unit with respect to another will increase.

1.4.2 Effect of Composition on Activation Energy

Effect of composition on activation energy of viscous flow has been studied. The increase in SiO_2 content from 31.3 to 53.9% decreases the activation energy from 40.9 to 18.9 Kcal/mole [45]. The activation energy of various CaO/SiO_2 ratios have smoother decrease with increase in CaO content at temperatures >1973 K compared to that at temperature below1973 K. This is because, as explained above, the breaking of SiO=O covalent bonds in presence of Ca^{++} ion at high temperature is more [9]. The affinity of Ca^{++} ions with oxygen is high, hence the broken Si-O structure requires less energy for displacement. The increase of SiO_2 content increases activation energy, especially above the 88 % level in CaO/SiO_2 melts. Conversely, if the alkaline earth metal oxide is added in the silicate melts, the activation energy decreases gradually due

to bridging of these metal ions with oxygen and subsequent collapse of the silica tetrahedral network.

As explained, liquid slag consists of, among others, discontinuous ionic structures, whose activation energy is closely connected to the type of ions and ionic complexes present in the system as well as to inter ionic forces. Due to the fact that the type and size of ion changes in temperature, the activation energy changes significantly with temperature too [51]

Metal oxides with smaller cations are less efficient in reducing the viscosity by bringing down the Eμ. In the case of the smaller cations, due to the spatial arrangement of atoms in the molecule, the Columbic interactions between metal cations and single bonded oxygen will be relatively smaller. The tendency to form more extreme depolymerized (e.g. SiO_4^{4-}) and polymerized (e.g. SiO_2) anionic units can be ranked in terms of the parameter, Z/r^2, where 'r' is the radii and 'Z' is the valency; the higher the ratio, the higher is the tendency. This tendency of the metal oxides can thus be given in the order $Mg^{2+} > Ca^{2+} > Sr^{2+} > Pb^{2+} > Ba^{2+} > Li^{+} > Na^{+} > K^{+}$.

Again, the addition of x moles of Na_2O to a given amount of a given silicate slag should result in greater lowering in viscosity in comparison with the lowering observed due to the addition of x moles of CaO to the same amount of the same silicate slag. This is because the alkaline earth cations having a bridging tendency would not permit the O^-—O^- interactions to be as effective as the case when only alkali metal cations are involved.

The cations, randomly distributed throughout the lattice of the silicate network introduce weak points into the network and also weaken the Si-O bonds near the metal ion due to a polarization effect. This causes a general loosening effect in the lattice.

1.5 Flow characteristics

1.5.1 Characteristic Temperature

The ultimate objective of metal gangue separation is dependent to a large extent on the fluidity of the slag at different stages of BF operation. The slagging oxides react, form liquid, flow down and finally at the hearth level the viscosity of both the fluid slag and liquid metal is so low that effective metal separation takes place.

Role of liquid slag is also to receive all the gauge materials besides its role to keep the metal protected from oxidation and provide alloying element. Therefore the basic characteristics of the slag required, are that it should have low cohesiveness, low viscosity and lower melting temperature at final stages to help drainage and as mentioned above on affinity towards non ferric metal oxides so that partial refining of iron also takes place.

Study on the behavior of slag in blast furnace has been summarized [10]. The study of measurement of viscosity, physical properties of liquid, quantitative evaluation of molten pig iron and slag tapping phenomena, evaluation of the effect of pressure drop in liquid flow in dripping zone, are some of the behaviors needing study and evaluation.

Togobistakaya [52] reports that in an experimental condition, the most suitable range of viscosity for smooth BF operation should be as under:

1. During blowing, the viscosity should vary from 0.4 – 2.0 PaS at 1623 K.
2. While working, the viscosity at optimum slag temperature of 1723 K-1773 K should be less than 0.25-0.2 Pa.S
3. During blowing out period the viscosity should not exceed 0.2-0.3 Pa.S at 1723 K-1823 K

These are, however viscosities of the end slag. The formation of slag which starts early in the BOF operation has been identified as [53] primary slag at cohesive zone, bosh slag at dripping zone, tuyere slag at tuyere zone and final slag at the hearth.

Final slag consists of mainly SiO_2, Al_2O_3, CaO and MgO and must have good fluidity to ensure good tapping. This requires a low liquidus temperature & low viscosity [53]. Considering above requirements of slag behavior, efforts have been made in the present study to examine the fusion behavior of compositions based on finishing slag of a blast furnace.

1.5.2 Fusion behavior – Stages of Fusion

Primary slag formation in the blast furnace at early stages of burden plays a very important role. Strongly dependent on reduction of metal oxides, the liquid becomes highly viscous. It may lead to deformation of the burden before the flow starts. The need is of a slag of high softening temperature coupled with a relatively low flow temperature [41]. This will form a narrow cohesive zone and lower down it [54]

With two distinct requirements of slag i.e. a final slag which starts flowing as soon as it softens (short slag) and slag of high softening temperature and low flow temperature of the cohesive zone area, necessitates the study of fusion behavior and flow characteristics of the slag.

The fusion behavior is defined in terms of four characteristic temperatures [55]. These are: IDT – Initial Deformation Temperature symbolizing stickiness with surface, ST – Softening Temperatures symbolizing the start of Plastic Deformation. HT – Hemispheric Temperature indicates the liquidus temperature and FT – the flow temperature. Here the HT of the slag – liquidus temperature, plays a very important role in maintaining the gas flow, reduction mechanism and heat transfer. Flow Temp (FT) symbolizes the liquid mobility.

1.5.3 Effect of composition on flow behavior

The fusion behavior of the slag and that of the metal has been well studied. Wherever metal is entrapped in slag in the form of bubble–occurring because of the sudden fluidity of slag immediately after the reduction of Fe, the surface area of slag – Fe and its oxide increases and becomes much larger than that postulated in two film theory [56]. This envelope of large surface area due to the fluidity of the slag initiates mass transfer in solid, liquid and gaseous phases. Slag formation and state of reduction can be driven by the much larger volume obtained out of such entrapment [10].

With an increase in Al_2O_3, drainage rate decreases due to increase in viscosity. However, due to increase in MgO content, the viscosity reduces and drainage improves. MgO addition (8.5-10.6%) in slag increases the crystallization temperature, whereas MgO addition content of 4.6 to 5.3% reduces the crystallization temperature at two CaO/SiO_2 ratio of 1.20 and 1.45. [57]

As the slag formation and its various states are complex, in Japan people have even tried to study the exact working of a blast furnace by quenching & dissecting a working furnace. Their study reveals that, the cohesive zone in the furnace greatly influences the process of iron making in the blast furnace- being practically working as a gas distributor - thus controlling the permeability, heat and mass transfer in the furnace.

FeO remains in slag initially, but is removed from the slag gradually and finally in the dripping zone slag becomes a non-FeO system. Similarly CaO/SiO_2 ratio is around 2.0 in the beginning as is in gangue material and then reduces to about 1.4 at a slag discharge level in EBF.

It has been reported [10] that the addition of FeO up to 20% max in the CaO-SiO_2-MgO-Al_2O_3 system decreases the softening and melting temperature. Further addition of FeO does not have any appreciable impact.

Al_2O_3 increases in the upper part of dripping zone as the slagging with coke ash – Al_2O_3, SiO_2 increase, coke being the major source of these oxides. The viscosity increases, but due to high temperature at tuyer it remains at 1.3 Poise.

The flow of the slag in the burden and coke slits is responsible for the pressure drop. Sumahara [10] studied the EBF and found that the pressure drop is not only dependent on viscosity and crystallization temperature, but also on the CaO/SiO_2 ratio. The CaO/SiO_2 ratio increase leads to higher pressure drop and vice-versa. However, at the same CaO/SiO_2 ratio with equal crystallization temp, the pressure drop varies. This brings in Al_2O_3 and MgO to play a role. If CaO/SiO_2 is, say around 1.18, the impact of Al_2O_3 in pressure drop is low. In case of MgO, if CaO/SiO_2 is low and MgO is high, the drop is small even if Al_2O_3 is high.

The flow is also dependent on wettability and if CaO/SiO_2 is 1.5 or greater, the slag does not wet with coke, etc., whereas if CaO/SiO_2 reduces, say to 1.4 or 1.3, a lower contact angle is obtained and wettability improves [10]

The molten slag at the burden stage contains solid particles and therefore, till the compete liquidification of slag components the fluid flowing through the blast furnace

can be considered to be a non-Newtonian liquid [51]. Synthetic liquid slag of CaO-SiO_2- Al_2O_3 at 1673 K shows fully Newtonian viscous fluid. However, with solid particles the above liquid behaves like a pseudo plastic system where shear stress influences the value of the dynamic viscosity coefficient. This is possible even at solid contents in the range of 11.46-17.55% also [51]

The presence of solids will influence the rheological properties of the system. The type of solids and their amount and types of anions in the liquid part of the fluid influence the changes in viscosity. The addition of Al_2O_3 changes the rheological character by increasing the solid content at lower temperature and polymerize the liquid part of the system. If added into a Newtonian slag melt, the Al_2O_3 changes it to pseudo plastic. The viscosity of such systems containing solid is described by the following equation of Einstein Roscoe [58].

$$\mu=\mu_0 (1-\alpha/\beta)^{-q} \qquad \textbf{Equation 1.22}$$

Where μ_o is crystal free viscosity,

α is the fraction of crystals,

q is approximately taken as 2.5 &

β is given by, $\beta=1-\alpha (1-\alpha_0) /\alpha_0$;

with α_0 is approximately 0.7.

The dissolution of Al_2O_3 in slag is studied for identifying the reason of the nonmetallic inclusion and it is found that with increase of Al_2O_3 content in slag, the mass flow density reduces [59]. This implies that the addition of Al_2O_3 restricts the flow due to reduced fluidity. It confirms that Al_2O_3 addition polymerizes the slag. Impact of MgO on Al_2O_3 is also studied. More addition of MgO initially forms spinel $MgO.Al_2O_3$ which reduced the mass flow rate, but as soon as $MgO.Al_2O_3$ dissolves in slag the mass flow rate doubled indicating breaking of the structure of liquid slag by MgO.

1.5.4 Pore blockade by molten slag

Nakamoto [60] studied the impact of the pore blockade on reduction of FeO containing slag {FeO-SiO_2 (Fayalite System,FS) and FeO-SiO_2-CaO (FSC)} system. These systems represent a primary slag system in the Blast Furnace. The Fayalitic Slag is more viscous than FSC (almost 4 times), the mechanism of flow is found to be different for both. FSC is found to be present in greater extent in the interspaces of the grain than along the grain boundary. This creates a blockage of pores with respect to reducing gases. FS slag is found more in the grain boundary spaces, thereby creating the space between the grains and permitting the flow of reducing gases.

The impact of surface tension vis-à-vis viscosity on downward flow is assessed by the following formula of penetration [61]

$$dL^2/dt = r \gamma_{LV} CosQ/2 \eta_L \qquad \textbf{Equation 1.23}$$

Or, integrating, $L^2 = t.\ r.\ \gamma_{LV}.\ cosQ\ /2\eta_L$ **Equation 1.24**

And the fluid volume V absorbed by N such capillaries of the coating is given by the following relation:

$$V=\alpha/K(r \gamma_{LV}.cosQ\ t/2\eta L)^{1/2} \qquad \textbf{Equation 1.25}$$

Where

L is penetration length of the fluid,

r = average pore radius,

K = constant for tortuosity of capillary pores=L/E, where E= coating thickness,

& $\alpha = Np.\pi r^{2;}$ where Np is number of pores per unit area, α signifies porosity .

γ_{LV} = surface tension of the fluid ,

Q = contact angle between the liquid and solid,

η_L = viscosity of the liquid, and

t = time of penetration

If K is constant for all the feed materials, then the flow through penetration will be dependent on the physical properties of the molten slag e.g. contact angle between

slag and FeO, surface tension and viscosity. It has been found that the viscosity variation due to composition is lower than surface tension, hence the flow behavior in penetration of the molten slag is mainly dependent on viscosity.

1.5.5 Effect of Feed material on flow

It is found that addition of BOF slag in the blast furnace burden along with dolomite and limestone increases the softening & melting temperature of the slag. In case of BOF slag with 41.09 % of CaO and C/S ratio of 4.18 raised the melting temperature from 1430°C to 1520°C and above, while softening temp is increased only by 25°C [62]. This increases the gap between softening and melting temperature.

However, with additions of other CaO/MgO bearing materials in form of dolomite and/or the BF slag the softening and melting temperatures increase by 25°C and 30ºC respectively.

The different behavior of BOF slag and other additions is due to the formation of high CaO/SiO_2 ratio slag material as evident from the phase diagram [62]

The literature has shown that there are three mechanisms of melt down [63]. However, it is generally believed, because it is not possible to replicate the internal BF situation completely as of now, that the slag in the core melts and comes out breaking the iron shell of the BF feed. This is possible only when reduction of the outer shell proceeds continuously to increase the % of reduced ore. It is found that increase in reduction from 60% to 90% in a pre-reduced pallet increased the softening temperature by 70°C [62]

1.5.6 Effect of Reduction degree on flow

The flow of the slag in the blast furnace (where pallets of predefined composition are charged) is also dependent on reduction degree and distribution chemistry of constituents in the pallet.

It is observed that outer surface, still in contact with carbon by way of coke or graphite of experimental crucible, melted earlier and then the primary slag exuded out of the shell. This role of carbon surrounding the BF feed will lead to change in melting

behavior and flow behavior of the slag due to different degrees of rejection along with the degree of carburization. [62]

1.5.7 Flow at the bottom of the furnace

The lower portion of blast furnace has flowing liquid slag, liquid metal and the coke burden. Considering this portion as a packed bed, the flow characteristics of slag are experimentally studied [64]

Liquid flow through packed bed occurs because of force applied on the liquid. Six major forces are discussed by Fukutake [65].

Following equation is given by Husslage [66] to define the forces acting on a static liquid phase suspended at the top of an inter particle void.

$$Pgh = -\frac{4s\cos Q}{d}$$ **Equation 1.26**

where

P is slag density,

g = gravitational acceleration,

s = surface tension of the slag;

Q is contact angle between slag and coke.

d = channel diameter,

h = molten slag head over the opening top.

This equation does not consider the forces due to the movement and that of gaseous phases present. The flow starts only when the liquid slag hydrostatic pressure overcomes the capillary pressure for a given channel diameter [64]. It is established that minimum channel diameter between 4 to 4 5 mm are required to allow the slag to drip freely in the experimental condition at 1500°C. This is confirmed by using the above equation with data from literature. The calculation range is found to be 2.6 to 5.4 mm.

1.6 Impact of Viscosity on Slag – metal reaction/exchange

Andre Wu et al [67] have studied slag metal exchanges/reactions in details regarding the partition ratio of silicon and manganese. They suggest that the viscosity and flow characteristic of the slag are responsible for the silicon pick up and that the

silicon partition ratio depends on the percentage of silicon in the metal droplets. They found that the Silicon exchange takes place in very short period (1 second) and the reverse, i.e. Silicon from metal to slag goes, if the % of Silicon is more than 1.1% in metal droplet. The slag and metal droplets both are at 1500°C in this experiment indicating low viscosity for both slag and metal.

They also conclude that the thermodynamic driving force is responsible for the Si pick up by the metal droplet. The thermodynamic driving force is proportional to viscosity i.e. more viscous is the slag, higher thermodynamic force is required for silicon pick up by the metal droplet.

1.7 The viscosity models

Several viscosity models have been reported for calculating the viscosity. The models have been designed on various empirical parameters. Factors which effect the viscosity is also considered. These can be listed as-

1. Temperature dependence
2. Chemical composition dependence
3. Structure dependence
4. Thermodynamic consideration

1.7.1 Temperature dependence relationship

The temperature dependence of blast furnace slag viscosity is governed by Arrhenius equation. The change in temperature of a liquid effects its bond strength and it can be presumed therefore, that it will affect the viscosity as per following equation[68].

$$\eta = A \exp\left[\frac{EA}{RT}\right] \qquad \textbf{Equation 1.27}$$

where η = viscosity, A is pre-exponential coefficient and EA is the activation energy of the process of fluid flow.

Weymann-Frankel modified above equation[69] considering temperature dependence of constituents as follows

$$\eta = AT \exp\left[\frac{EA}{RT}\right] \qquad \textbf{Equation 1.28}$$

This equation is subsequently used to describe the slag viscosity.

1.7.2 Composition dependence relationship

Chemical composition of slag shows the constituents as well the species of these constituents. Kondratiev et al [70] referred models based on composition. The slag constituents have been defined as glass forming, modifier and amphoteric oxides. While SiO_2 is glass former, the oxides of Ca^{2+}, Fe^{2+}, Na^{+}, K^{+} are modifiers. Al_2O_3 and Cr_2O_3 are considered amphoteric. Behavior of Al_2O_3 and Cr_2O_3 is therefore dependent on their content and state in which other oxides exist (Slag Atlas). [82]. The most prominent model in this category is developed by Urbain.

1.7.2.1 Urbain Model [70]

Urbain studied the viscosity in system Al_2O_3-MgO-SiO_2 and Al_2O_3-CaO-SiO_2. It is to be extrapolated by the suggested method to predict the viscosities for multi-component system. It has however been found that the predicted data and those found in experiments in the full composition range of Al_2O_3-CaO-MgO-SiO_2 system are not in close agreement.

The model follows Waymann type relationship [33]

$$\eta = A_w T \exp\left[\frac{Bw}{T}\right] \qquad \textbf{Equation 1.29}$$

where η is (dPas) have following relationship.

$$-\ln A_w = 0.29Bw + 11.57 \qquad \textbf{Equation 1.30}$$

The Bw is calculated as under:

$\pounds^* = X^*_m / (X^*_m + X^*_A)$, where X^*_m, X^*_A, X^*_{SiO2} are modified normalized for m for the molar fraction of network modifier(X_m), amphoteric(X_A) & network former(X_{SiO2}) respectively. The modified figure is obtained by dividing each term by $(1+0.5X_{FeO1.5}+X_{CaF2}+X_{TiO2}+X_{ZrO2})$.
[i.e. $X^*m=Xm/(1+0.5X_{FeO1.5}+X_{CaF2}+X_{TiO2}+X_{ZrO2})$, $X^*_A= X_A/(1+0.5X_{FeO1.5}+X_{CaF2}+X_{TiO2}+X_{ZrO2})$ etc]. This normalization is needed as this model acts only in M_xO oxide system.

$$Bi = a_i + b_i\alpha + ci\ \alpha^2$$

where subscript I = 0, 1, 2, 3 and a, b, c are given constituent for each case of 0, 1, 2 and 3.

$$B = B_0 + B_1X_{SiO2} + B_2X^2_{SiO2} + B_3X^3_{SiO2}$$

Different values for a, b, c are given for 0,1,2,3 to calculate the B value for a different system of divalent cations i.e. $CaO-Al_2O_3+SiO_2$, $MgO-Al_2O_3+SiO_2$ and $MnO-Al_2O_3+SiO_2$.

1.7.3 Structure dependence relationship

The structure of the viscous melts is very important. It is temperature dependent and establishes the flow units. Models have been developed to predict the viscosity considering structure in view and Iida model is one of the more prominent one. [83]

Viscosity is expressed as

$$n=A\mu_0 \exp\ (E/B_i^*) \qquad \textbf{Equation 1.31}$$

E is the activation energy

A is pre-exponent term and both are functions of temperature

μo is hypothetical viscosity and is a function of molar volume, melting point and chemical composition

Bi* is the modified basicity index and is a function of chemical composition [83, 84]

[Modified basicity index $=B_i^*= [\sum (\alpha_i W_i)_B + \alpha Fe_2O_3 * WFe_2O_3 + \alpha Cr_2O_3 * WCr_2O_3]/[\sum(\alpha_i W_i)_A + \alpha Al_2O_3 * WAl_2O_3]$

& primary basicity index $Bi==\sum (\alpha_i W_i)_B / \sum(\alpha_i W_i)_A$

Where suffix B & A stand for basic & acidic oxides respectively.
W_i=Wt. % of component oxide I,

α_i = specific constant for each component i]

The original Iida model had equations for calculating A, E and μo and various constituents are categorized into acidic, basic, and amphoteric. [85]

It is modified due to the change in behavior of amphoteric oxides with respect to temperature. Basicity index calculations are modified [84]

This model gets complicated because the specific coefficient α used in Basicity index calculation is first measured for saying Al_2O_3 and then used in the equation [33]

$$\alpha^* Al_2O_3 = a B_i + b W Al_2O_3 + c \qquad \textbf{Equation 1.32}$$

A, b, c values of above equations for $CaO+MgO+Al_2O_3+SiO_2$ system are defined as given below

$$a = 1.20.10^{-5} T^2 - 4.3552.10^{-2} T + 41.16 \qquad \textbf{Equation 1.33}$$

$$b = 1.40.10^{-7} T^2 - 3.4944.10^{-4} T + 0.2026 \qquad \textbf{Equation 1.34}$$

$$c = -8.00.10^{-6} T^2 + 2.5568.10^{-2} T - 22.16 \qquad \textbf{Equation 1.35}$$

Due to calibration with experimental data for each family of slag, the model is reported to be very accurate, however ,this makes this model a difficult one to implement because no general value of constituents can be considered because $a^* Al_2O_3$ is to be calculated for each family of slag[33]

1.7.4 Thermodynamic Considerations

KTH model is based on Eyring equation which takes Gibbs free energy, a thermodynamic property in consideration

1.7.4.1 KTH Model

$$\eta(PaS) = \frac{hNA\rho}{M} \exp\left(\frac{\Delta G}{RT}\right) \qquad \textbf{Equation 1.36}$$

where

h is the Planck's constant;

NA is Avogadro's numbers;

ρ and *M* are the density and molecular weight of the melt, respectively;

R is the gas constant;

T is temperature in Kelvin.

ΔG^* is the Gibbs energy of activation for viscosity,

ΔG is considered to be a function of both temperature and composition of the melt.

For multicomponent systems, the molecular weight M and density can be calculated as the weighted average as per following equations

$$M = \sum_{i=1}^{m} X_i M_i \qquad \textbf{Equation 1.37}$$

where

Xi and *Mi* are mole fraction and the molecular weight of component *i* in the solution, respectively

$$\rho = \sum_{i=1}^{m} X_i \rho_i \qquad \textbf{Equation 1.38}$$

where

ρi is the density of pure component *i* in the liquid state.

The Gibbs energy for activation of viscous flow can be calculated by following equation.

$$\Delta G^* = \sum_{i=1}^{m} X_i \Delta G^*_i + \Delta G^*_{mix} \qquad \textbf{Equation 1.39}$$

ΔG_i^* is Gibbs activation energy of pure component in liquid state

ΔG_{mix}^* is a term used to define Gibbs energy arising out of due to the mutual interactions between different species of the constituents of slag and therefore is expected to be a function of composition.

Different equations have been derived for ionic solutions.

This model has been reported to be applied in various systems.

Fact stage software has been used to calculate the viscosity and the comparison between the calculated and measured [86] ones. It has been found that at lower viscosity levels, there is fare correlation, but at higher viscosity levels, there is deterioration in the relationship [7].

1.8 Summary

Various viscosity models have been proposed based on temperature, composition, structure and thermodynamic considerations. Each model has its limitations. Temperature dependent models follow Arrhenius equation and there is a straight - line relationship between viscosity and ln1/T. In all other models the measured values and calculated values differ. Some of the original models have been modified subsequently by other researchers to make them more predictive than originally designed e.g. Urbain model, Iida model, etc. Wherever the differential is less, models can be used for predicting the viscosity. e.g. Iida model. Several Researchers, including Iida himself have commented that this model is more reliable compared to other models in predicting the blast furnace slag viscosity.

Thus an exhaustive literature survey has been made prior to conducting the experiments. On the basis of the finding of various experimenters, the experimental data have been thoroughly analyzed with specific comments wherever necessary.

Chapter 2

MATERIALS EXAMINED AND EXPERIMENTS CONDUCTED

2.1 Work plan

In this chapter experiments conducted for measurement of flow characteristics, viscosity and chemical analysis required for characterization are explained. The determination of chemical compositions of the collected industrial slag samples is also discussed. The materials used for making synthetic slag, the sample preparation for all the tests are also mentioned. The equipment used for conducting the experiments is explained along with special literature references for viscosity and flow characteristic, measurement procedures. Finally, procedures for conducting tests are also given in explicit details.

2.2 Collection of Industrial Blast Furnace slag and its characterization.

2.2.1 Sample collection of Industrial Blast Furnace Slag

40-50 Kg blast furnace slag is picked up from different steel plants. Approximately 5 Kg representative samples are made by coning and quartering. The samples are characterized with respect to chemical constituents.

2.2.2 Chemical Composition of Industrial Blast Furnace Slag

Chemical analysis of the slag samples collected from Industrial Blast Furnace as per the procedure mentioned in Para **2.8** is done and results are presented in **Table 2.1** below. While CaO, SiO_2, Al_2O_3 and MgO are determined chemically for all the slag, minor constituents like Na_2O, K_2O, TiO_2, MnO are determined only for selected slag samples.

Table 2.1 Chemical Analysis of Industrial Blast Furnace slag.

SL. NO	Al_2O_3	CaO	MgO	SiO_2	Na_2O	K_2O	Fe_2O_3	CaO/ SiO_2	TiO_2	MnO
1	16.95	36.06	9.09	36.58	0.07	0.10	0.24	0.99	0.22	
2	16.76	36.95	7.66	36.49	0.01	0.19	1.38	1.0	0.1	
3	17.66	38.93	7.52	32.6	0.05	0.09	0.47	1.19	0.3	
4	20.57	37.55	8.82	26.77	0.08	0.14	1.97	1.40	0.25	
5	13.8	35.11	9.57	36.5	-	-	2.52	0.96	0.8	
6	21.97	34.12	8.87	32	-	-	1.08	1.07	0.8	
7	19.0	34.04	10.09	32.05			1.02	1.06	0.7	
8	20.89	43.25	11.01	30.84			0.44	1.40	0.7	
9	18.77	35.10	10.4	32.24			0.92	1.088	0.76	
10	19.0	33.4	10.4	31.3			3.7	1.067	0.7	
11	20.28	32.55	10.4	31.58			0.74	1.03	0.76	
12	20.05	33.61	10.09	32.05			0.62	1.04	0.82	
13	18.54	30.85	9.79	30.85			11.68	1	0.82	
14	16.92	38	10.23	31.86	0.98	0.48	0.66	1.19	0.7	0.05
15	16.31	36.84	10.56	33.25	1.1	0.52	0.54	1.1	0.82	0.055
16	17	35.78	11.88	32.48	1.1	0.52	0.6	1.1	0.55	0.051
17	17.04	36.96	11.22	31.08	1.8	0.88	0.40	1.18	0.5	0.053
18	16.58	36.2	9.57	34.32	1.36	0.82	0.53	1.05	0.55	0.055
19	17.45	35.03	11.11	31.8	2.54	0.92	0.6	1.1	0.5	0.055
20	17.32	37.7	10.89	30.77	2	0.52	0.45	1.2	0.2	0.072
21	17.56	34.97	11.75	31.90	2.12	0.82	0.53	1.096	0.175	0.084
22	20.58	33.7	9.58	30.92				1.09		
23	16.73	38.80	9.74	30.87			1.4	1.256	0.4	
24	17.9	36.2	7.05	34.6				1.046		
25	19.04	34.57	6.51	36.72				0.941		
26	18.07	34.15	6.5	34.06				1.003		

It is found that CaO/SiO_2 ratio varied within a range of 0.94 to 1.4 with an average of 1.102. This Avg change to 1.09 if two extreme values of 0.94 and 1.4 are ignored. Al_2O_3 has an Avg value of 18.44% after ignoring two of the lower extremity values. MgO (Avg 9.62%) and TiO_2 (Avg 0.55%) are the other constituents of the slag. . This

forms the basis for making synthetic slag for the study of characteristic temperature and viscosity.

2.2.3 Phase Analysis of Industrial Blast Furnace Slag

Phase analysis of Industrial blast furnace granulated slags reveal glassy phase. X-ray diffractogram of slag no 12 which contains 20% Alumina with C/S ratio 1.04 is given in **Fig No.2.2.3A**. The melted slag of slag no 12 is quenched slowly to crystallize the slag. X-ray diffractogram of crystallized slag is given in **Fig no 2.2.3B**.The only crystalline phase found is mellilite.

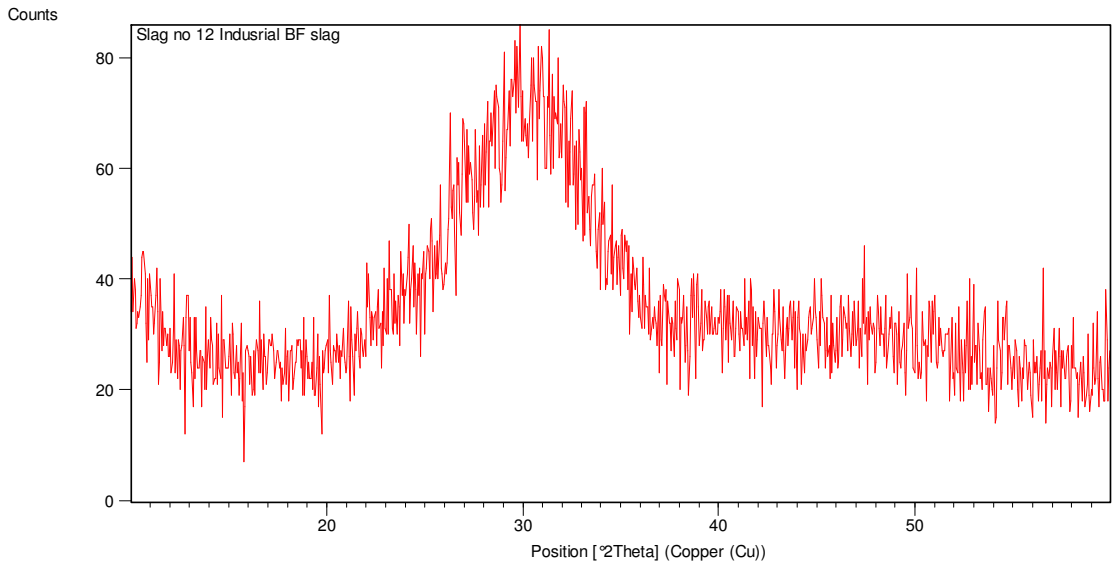

Figure 2.2.3A: XRD of Industrial slag no 12 (Granulated)

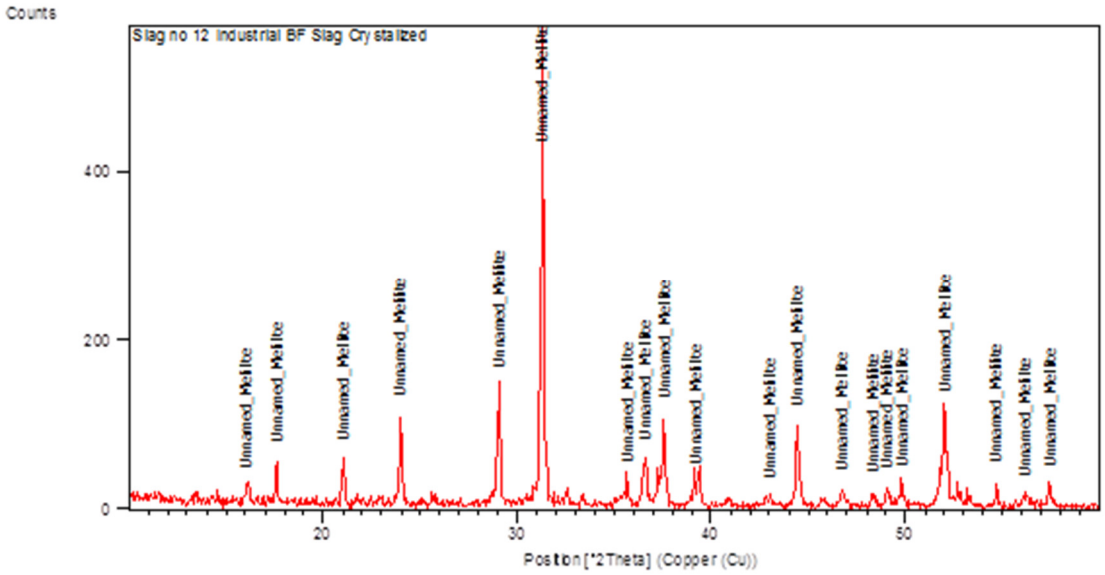

Figure 2.2.3B-: XRD of Industrial slag no 12 (crystallized)

2.3 Characterization of Synthetic Slag

Synthetic slag samples are prepared after critically examining the industrial blast furnace slag with respect to chemical constituents. Analytical grade oxides are used for preparing the synthetic slag within the range of compositions as obtained from the chemical characterization of industrial blast furnace slag. The detailed composition of synthetic slag samples is presented in the respective chapters. However the group detail is given here.

2.3.1 Chemical composition of prepared synthetic slag

Preparation of synthetic slag is done for two purposes.

a. For flow characteristic measurement to develop a relationship with composition. First set of 8 slag is prepared and their characteristic temperatures are measured. By using the factorial design techniques, equations are developed. The 2nd set of the compositions are made and their characteristic temperatures are measured to validate the formula developed by use of the first set of 8 slag.

b. For measurement of viscosity and calculation of activation energy for different composition

Thus the total slag preparation is in 6 groups as detailed below.

Group-1

This is a single slag which formed the base for statistical analysis (**Table 3.1**)

Group-2

This group of slag is designed to measure the flow characteristics with composition having two ranges of C/S ratio, TiO2 and MgO, keeping other constituents constant. (**Table 3.2**)

Group-3

This group of slag is prepared to validate the statistical calculation obtained by factorial design. (**Table 3.3**)

Group-4

In this group of 5 nos. of slag are prepared where, CaO/SiO_2 ratio (C/S) is varied from 0.9 to 1.1 with steps of 0.05 for measurement of viscosity (**Table 4.1**)

Group-5

In this group of 5 nos. of slag are prepared where MgO content is varied from 4% to 12% in steps of 2% for measurement of viscosity. (**Table 4.6**)

Group-6

In this group 5 nos. of slag is prepared where TiO_2 content is varied from 0.2% to 1.0% in steps of 0.2% for measurement of viscosity (**Table 4.8**)

Group-7

In this group of 5 nos. of slag samples are prepared to assess the effect of simultaneous variation of C/S ratio and MgO content on the slag viscosity. The slag composition is so chosen that the slag with least MgO content has the highest C/S ratio within the specified range of variations. (**Table 4.12**).

The purity of different analytical grade oxides used in preparing the synthetic slag in the laboratory, is presented in **(Table No 2.2).** FeO is prepared in the laboratory according to the following equation;

$$Fe_2O_3 + C = 2FeO + CO$$

Stoichiometric amount of Fe_2O_3 and Carbon are mixed thoroughly and heated at 900°C for about 6 hours. The process is repeated till it is confirmed that no magnetic material is left. Complete conversion to Wustite is also confirmed by XRD. The FeO so generated, is immediately used for synthetic slag preparation.

Table 2.2

Minimum percentage of constituent in the oxide used for preparing Synthetic slag (Purity %)

Sl. No.	Oxide	Purity %
1	Al_2O_3	99.90
2	$CaCO_3$	98.50
3	MgO	98.53
4	SiO_2	99.50%
5	Na_2CO_3	99.50%
6	FeO	99.00%

2.3.2 Preparation of synthetic slag samples for characterization and Viscosity measurement

The oxides are weighed in the proportion designed for each composition. These are put in a glass bottle and shaken well for a few minutes with the lid of the bottle tightly secured in place and then transferred to a stainless tray for calcinations at 900ºC for four hours. After calcinations, for the purpose of homogeneity the samples are mixed in a planetary ball mill. The mill contains one 250 ml volume Zirconia bowl and mixing is gone by the 10 mm Zirconia ball. The sample is mixed for 24 hours.

Half hour break after every one hour run is used to release the material stuck at the side wall as well as cooling off of the motor.

The ground sample is used for making the molten slag – quenched – ground finally for experimental. This process adopted is as under:

The ground sample is transferred to a platinum crucible which is put in a raising hearth furnace at 1550°C in air atmospheric and held for 2 hours in which period it becomes a melt. This melt is quenched in the water and solidifying glassy mass. This mass is dried in oven at 110°C for 24 hours, crushed and mixed in an agate motor. The crushed material is ground in the planetary ball mill for 6 hours total in the process of one hour run and half an hour stop as above. The ground samples are re-melted in the process explained above, however the holding time is increased to 4 hours with intermittent stirring by Platnum-Rhodium (Pt-Rh) rod for homogenization.

The molten samples are quenched dried and again ground in the planetary ball mill for 2 hours actual grinding as per the previous process and the ground samples are transferred to glass bottles for experimentation.

2.4. Experiments conducted

For the characterization of the slag samples, following experiments are conducted

a) Measurement of flow characteristic

b) Measurement of viscosity & activation energy,

c) Chemical analysis.

d) XRD and Phase analysis

The details of the processes and equipment used are discussed herein. Activation Energy is calculated from the viscosity data.

2.5 Measurement of Flow Characteristic of slag

2.5.1 Definition of flow

The flow characteristics of slag are presented in the form of four characteristic temperatures. These are (a) Initial deformation temperature (IDT), (b) Softening temperature (ST) (c) Hemispherical temperature (HT) (d) Flow temperature (FT). The definitions given below are as per German Industrial Standards 51730. [55]

a. Initial Deformation Temperature (IDT): Initial deformation temperature is the temperature at which the first rounding up of the edges of the cube-shaped sample specimen takes place. In fact, this is the temperature at which the first sign of the change in shape appears. Rheologically, this temperature symbolizes the surface stickiness of the slag.

b. Softening Temperature (ST): It is the temperature at which the outline of the shape of the sample starts changing and is reported as the temperature at which the sample shrinks by one division or the temperature at which the distortion of the sample starts. Rheologically this temperature symbolizes the start of plastic distortion.

c. Hemispherical Temperature (HT): It is the temperature at which the sample has fused down to hemispherical shape and is measured as the temperature at which the height of the sample is equal to the half of its base length. This is defined as the fusion point or the melting point. Rheologically this temperature symbolizes the sluggish flow of the slag.

d. Flow Temperature (FT): It is the temperature at which the sample liquefies and is reported as the temperature at which the height of the sample is equal to one-third of the height that it had at HT. The typical shapes of the samples at the respective temperatures are presented below.

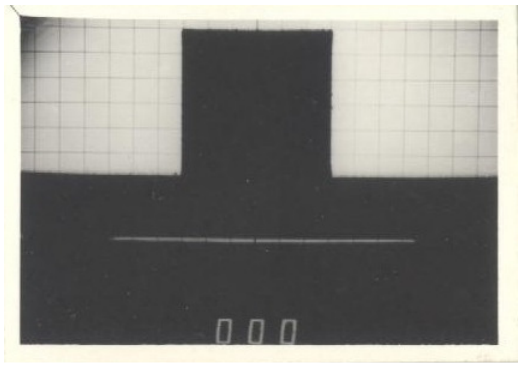

(a)

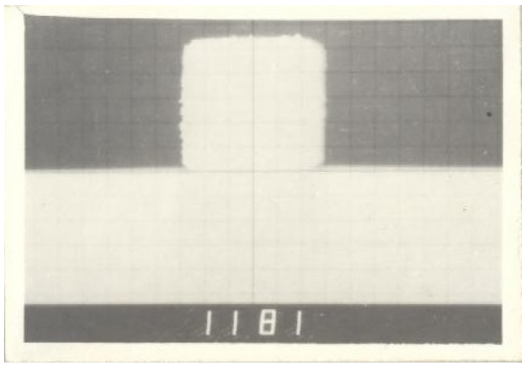

(b)

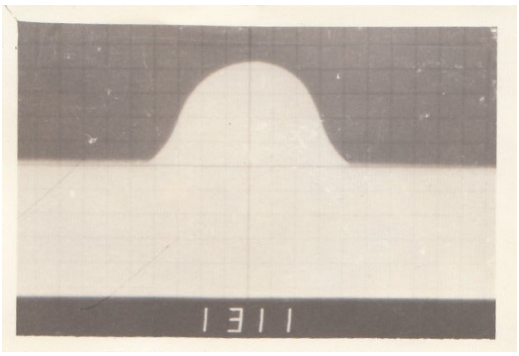

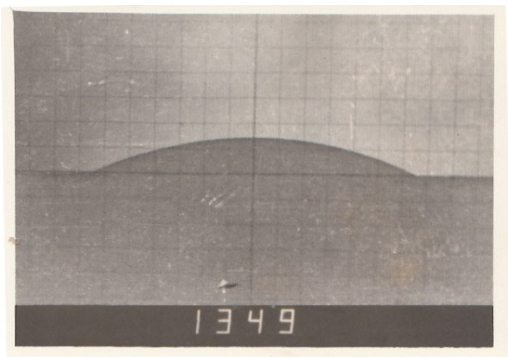

(c) (d)

Figure 2.1
Photographs illustrating the characteristic temperatures of a slag owing to its shape change on deformation as a consequence of heating: (a) Original shape of the sample, (b) ST, the Softening Temperature in ^{o}C, (c) HT, the Hemispherical Temperature in ^{o}C and (d) FT, the Flow temperature in ^{o}C.

2.5.2 Heating Microscope

Heating microscope has been successfully used [8] for determining the softening /fusion behavior of the slag. The melting point as defined by the hemispherical point is also determined by this microscope.

In this experiment the microscope used is of Leitz make and is shown in **Photograph no 1** in **Annexure 4** It also contains a furnace, which can be heated up to 1750deg C and has a Leica camera as an attachment. The heating microscope consists of 1. Light source, 2. Electric furnace having a specimen carriage and 3. Observation and photo camera. A line diagram (**Figure 2.2**) of the same is provided below to show all the detailed components of the instrument.

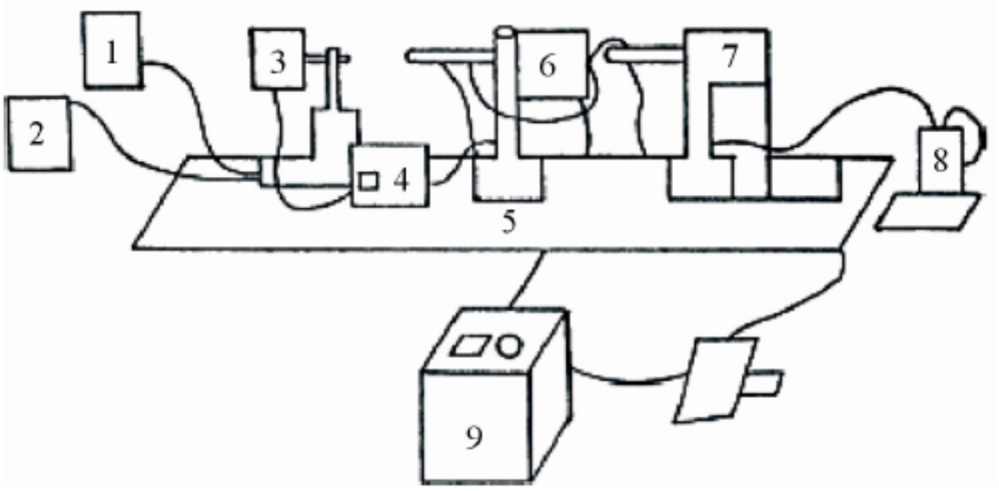

Figure 2.2
Line diagram of hot stage microscope.
1. Cooling water tank; 2. Cooling water re-circulating tank; 3. Light source; 4. Regulating transformer for light source; 5. Optical bench; 6. High temperature electrical furnace with specimen carriage; 7. Observation and photo microscope; 8. Digital thermometer; 9. Regulating transformer for high temperature electrical furnace.

2.5.2.1 Construction of heating Microscope

The microscope has the following components-

a. Optical bench-a prismatic bar of about 1400mm length holds the main elements which can be adjusted in any position with respect to others, as per the need.
b. Light source- A 12 V, 100 W filament lamp is connected to 110/240 V, 50-60 c/s mains. A transformer regulates the voltage. Full and uniform illumination is obtained by adjusting the spherical condenser along with the optical axis of the instrument.

2.5.2.2 Electric Furnace with specimen carriage

The heating element is of 19 mm ID Rhodium wound, so as to raise the temperature up to 1750° C. Alumina boat of 99.5% crystallized Al2O3 holds the specimen and is inserted in the furnace with sample holder also carrying the thermocouple of Pt-6Rh /Pt-13Rh.The front and rear apertures are closed by interchangeable quartz discs to eliminate air currents and turbulence. A transformer (O-42A, 35A) is connected to the furnace and mains.

2.5.2.3 Observation and photo microscope

Observations are made through three built in eye pieces on a revolving turret with a graticule division, which correspond to that of 0.5 mm in the object place. The temperature and the photographic/video display is made visible by a reflection device at the back of the microscope housing. Leica camera is connected through a tube to mirror reflex housing, situated behind the microscope tube. The magnification of the microscope is 5:1 and thus 4X magnifier gives a total magnification of 20X.

2.5.2.4 Sample preparation for experiments for Flow Characteristic

For characteristic temperature measurement in the hot stage microscope, ground slag is pressed by a die-assembly in a hand press (presented in Photograph**-6 in Annexure-4**) and specimen of 3 mm size cube is prepared.

The sample cube as prepared is placed on platinum substrate and put in the furnace chamber. Heating rate is controlled by potentiometer. The temperature is recorded using Pt Rh 10 thermocouple

2.5.2.5 Measurement and photography of specimen during experiment

The 3 mm cube specimen is kept in the object carrier. Thermocouple is adjusted properly so that it reads the temperature of the sample. The sample holder and the carrier assembly are inserted in the furnace. The furnace chamber is sealed from the outside. The microscope is adjusted to focus the sample in zero position on the grid. The external light source is used to adjust the positioning of the sample.

After ensuring continuous water supply in the furnace, the temperature is raised up to 1000ºC @ 10ºC per minute maximum. Once the temperature reaches to 1000ºC the rate of heating is maintained between 4 to 6ºC per minute. The sample is viewed through the microscope and fusion behavior is recorded separately represented by the ITD, ST, HT & FT. Two sets of reading are obtained for each sample. If the reading varies by more than 5ºC, the readings are cancelled and fresh samples are prepared and subjected to investigation. If not, the average of two readings is reported.

2.6. Viscometer used in the present investigation

The viscosity of the blast furnace slag, in the present investigation, is measured at different temperatures in High temperature Viscometer. Model VIS 403 HF of Bahr. This model is a rotating Viscometer where dynamic viscosity is calculated by measurement of torque of a rotor immersed in molten liquid.

Calibration of the Viscometer is done by reference glass sample of known viscosity. The measurement of viscosity is possible when the liquid shows Newtonian behavior. A general principle is to first heat the sample until it melts and reaches to an approximate viscosity of 100 dPas. The rotor is then immersed into liquid. The temperature is lowered linearly and the torque is measured simultaneously.

Once the maximum torque is reached the test stops automatically. Rotor is removed after resetting the temperature programme for removal of rotor approximately at 200ºC higher than the temperature at which test stops.

The sample temperature measurement is done at the base of the platinum crucible. It is possible to measure viscosity between 10^{1} dPas and $10^{4.5}$ dPas. The actual procedure is explained here- in-after.

. The technical specification of the Viscometer-as supplied by the manufacturer is given in **Annexure-1** and the photograph is given in **Annexture-4, Photograph -2**

2.6.1 Test Procedure for measurement of viscosity.

Ground slag samples of approximately 130-150 grams are used in each experiment for measurement of viscosity. The utmost precaution is taken to ensure the homogeneity while preparing the samples by coning and quartering method.

2.6.1.1 Calibration of the Viscometer

The Viscometer is calibrated by using standard glass granules supplied with the m/c with known viscosity at specified temperature in dPaS (Deci Pascal second) units.

The viscosity of the standard sample is measured in the m/c using the usual procedure at different temperatures, within the range of temperature in which viscosity of the slag samples is to be measured. Now these measured values are compared with given standard values supplied with the instrument at 1°C interval. From the difference between the measured and standard viscosity values of the standard sample a correction factor is arrived at, using the software provided with the m/c which automatically records the corrected measured values applying the correction factor so incorporated.
The initial correction factor is found to be 5.5. This correction factor is checked time to time and incorporated into the m/c by running the m/c with standard sample as stated above.

Initially, before starting the experiments at 40:40:20 slag having 40% CaO; 40% SiO_2 and 20% Al_2O_3 respectively, is synthetically prepared in the laboratory. This is a standard slag with standard viscosity values, available in the literature [71] and is selected to check the calibration of the m/c. The viscosity of the slag is measured adopting the procedure described above. The viscosity values are compared. The data are provided in **Table 2.3** and the deviation is seen to be max 5.0%. It establishes the

calibration of the Viscometer and also provides the check on the correctness of the procedure adopted for measurement.

Table 2.3
Comparison between measured viscosities V/s mentioned in literature

Slag No.	Temperature K	Viscosity (Poise) (Measured)	Viscosity (Poise) (From literature)	% difference
1	1678	21.96	22.53	2.6
2	1718	14.50	15.19	4.2
3	1758	9.79	10.28	5.0

2.6.1.2 The stepwise procedure adopted for the measurement of viscosity

The stepwise procedure adopted to measure viscosity is presented below:

(i) The electrical connections as well as the cooling water connections are checked and the cooling water through the chiller is made to pass through the m/c and the induction-heating-coil. The m/c would not start if the circulation of cooling water through the chiller is not established.

(ii) The heating cycle, i.e. the maximum temperature up to which the slag melt has to be heated – the residence time at the highest temperature and the heating rate are all set using the software WIN TA 10 provided with the m/c. The heating rate could be 0.5°C/min, 10°C/min or 20°C/min. It is possible to set this rate manually or by programming.

In our case the max temperature is set at 1600°C. The heating rate is set at 20°C/min manually. The residence time at 1600°C is selected to be ½ hr for ensuring uniform heating of the entire mass of the slag sample.

(iii) The cooling rate has to be programmed. It can be 3°C/min, 5°C/min or 10°C/min. In our case a cooling rate at 5°C/min throughout the cooling cycle is selected.

(iv) The platinum crucible is filled with the powdered slag sample and melted in the Electric Raising Hearth furnace. The level of slag in the crucible is checked and if required additional slag powder is added and the same is melted till the liquid slag reached the required height in the crucible. The crucible is cooled to room temperature by quenching to ensure glassy phase of the slag.

(v) The crucible with the melted and cooled slag sample is put in place in the Viscometer for viscosity measurement.

(vi) Now the machine is switched on. The rotor is kept at the highest position in the static state.

(vii) Once the highest set temperature (1600°C in our case) is reached, the rotor is inserted in the melt gradually into a pre-determined level such that its front end rests at a height of about ½ cm from the bottom of the crucible.

(viii) The speed of rotation of the rotor can be programmed. Initially, a speed of 100 RPM to bring about stirring of the liquid-slag-melt to ensure homogenization of heat and composition, is selected. The speed is then fixed at 50 RPM throughout the entire period of measurement.

As soon as the target condition, as programmed earlier, is achieved data recording is started by the m/c. Both the torque and the viscosity vs. temperature are recorded graphically. For our purpose, we recorded the viscosity readings at the specific temperatures. The viscosity data are obtained in Deci-Pascal-Second.

After calibration run as per above process, the measurement of viscosity of the test samples is done. Reuse of the platinum crucible needs its cleaning. For the cleaning purpose, the crucible is heated in the electric raising-hearth-furnace in the inverted position. Most of liquid slag on its melting drains out of the crucible in this position and collected in another platinum crucible. The smallest amount of slag sticking to the walls of the measuring crucible is removed by boiling it in hydrofluoric acid.

2.7 Calculation of Activation Energy

The activation energy of viscous flow is calculated from the viscosity versus temperature curve using the Arrhenius equation. Values of logμ versus 1/T graph is plotted where μ is the viscosity in Pascal second and T is the corresponding temperature in K. The slope of the plot is calculated to determine the activation energy of the viscous flow.

2.8 Chemical Analysis Method of slag samples

The chemical analysis of industrial blast furnace slag and synthetic slag are determined by following standard method. Before analysis all the samples are dried in an oven at 110°C for 24 hrs. The loss on ignition is determined by igniting 1 gm of sample in a dry platinum crucible at a temperature of 1000°C till the constant weight is obtained. SiO_2 is determined by potassium silico-fluoride method [76]. Al_2O_3 is determined by EDTA method [77] TiO_2 is determined by colorimetric method using hydrogen peroxide [78]. Na_2O and K_2O are determined by flame photometer [79]. The Fe2O3 are determined by colorimetric method using orthophenanthrolin as a color developing agent [80]. CaO content is determined by precipitating as calcium oxalate and titrating with standard KM_nO_4 solution [81]. The MgO percentage is determined by gravimetric method by precipitating with hydrogen phosphate and igniting in a porcelain crucible at about 1000°C. From the weight of $Mg_2P_2O_7$ percentage of MgO is calculated [81].

2.9 Other Equipment used in sample preparation and investigation

2.9.1 Mixing Equipment

For the purpose of homogenized mixing of various oxide constituents a laboratory –planetary mill has been used. (**Photograph 3** in **Annexure 4**)

The mill consists of a drive arrangement to rotate the bowls of Zirconia. The bowl is about 250 ml capacity. The grinding balls are also of Zirconia and are about 10 mm diameter.

While starting the operation the grinding media are put in the bowl and then the constituents for mixing/homogenization are poured. The mixing and homogenization is done by centrifugal force generated due to rotation of the bowl, rotating on their own axis and the plate on which these are properly secured. It is therefore important that the sufficient gap is left in the bowl for allowing centrifugal force to generate. In practice only 66% volume of the bowls is utilized for materials and grinding media.

Mill runs for 1 hour for homogenization and 10 nos. of grinding media are used for this purpose. After every two hour run, the machine is switched off for 30 minutes.

2.9.2 Melting Furnace

Melting of blast furnace slag and preparation of synthetic slag is done in a rising hearth furnace. (**Photograph 4** in **Annexure 4**)

This furnace is heated by super Kanthal Supar heating elements .The maximum temperature, which can be raised is 1700ºC.

The furnace is connected to mains supply through a transformer specially designed for this. The temperature is controlled by a microprocessor designed to control all the heating elements.

The temperature is measured by Pt-6 Rh/ Pt-30 Rh thermocouple and is controlled within ±3ºC in the range of 1200ºC - 1700ºC.

2.9.3 Hand Press

The samples for flow characteristic are prepared in a hand press by 4 interchangeable plungers housed in the handle of the press. Specimen size is 2x2x2 mm or 3x3x3mm cube as well as 2mm/3mm dia cylinders. For this experiment specimen are made in a die/plunger of 3x3x3 mm cube**.(Photograph 5** in **Annexure 4**)

2.10 Summary

Slag Samples are prepared with analytical grade materials by adopting a standard procedure mentioned herein. The sample preparation of slag fused and ground is done as per the requirement of the equipments used for the purpose of measurement of Flow Characteristic, viscosity and chemical analysis. The Viscometer is calibrated with standard samples and variance is found to be within limits mentioned in literature.

CHAPTER 3

FLOW CHARACTERISTIC OF BLAST FURNACE SLAG

3.1 Importance of flow characteristic

The flow characteristics of the Blast Furnace (BF) slag constitutes an important tool for assessing the behavior of the BF burden during its descent in the furnace. More importantly, it decides the location and extent of the cohesive zone, which should form lower down the furnace and should be a narrow one for a smooth and efficient operation. The flow characteristic of a slag is presented in terms of four specific characteristic temperatures, which have rheological importance relating to the deformation and flow of the slag. In German standard 51730, these four specific characteristic temperatures are presented as IDT: the initial deformation temperature, ST: the softening temperature, HT: the hemispherical temperature, which is also considered to be the liquidus temperature and FT: the flow temperature. These characteristic temperatures are measured by noting the specific shape changes undergone by the slag samples as a consequence of the deformation caused on heating the same. These shape changes are specific to the sample at a specific temperature as observed continuously during heating in a heating microscope. **(Para 2.5.2)** Though, initially the provisions in the German standard 51730 were used to measure the ash fusion behavior of coal samples, these have also been used successfully by many workers [23,87,88] to explain the characteristic behavior of slag generated in a smelting unit. It may be of interest to note that the flow characteristic of a slag may offer some indications about the viscosity of the slag (high/low) but the characteristic temperatures and viscosity of the slag are not interrelated. Viscosity, which is a measure of the resistance offered to the flow between two adjacent layers of a fluid, is a function of temperature and obeys the Arrhenius equation. This is not true for the characteristic temperatures, which are specific temperatures indicating rheological status of the slag. However, both viscosity and flow characteristics are structure dependent. Viscosity values, so also the characteristic temperatures vary as a consequence of polymerization/depolymerisation as well as loosening/tightening of the ionic bonds between the cat -ions and the anions. Hopkins [89] has established this statement with the example of an eutectic with 23.25% CaO, 14.75% Al_2O_3 and 62% SiO_2. This eutectic has a HT (liquidus temperature) of 1170^oC though it is extremely viscous even

at 1600°C with superheat pertaining to more than 400°C rise of temperature. On this basis viscosity and characteristic temperature may be considered to be related qualitatively, but it is difficult to predict an interrelation quantitatively.

The BF process is a counter-current process. The efficiency of the process depends on the permeability of the burden that controls the flow of the up-coming gases, which greatly influence the slag-metal reactions/exchanges and heat transfer in the furnace etc. [90]. In light of the above, it is only pertinent that the permeability of the bed in the blast furnace under the prevailing conditions of temperature and pressure must be conducive to accelerated rates of slag-metal reactions and heat/mass transfer. Therefore, then softened and subsequently melted slag as influenced by its chemical composition must acquire adequate flow ability as soon as it melts and the difference between its melting and flow temperatures should be as low as possible. Such a slag with a small difference between HT and FT is known as short slag and without the requirement of higher additional heat input, soon after it's melting, it trickles down the furnace, leaving behind paths for upward movement of the ascending gases resulting in an efficient heat transfer from the hot gases to the burden material. Also the trickling slag meets with freshly-exposed, partly-reacted burden surfaces along which it trickles down, accelerating the possibilities of enhanced chemical reactions between the two. Thus, the flow characteristics of the blast furnace slag constitute an important parameter for the evaluation of the blast furnace process of iron making. This is true for the high alumina Indian BF slag where the amphoteric alumina (Al_2O_3) exhibits a big-brotherly attitude for deciding the characteristic properties of the slag.

Besides Al_2O_3, the components like CaO, MgO, SiO_2 etc. form the major constituents of the BF slag, that control the characteristic properties of the slag [1, 7, 23, 33, 91-96]. Both CaO and MgO provide metal cations to the slag melt, which are randomly distributed throughout the lattice of the silicate network introducing weak points to the network. The presence of these cations weakens the Si-O bonds in general, causing a general weakening effect in the lattice which renders the slag more fluid [87, 89]. Therefore, the general effect of the presence of these alkali metal oxides in the slag is to bring down its flow temperature. The presence of CaO in the slag renders it sufficiently basic to react with and retain sulfur. However, an increase in the basicity

beyond certain levels in the presence of the strongly basic CaO in the slag may intervene with the free flowing nature of the increase in the chemical potential of some primary solid phases that may precipitate out. Therefore, it may be advisable to replace some CaO by MgO, an alkali metal oxide, such that the optimum basicity is maintained and the enhanced degree of weakening of the network, caused by the basic constituents, responsible for making the slag more fluid, is not affected [1, 95].

It is also important to consider a factor, NBO/T, the non-bridging oxygen per tetragonally bonded oxygen, which is a measure of the degree of depolymerisation responsible for modifying the slag structure, thus influencing its free flowing nature. It is reported that [7, 33] besides other oxides, TiO_2 contributes considerably towards NBO/T. In the present investigation, therefore, besides CaO/SiO_2 (C/S) ratio and MgO content, TiO_2 contents are also considered as a significant variable while preparing the high alumina synthetic slag in the laboratory to estimate the effect of their simultaneous variations on its flow characteristics. Al_2O_3 is kept constant at 20 wt. % for all the slag investigated while C/S ratio, MgO and TiO_2 contents are suitably varied in line with the chemical compositions of BF slag as encountered in the related industry.

Regression equations have also been developed using a factorial design technique to predict the combined effect of the significant variables on the flow characteristics of the slag. An extensive study on the prediction of characteristic temperatures of Alumino-thermic ferrochrome slag by factorial design technique is reported in our publication [87]. The equations developed, using the factorial design technique, are validated in the laboratory with further ten numbers of synthetically prepared BF slag. A careful analysis of the results establishes the interdependence of all the three significant variables, namely C/S ratio, MgO and TiO_2 contents, in deciding the flow characteristics of the BF slag, with a major impact on the process of iron making in the BF route. The equations developed may be used for the prediction of characteristic temperatures of BF slag in the range of composition investigated in the present study.

3.2 Experimental Work

3.2.1 Chemical Composition of the Synthetic Slag*:*

Synthetic BF slag was prepared by using analytical grade oxides available in the commercial market. The purity of such oxides is presented in T**able 2.2**. As mentioned earlier three significant variables, namely the CaO/SiO2 ratio (R), MgO content (M) and TiO_2 content (T) is considered in the regression analysis. The amount of other oxides like Al_2O_3, Na_2O, K_2O, Fe_2O_3 and MnO are kept constant in all the slag at 20 wt.%, 1.1 wt.%, 0.5 wt.%, 1.0 wt.% and 0.1 wt.% respectively. The base levels for the three significant variables are set at 1.15, 9.0 wt. % and 0.55 wt. %, respectively. **Table 3.1** shows the chemical composition (in wt. %) of the base slag. The chemical composition (in wt. %) of slag for factorial design calculation are presented in **Table 3.2**. **Table 3.3** represents the composition of the ten numbers of slag exclusively prepared within the prescribed ranges of the variation of significant variables for validation of the developed equations.

Table 3.1
Chemical composition (in wt. %) of base slag used for statistical calculation.

Al_2O_3	CaO	MnO	Na_2O	K_2O	Fe_2O_3	SiO_2	MgO (M)	TiO_2 (T)	CaO/SiO_2 (R)
20.0	36.29	0.1	1.1	0.5	1.0	31.56	9.0	0.55	1.15

Table 3.2
Chemical composition (in wt. %) of slag used for statistical calculation.

Sl. No.	Al_2O_3	CaO	MnO	Na_2O	K_2O	Fe_2O_3	SiO_2	MgO (M))	TiO_2 (T)	CaO/SiO_2 (R)
1	20.0	37.57	0.1	1.1	0.5	1.0	26.83	12.0	1.0	1.4
2	20.0	41.59	0.1	1.1	0.5	1.0	29.71	6.0	0.1	1.4
3	20.0	30.93	0.1	1.1	0.5	1.0	34.37	12.0	0.1	0.9
4	20.0	33.35	0.1	1.1	0.5	1.0	37.05	6.0	1.0	0.9
5	20.0	41.07	0.1	1.1	0.5	1.0	29.33	6.0	1.0	1.4
6	20.0	30.50	0.1	1.1	0.5	1.0	33.89	12.0	1.0	0.9
7	20.0	33.77	0.1	1.1	0.5	1.0	37.53	6.0	0.1	0.9
8	20.0	38.09	0.1	1.1	0.5	1.0	27.21	12.0	0.1	1.4

Table 3.3
Chemical composition (in wt. %) of slag used for testing accuracy statistical calculation.

Sl. No.	Al_2O_3	CaO	MnO	Na_2O	K_2O	Fe_2O_3	SiO_2	MgO (M)	TiO_2 (T)	CaO/SiO_2 (R)
1	20.0	34.44	0.1	1.1	0.5	1.0	36.25	6.5	0.20	0.95
2	20.0	35.05	0.1	1.1	0.5	1.0	35.05	7.0	0.30	1.00
3	20.0	35.09	0.1	1.1	0.5	1.0	34.40	7.5	0.40	1.02
4	20.0	35.29	0.1	1.1	0.5	1.0	33.60	8.0	0.50	1.05
5	20.0	35.46	0.1	1.1	0.5	1.0	32.83	8.5	0.60	1.08
6	20.0	35.22	0.1	1.1	0.5	1.0	32.02	9.5	0.65	1.10
7	20.0	35.38	0.1	1.1	0.5	1.0	31.31	10.0	0.70	1.13
8	20.0	36.41	0.1	1.1	0.5	1.0	29.13	11.0	0.85	1.25
9	20.0	36.73	0.1	1.1	0.5	1.0	28.26	11.5	0.90	1.30
10	20.0	37.16	0.1	1.1	0.5	1.0	27.53	11.75	0.95	1.35

3.2.2 Preparation of Synthetic Slag:

Oxides of given purity **(Table 2.2)** are weighed in given proportions, mixed, melted, quenched in water, ground, re-melted, quenched and ground again by using the digital analytical balance, planetary ball mill with Zirconia balls and the raising hearth electric furnace respectively to obtain the synthetic slag as discussed in **Chapter 3** in Experimental. The detailed process is also mentioned therein. These glassy synthetic slag samples are used for experimentation.

3.2.2.1 Phase analysis by XRD

In the present investigation all the synthetic slags prepared in the laboratory are in granulated state. Out of these slags, 8 slags have been selected for phase analysis on the basis of CaO/SiO2 ratio & MgO content. (Slag no 1-5 & 8-10). X-ray diffractogram of these granulated synthetic slags **(Table No 3.3)** are given and in Figure No. **3.1 & 3.2**. The diffractogram shows that all the above slags do not contain any crystalline phase and are in glassy form.

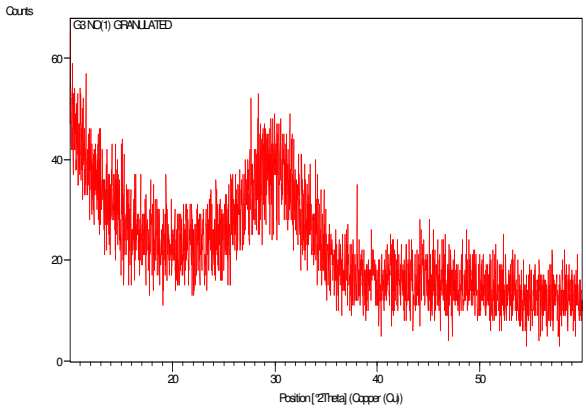

Slag No.1: Granulated

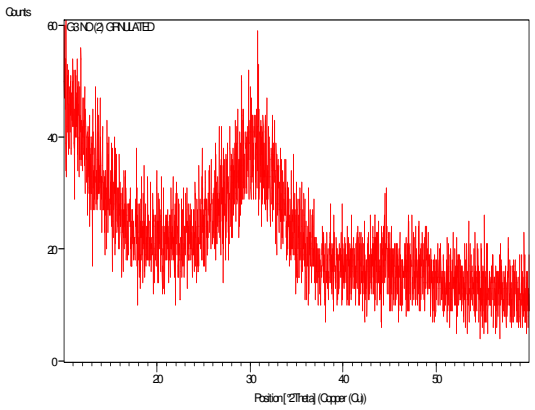

Slag No.2: Granulated

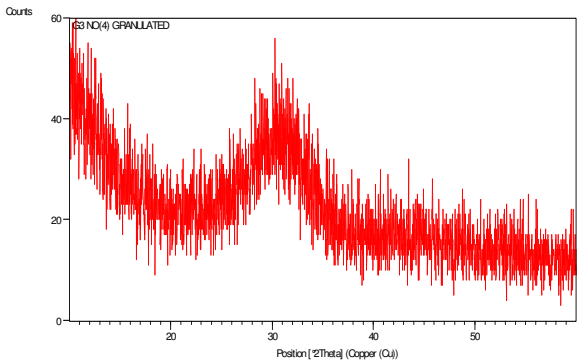

Slag No.3: Granulated

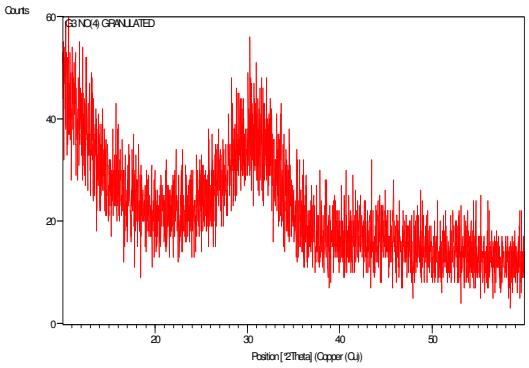

Slag No.4: Granulated

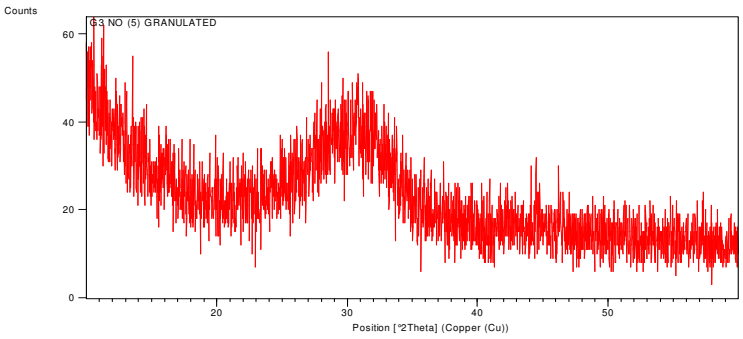

Slag No.5: Granulated

Figure 3.1: XRD of slag no 1-5(Granulated)

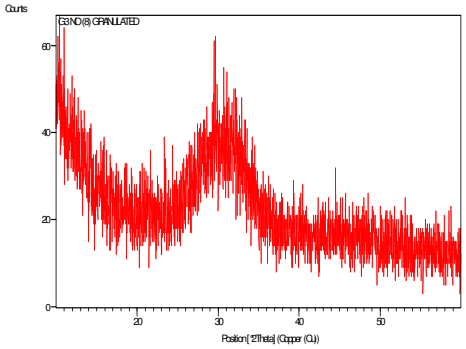

Slag No8: Granulated

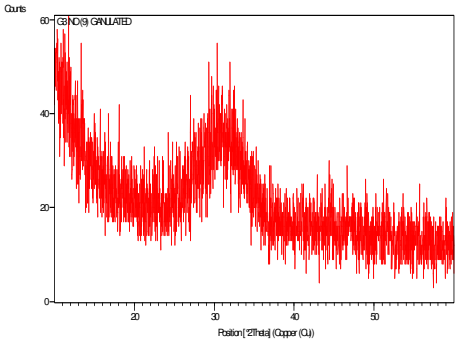

Slag No 9: Granulated

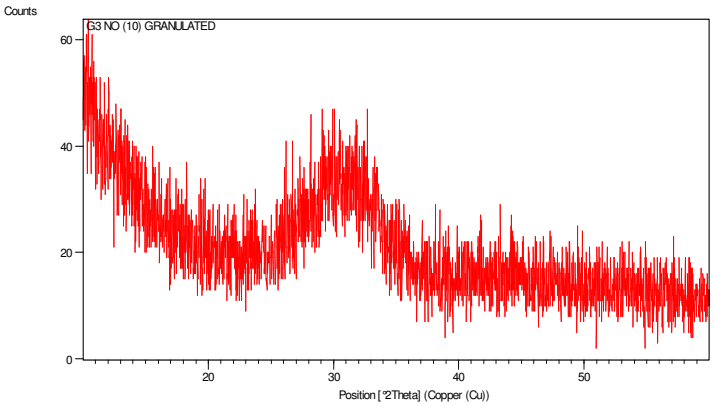

Slag No 10: Granulated

Fig 3.2 XRD of slag no 8-10(Granulated)

In order to verify the crystalline phases, these synthetic slags (**Table 3.3)** are quenched slowly @ 5˚C/min from 1400˚C to 200˚C (soaking at 1400˚C/1 hour). From 200˚C to room temperature samples cooled overnight in the furnace. X-Ray diffractogram of these crystalline slags are given in **Figure No 3.3 & 3.4**.

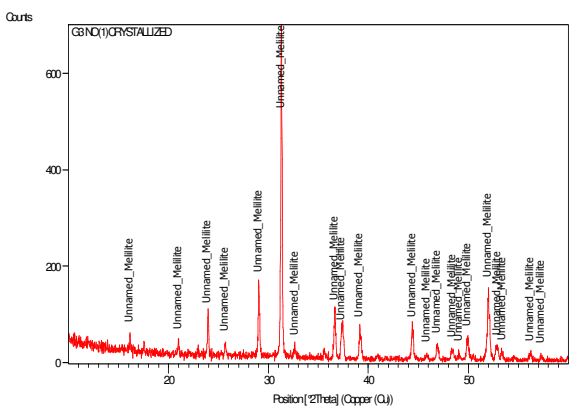

Slag No.1: Crystallized

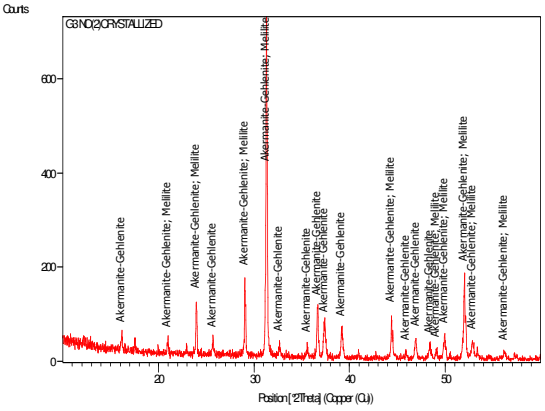

Slag No.2: Crystallized

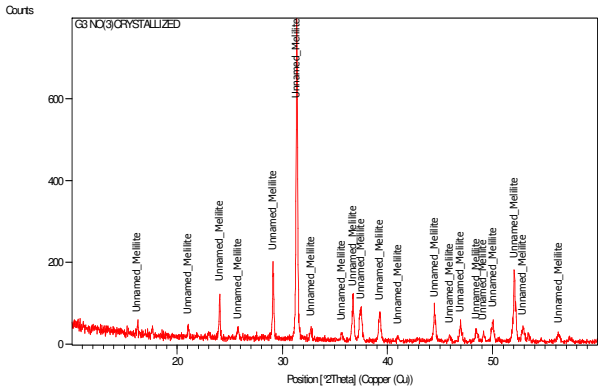

Slag No.3: Crystallized

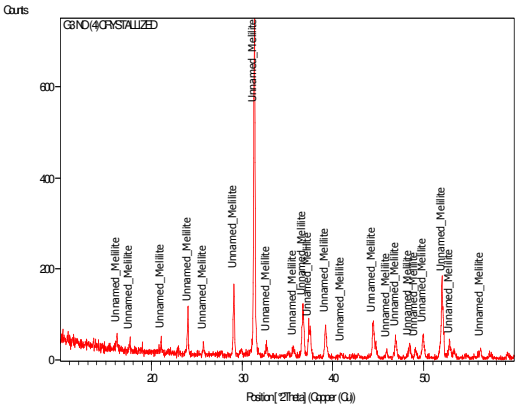

Slag No.4: Crystallized

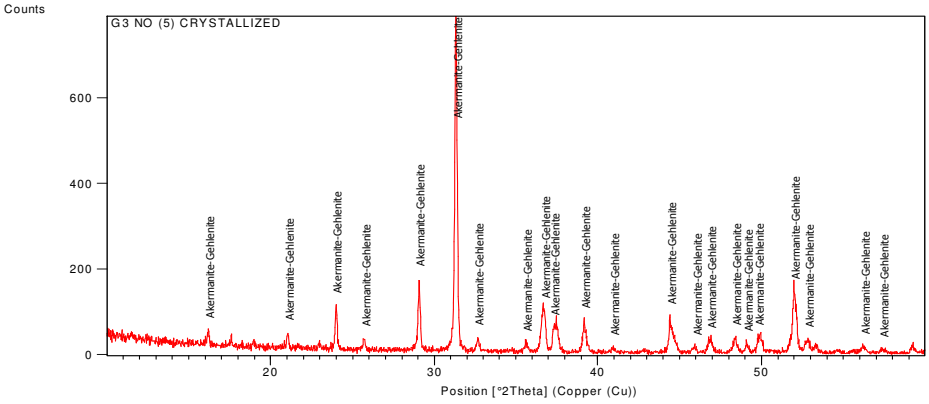

Slag No.5: Crystallized

Figure 3.3: XRD of crystallized slags 1-5

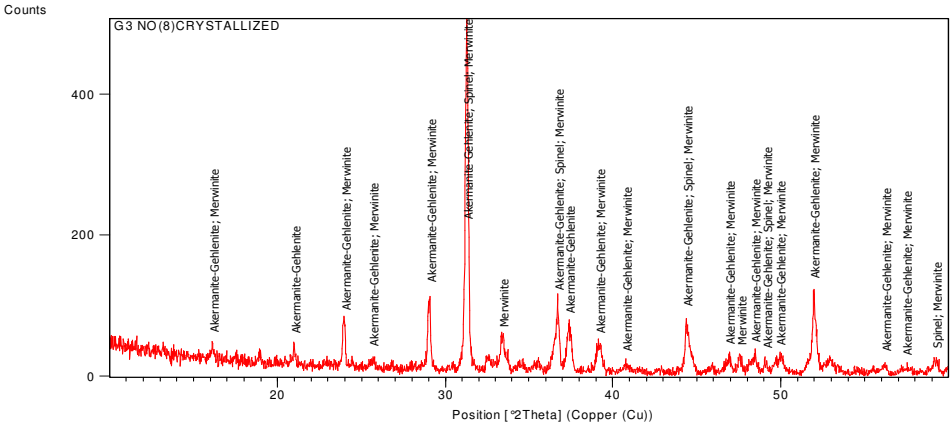

Slag No.8:Crystallized

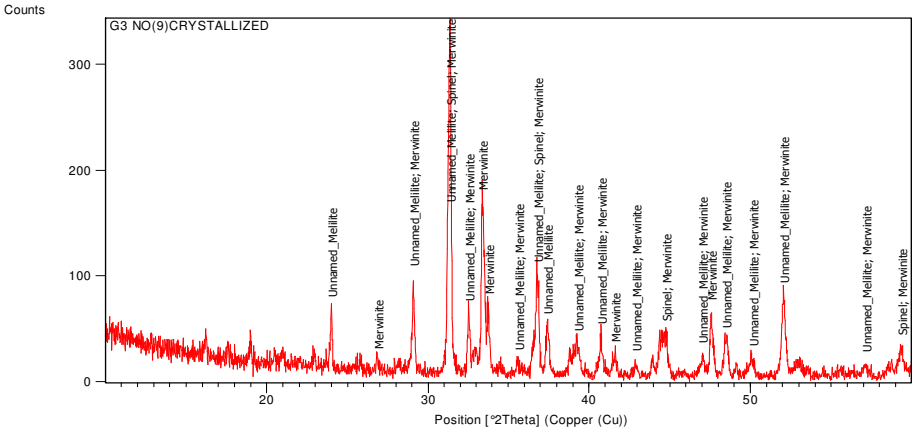

Slag No.9: Crystallized

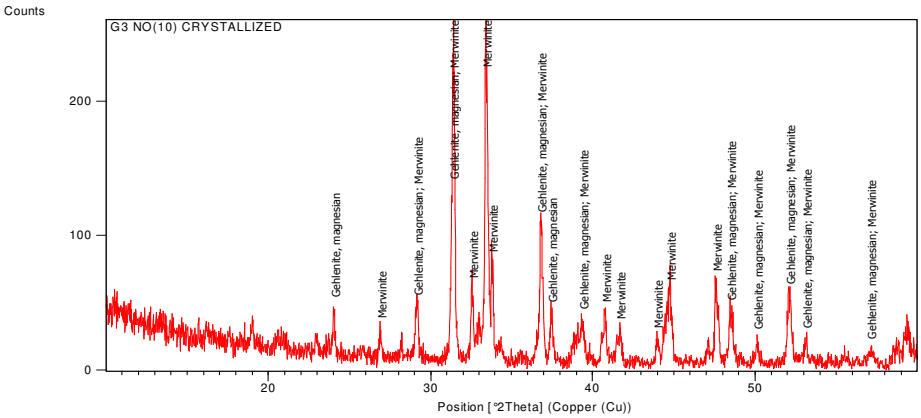

Slag No.10: crystallized

Figure 3.4: XRD of crystallized slags 8-10

Major and minor phases of the crystalline slags are tabulated in **Table No. 3.4** and compared with C/S ratio and MgO content.

Table no 3.4: Phases of Crystallized slags

Sample no	Major phases	Minor phases	C/S ratio	MgO%
1	Un named Mellilite		0.95	6.5
2	Mellilite, Akermanite-Gehlenite		1.00	7.0
3	Un named Mellilite		1.02	7.5
4	Un named Mellilite		1.05	8.0
5	Akermanite- Gehlenite		1.08	8.5
8	Akermanite-Gehlenite, Merwinite	Spinel	1.25	11.0
9	Un named Mellilite, Merwinite	Spinel	1.30	11.5
10	Un named Mellilite, Merwinite		1.35	11.75

Discussion:

The phases present in the slags is compared with CaO-MgO-SiO_2 ternary phase diagram with 20% Al_2O_3[97] Fig 3.5

Slags having C/S ratio (Table No 3.4) of 0.95, 1.00, 1.02, 1.05 and 1.08 with respective MgO content 6.5%, 7.0%, 7.5%, 8.0% and 8.5% fall in the Mellilite region. No other phase is present as shown in the X-Ray diffractogram. (Figure No 3.5). Slag having C/S ratio 1.25, 1.30 and 1.35 with respective MgO content 11%, 11.5% and 11.75% shows Merwinite and spinel apart from Mellilite. Comparison with CaO-MgO-SiO2 ternary phase diagram with 20% Al2O3 shows these slags fall in the interface of Mellilite- Merwinite- Spinel region. When the Al2O3 content of these slag will be 25%, Phase diagram of Cao-MgO-SiO2 with 25% Alumina Fig no 3.6 shows these slags will enter Anorthite-Mellilite- Spinel region where the liquidus temperature is comparatively higher than slag containing 20% Al2O3.

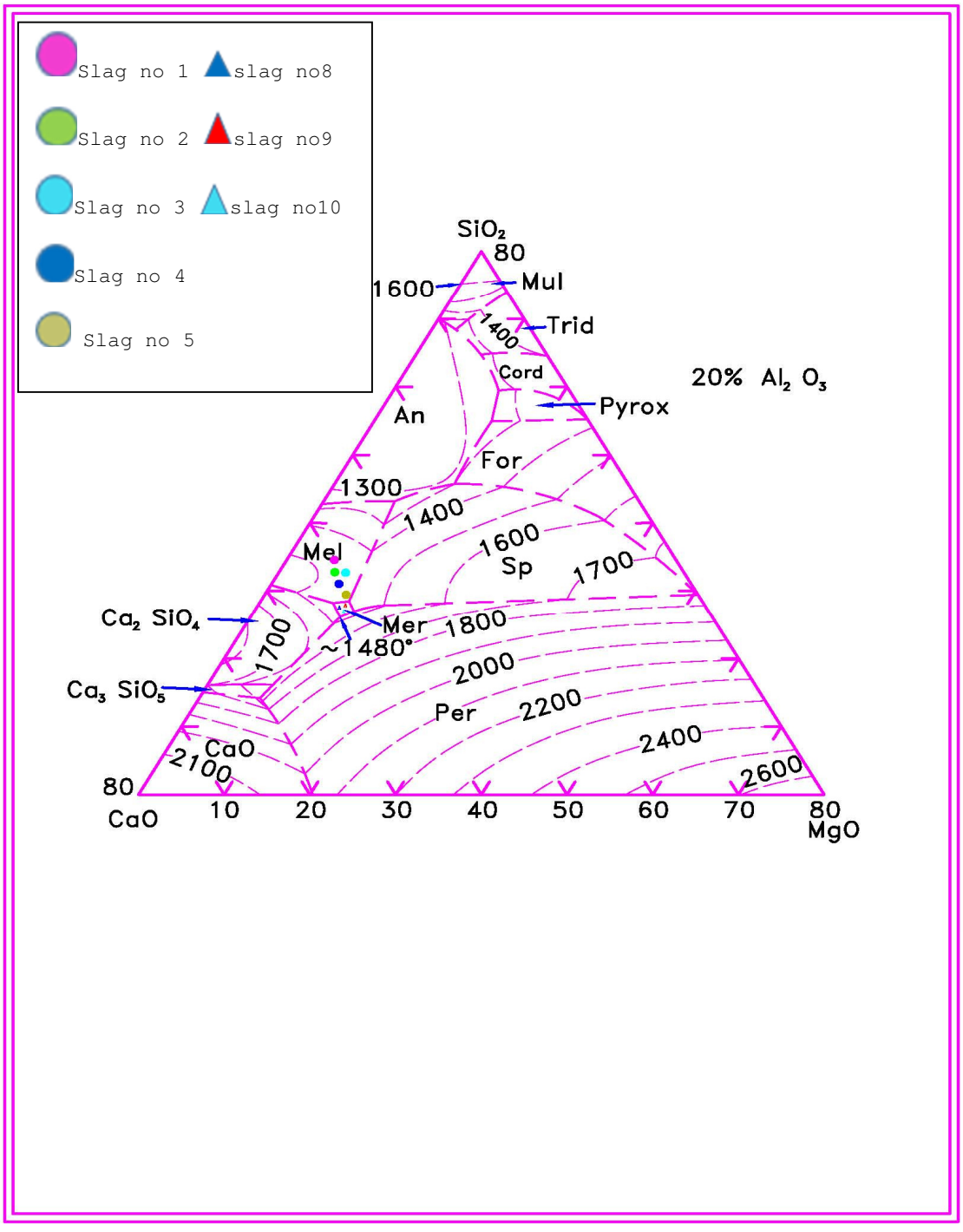

Figure 3.5 Phase diagram showing slag compositions in melilite & merwenite regions with 20% Al_2O_3

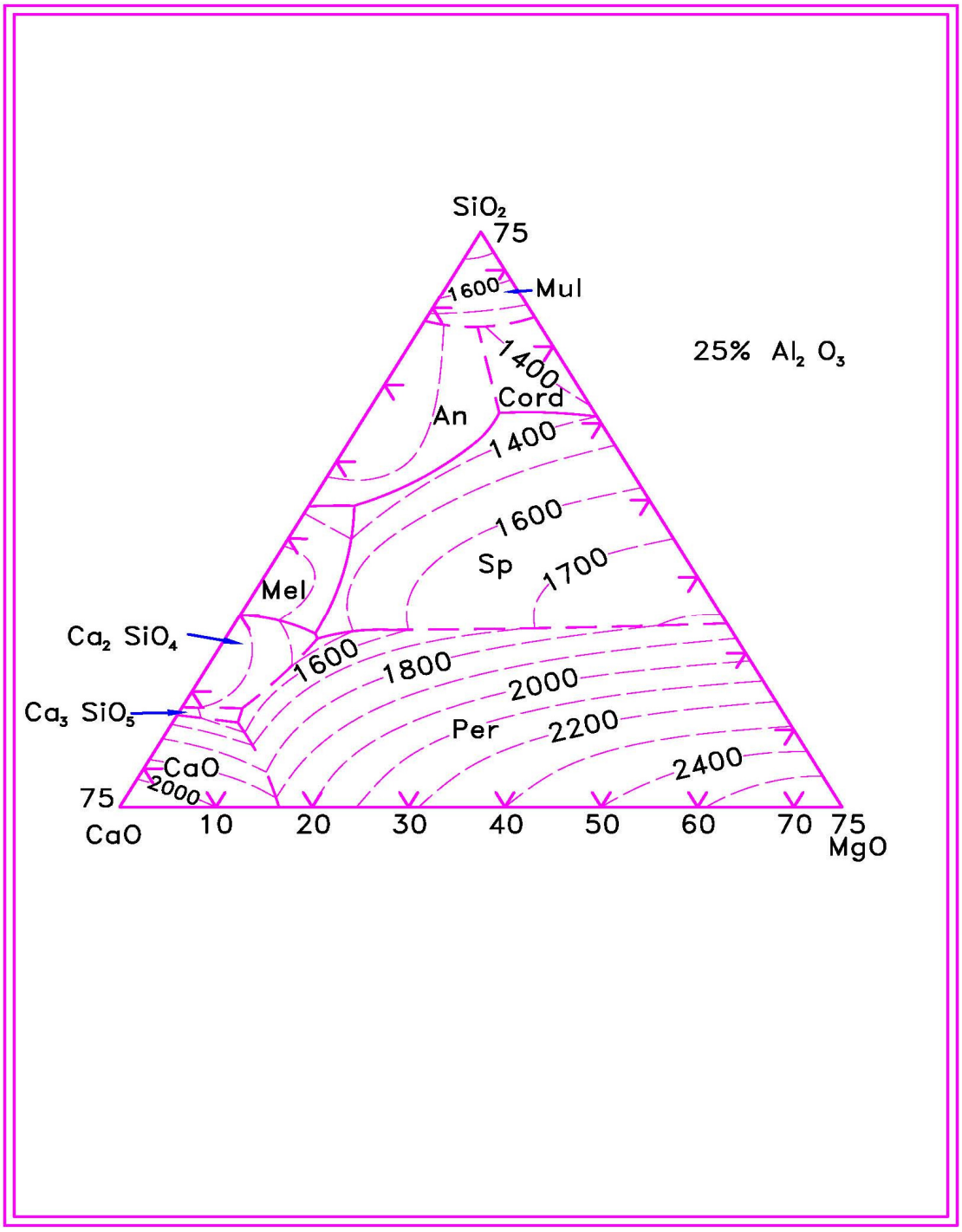

Figure 3.6 CaO.MgO.SiO_2 phase diagram at 25% Al_2O_3

3.2.3 Measurement of Flow Characteristics:

A Leitz heating microscope, with a Leica camera and 1750^{o}C furnace as a supplementary attachment has been used in the present work to determine the flow characteristics of the slag samples as presented in **Chapter 2**. A schematic diagram of the assembly is presented in **Figure 2.2**.

In the present investigation, in order to avoid any likely reactions with the atmosphere and/or the re-crystallized alumina sample holder Argon gas is introduced into the furnace throughout the entire period of measurement and also a platinum sample holder is used in place of the re-crystallized alumina sample holder. The heating rate adopted is 10^{o}C/ min maximum up to 1000^{o}C and 4-6^{o}C/min maximum beyond 900^{o}C. Regular photographs are taken to record the readings. Two readings are taken per sample. If the readings differ by more than 5^{o}C the results are rejected and new sample is taken for test; if not the average of the two readings is reported.

3.2.4 Factorial Design:

A two-level factorial design technique [87, 98] is used in the present study. As per the design each factor, i.e. the slag composition in the present case, is assigned two levels w.r.to the base level slag: ±0. 25 for R, ±3. 0 for M and ±0. 45 for T. Initially, characteristic temperatures of different level slag are performed to develop the relationship and then 10 tests are conducted to verify the derived equations [88]. It can be stated with emphasis that statistical methods of designing of experiments by means of factorial design technique incorporate the manner in which all variables in an experiment are simultaneously varied according to predetermined rules. In the two level factorial design technique an experiment for obtaining optimum conditions is based on a variety of factors at two levels i.e. higher (+) and lower (-). The total number of tests to be conducted is given by $N=2^{k}$ where 'k' is the number of factors. Here in the present case the significant variables (factor) being 3 in number [CaO/SiO_2 (R), MgO (M) and TiO_2 (T)], the total number of tests conducted are $2^3 = 8$.

3.3. Results

The characteristic temperatures, ST, HT and FT, of the slag used for factorial design technique are shown in **Table 3.5**. It may be noted that the average characteristic temperatures only are presented here. However, the measurements are carried out four times for base slag and twice for other slag respectively. Using the two-level factorial design technique, the characteristic temperatures, namely ST, HT and FT, are found out as follows:

ST = 1502.375 + 20.125R + 9.375M – 13.625T ---------- **Equation 3.1**

HT = 1649.625 + 28.625R + 4.625M – 10.875T – 12.375 (M-R) **Equation 3.2**

FT = 1677.375 + 29.625R – 5.625M – 14.875T ---------- **Equation 3.3**

The detailed calculation for the ST is given in **Annexure 2.** The others follow.

Table 3.5.
Softening temperature (ST), hemispherical temperature (HT) and fusion temperature (FT) at different levels of R, M & T, measured by heating microscope. R_0 = 1.15, M_0 = 9.0, T_0 = 0.55, R_1 = 1.4, R_2 = 0.9, M_1 = 12.0, M_2 = 6.0, T_1 = 1.0 & T_2 = 0.1.

Test No.	Factors	Levels	Response (ρ)		
			ST, K	HT, K	FT, K
1	$R_0M_0T_0$	------	1474	1660	1673
2	$R_1M_1T_1$	+ + +	1518	1668	1681
3	$R_1M_2T_2$	+ - -	1534	1691	1726
4	$R_2M_1T_2$	- + -	1503	1653	1675
5	$R_2M_2T_1$	- - +	1451	1583	1623
6	$R_1M_2T_1$	+ - +	1499	1681	1718
7	$R_2M_1T_1$	- + +	1487	1623	1628
8	$R_2M_2T_2$	- - -	1488	1625	1665
9	$R_1M_1T_2$	+ + -	1539	1673	1703

The observed and calculated values of the response for ST, HT, and FT can be used to verify the fit of the above equations as per χ^2 test [99]. ST, HT, and FT are calculated according to the **Equation 3.1** through **Equation 3.3**, and the results are represented in **Table 3.6**. In the above mentioned equations, signs (not values) of R, M,

T, and R-M are taken to calculate ST, HT, and the FT. **Table 3.6** shows that the above equations fit into the result pattern because the $\sum \frac{(\rho_{obs} - \rho_{cal})^2}{\rho_{cal}}$ for all the three responses, namely ST, HT, and FT, lies much below the value of 2.17. According to the χ^2 test at 95% confidence, $\sum \frac{(\rho_{obs} - \rho_{cal})^2}{\rho_{cal}}$ should be less than 2.17 for the present investigation [98]. Finally, characteristics temperatures of ten slag of composition shown in **Table 3.7** are compared to verify the accuracy and usefulness of these equations. The observed and calculated values of all the three responses, i.e. ST, HT, and FT are presented in **Table 3.7**. The max percentage variation for ST, HT, and the FT is found out to be within 1.99%, 1.69%, and 1.74% respectively. This may, therefore, be concluded that the equations developed for the prediction of ST, HT, and FT of the blast furnace slag in the range of CaO/SiO2 ratios from 0.9 to 1.4, MgO percentage from 6 to 12 wt. %, and TiO_2 percentage from 0.1 to 1.0 wt. % give good fit for all the characteristic temperatures.

Table 3.6
Results of χ^2 test.

Test No.	Levels	Response Observed ρ_{obs} (in K)			Response Calculated ρ_{cal} (in K)			$\frac{(\rho_{obs} - \rho_{cal})^2}{\rho_{cal}}$		
		ST	HT	FT	ST	HT	FT	ST	HT	FT
2	+ + +	1518	1668	1681	1518	1660	1687	0.0000	0.0423	0.0179
3	+ - -	1534	1691	1726	1527	1697	1728	0.0344	0.0203	0.0013
4	- + -	1503	1653	1675	1505	1649	1657	0.0034	0.0106	0.1955
5	- - +	1451	1583	1623	1459	1593	1639	0.0466	0.0643	0.1466
6	+ - +	1499	1681	1718	1500	1675	1698	0.0001	0.0206	0.2415
7	- + +	1487	1623	1628	1478	1627	1628	0.0548	0.0105	0.0000
8	- - -	1488	1625	1665	1487	1615	1668	0.0015	0.0635	0.0063
9	+ + -	1539	1673	1703	1546	1681	1716	0.0273	0.0417	0.1023
							$\sum \frac{(\rho_{obs} - \rho_{cal})^2}{\rho_{cal}}$	0.1681	0.2737	0.7114

Table 3.7
Comparison of observed and calculated values of the response.

Test No.	R	M	T	Response Observed (in K)			Response Calculated (in K)			Percentage Variation		
				ST	HT	FT	ST	HT	FT	ST	HT	FT
1	0.95	6.5	0.2	1465	1625	1649	1487	1615	1668	+1.50	-0.62	+1.15
2	1.00	7.0	0.3	1476	1628	1641	1487	1615	1668	+0.75	-0.80	+1.65
3	1.02	7.5	0.4	1458	1629	1648	1487	1615	1668	+1.99	-0.86	+1.21
4	1.05	8.0	0.5	1465	1641	1657	1487	1615	1668	+1.50	-1.58	+0.66
5	1.08	8.5	0.6	1462	1618	1668	1459	1593	1639	-0.21	-1.55	-1.74
6	1.10	9.5	0.65	1470	1608	1650	1478	1627	1627	+0.54	+1.18	-1.39
7	1.13	10.0	0.7	1467	1600	1645	1478	1627	1627	+0.75	+1.69	-1.09
8	1.25	11.0	0.85	1516	1643	1682	1518	1660	1687	+0.13	+1.03	+0.30
9	1.30	11.5	0.90	1516	1658	1685	1518	1660	1687	+0.13	+0.12	+0.12
10	1.35	11.75	0.95	1518	1663	1688	1518	1660	1687	0.00	-0.18	-0.06

To predict a valuable relationship between the slag composition and the characteristic temperatures with flow characteristics of BF slag, slag listed in **Table 3.2** with a systematic variation of the significant factors (C/S ratio of 0.9 and 1.4, MgO content of 6 and 12 wt.%, and TiO_2 content of 0.1 and 1.0 wt.%) are analyzed. These compositional variations are in line with the same as obtained from chemical characterization of Industrial Blast Furnace slag. The results are presented in **Figure 3.7** through **Figure 3.9.**

3.4 Discussion

Correlation of phase analysis with melting characteristics indicates from Slag No.1 to 5 HT and FT are more or less similar and comparatively lower than Slag No.8, 9 and 10. This is in accordance to different phases present in these slags.

Irrespective of the compositional variations, when the temperature of the slag is increased, any one or both of the phenomena given below would take place.

(i) Weakening of the ionic bonds between the cations and the discrete anions.

(ii) Gradual break-down of the discrete anions to smaller flow units.

It is interesting to note (**Figure 3.7**) that at the same C/S ratio the characteristic temperatures are different at different levels (high/low) of other two oxides (MgO, TiO_2). The diagram further reveals that the effect of the C/S ratio at different combinations of the other two significant oxide components on the characteristic

temperatures is not the same as evident from the varied slopes of the plots. This establishes the interdependence of all the three significant variables in influencing the flow characteristics. The increasing trend of the characteristic temperatures, including the flow temperature, which indicates the free flow of the slag, with the increase of the C/S ratio at all levels of the other two oxides can be attributed to the following.

(A) Al_2O_3/CaO Ratio:

When Al_2O_3/CaO ratio is high (> unity), Al_2O_3 works as a network breaker [7, 33]. In the present case, however, the ratio is below unity (especially as the CaO/SiO_2 ratio increases, CaO increases and the Al_2O_3/CaO ratio are further decreased) for all the slag investigated. Therefore, in these slag both Al and Si are expected to occupy similar sites in the lattice [7] and the total network forming ions are presented by (Al+Si). Under such a situation Al_2O_3 will contribute towards an increase in the degree of polymerization, hindering the free flowing nature of the slag. In the entire range of compositions studied, therefore, the change in the characteristic temperature with C/S ratio is not caused by the breakdown of the discrete silicate anions; rather it is due to a general tightening (at increased degree of polymerization) effect on the ionic bonds between the cations (Ca^+) and the discrete silicate anions, as influenced by the compositional variations.

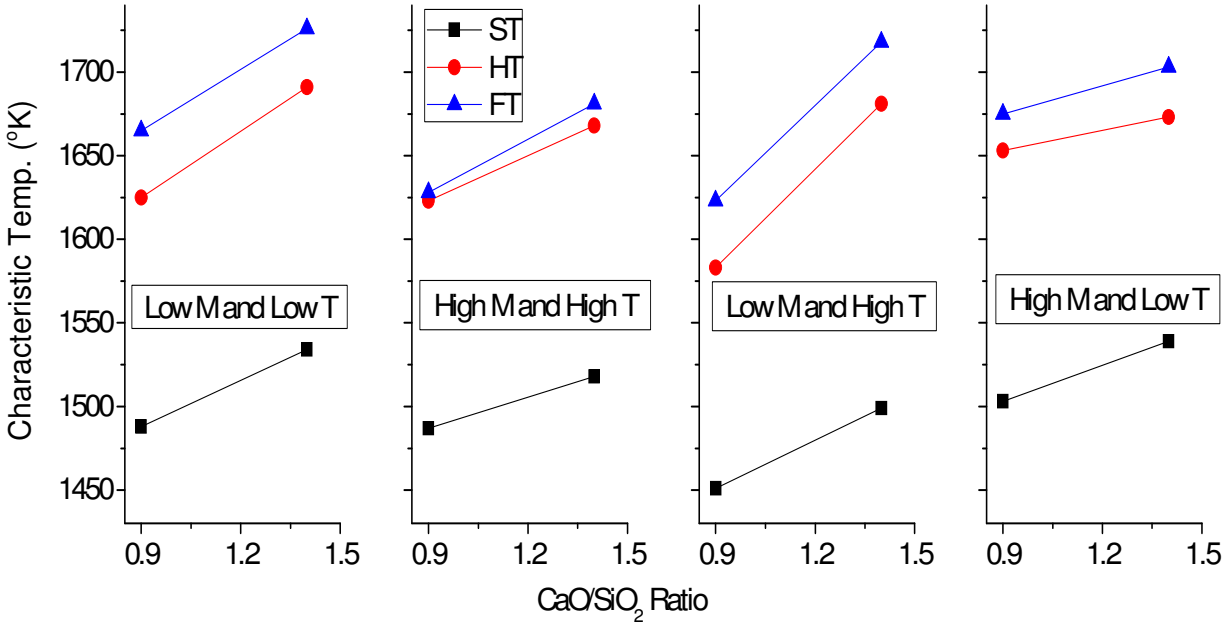

Figure 3.7
Effect of CaO/SiO_2 ratio on flow characteristics of BF slag. Low and high values for M and T are 6 and 12% & 0.1 and 1.0% respectively.

(B) Al_2O_3 / SiO_2 Ratio:

The discrete ion theory ignores the presence of free oxygen and its ions (O^-; O^{2-}) in the melt. However, in a silicate slag singly bonded oxygen (O^-), doubly bonded oxygen (O^o) and free oxygen (O^{2-}) ions are always present and the singly bonded ion interacts with itself as well as other metallic ions strengthening the ionic bond and thus assisting polymerization. In an Al-Si melt this phenomena is exhibited by O^-– O^-, Ca^{2+}– O^- and Al^{3+}– O^- type of interactions. The Al^{3+}– O^- type of interactions increase the degree of polymerization and the rate of this interaction is enhanced at higher Al_2O_3/SiO_2 ratio, i.e. at high values of the Al/(Al+Si) or simply at higher values of Al/Si ratios.

At a high C/S ratio in the silicate melt the SiO_2 content is low. Therefore, at a high C/S ratio the Al_2O_3/SiO_2 ratio increases resulting in higher extents of the Al^{3+}– O^- type interactions, enhancing the degree of polymerization as influenced by the presence of the other oxides. It can thus be inferred that under these conditions a general tightening of the ionic bond may occur requiring higher extents of heat input for the purpose of free flow. Based on the above Gupta and Seshadri[100] opined that flow unit size alone can't be taken as a measure of the free flow nature of a slag and that at a constant average flow unit mass the free flowing nature of the slag decreases with the increase in the Al/(Al+Si) ratio.

Form the flow point of view the industrial BF slag should be a 'short slag'. Such a slag has a small difference between the liquidus temperature (HT) and the flow temperature (FT) and acquires free flowing ability soon after it is rendered molten without needing any higher extents of heat input. Several advantages result with a short slag. The slag-metal reactions/exchanges is accelerated; the permeability of the bed is less affected and heat and mass transfer is assisted with the generation of a short slag. It is interesting to see (**Figure 3.8**) that a combination of high C/S ratio and high MgO contents result in the formation of a short slag irrespective of the TiO_2 variations[23,68,101] within the range of slag composition examined.

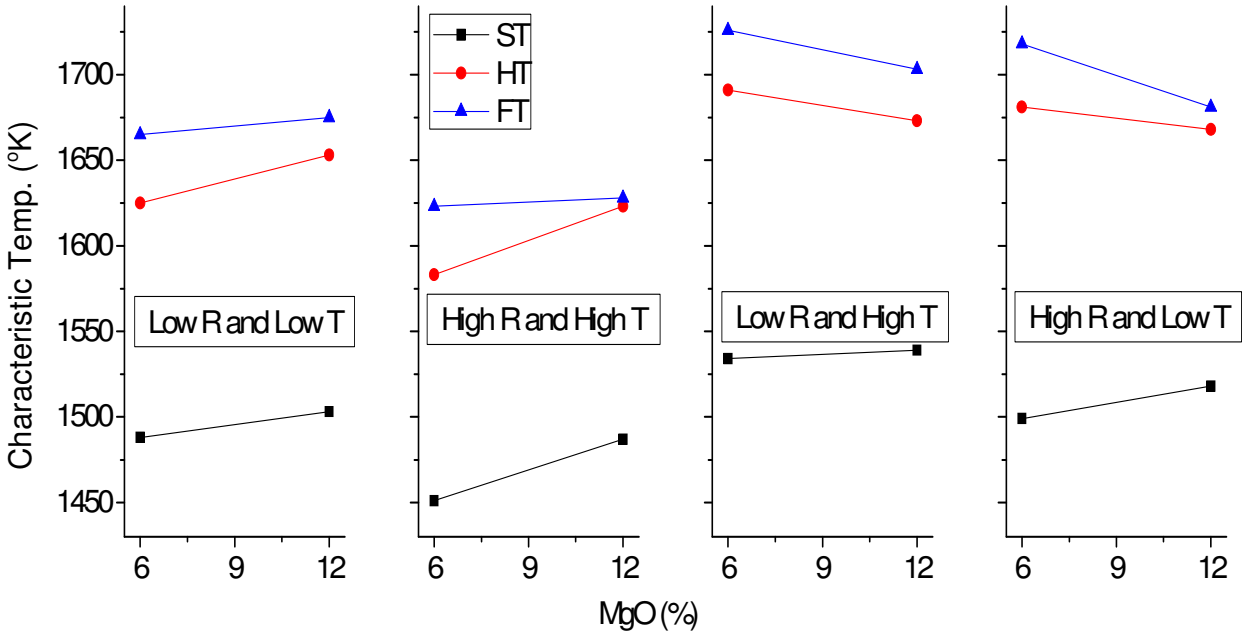

Figure 3.8
Effect of MgO content on flow characteristics of BF slag. Low and high values for R and T are 0.9 and 1.4 & 0.1% and 1.0% respectively.

It can also be concluded, by careful examination of figure (**Figure 3.8)**, that the variations of MgO differently affect the characteristic temperature at different combinations of C/S ratio and TiO_2 contents. Therefore, it will be futile to assess the effect of variation of any of the three factors independent of the other two.

Irrespective of the variations in C/S ratio and MgO additions, an increase in TiO_2 addition always brought down the characteristic temperatures **(Figure 3.9)**. This is in line with the findings of Park et. al [93]. They observed that TiO_2 up to 10 mass % additions behave as a basic oxide and depolymerizes the silicate network structure. Based on FTIR analysis, they also report that TiO_2 additions do not have any effect on aluminate network structure, whereas TiO_2 additions significantly depolymerize the silicate structure till about 5 mass%.

According to their findings TiO_2 additions beyond 5 mass% have negligible effect even on the silicate network structure. In the present case TiO_2 variations are 0.1 to 1.0 mass%, which is much below 5 mass%. Also the present slag analyzed is high in Al_2O_3 which is parallel to the high Al_2O_3 (17 mass %) slag examined by Park et. al. [93]. Thus TiO_2 additions depolymerize the silicate network, making the slag more fluid.

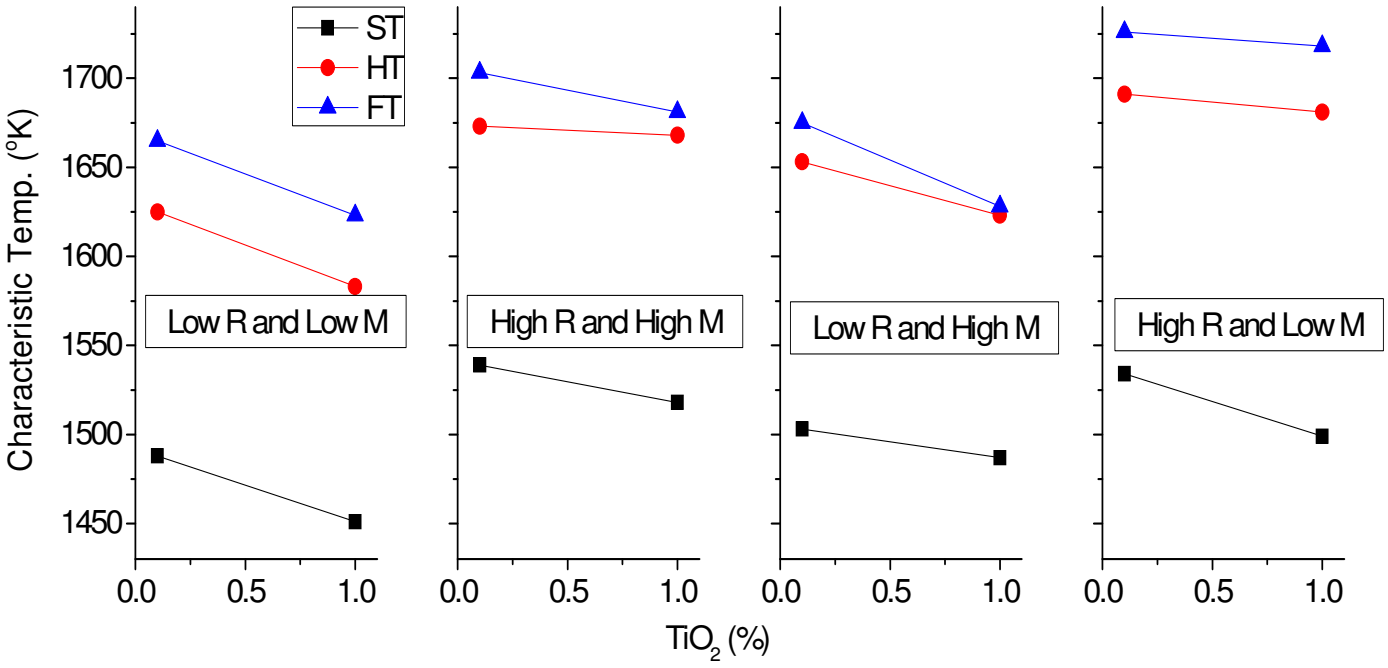

Figure 3.9
Effect of TiO_2 content on flow characteristics of BF slag. Low and high values for R and M are 0.9 and 1.4 & 6% and 12% respectively.

3.5 Conclusion

1. The empirical equations developed using the factorial-design-technique, can be used to predict the flow-characteristics of BF slag fairly accurately, within the range of compositions investigated.
2. The significant variables, viz. C/S ratio, MgO content and TiO_2 content of the BF slag are combinedly involved in influencing the characteristic temperatures of the slag. Any attempt at assessing the effect of any one of the variables, independent of the other two, will not be justified.
3. The combination of high C/S ratio and high MgO content at all levels (high/low) of TiO_2 content, within the range of compositions investigated, aids to the process of iron-making in the BF route in way of assisting the generation of a short slag.

Chapter 4

VISCOSITY OF BLAST FURNACE SLAG

4.1 Viscosity of blast furnace slag

The B.F Slag is a Newtonian fluid and its viscosity is a function of its composition and the prevailing temperature. On the other hand, the composition of the slag melt at the prevailing temperature conditions has a definite say in its ionic structure and the nature of the chemical bonding or the interactions between the various anions present in the melt. As a matter of fact, there exists a direct relationship between the viscosity and the structure of the slag melt. Therefore, it is possible to predict the structure of the B.F Slag from a measure of its viscosity and also it is possible to assess the viscosity from its structural details.

Viscosity of B.F Slag has an important influence on the furnace operation. From the operational point of view the slag should neither be too viscous nor too fluid. A viscous slag would not assist the slag metal interactions / exchanges and will not be easily separated from the metal. On the other hand, though a fluid slag may seem to be beneficial, it is likely to bring about a heat imbalance in the furnace. If the metal droplets are trickling through the slag, a relatively high viscosity of the slag may help the chemical exchanges between the slag and metal by increasing the residence time of the metal droplet in the slag. A viscous slag attacks the refractory lining of the furnace at a slower rate compared to a slag with low viscosity values. On the other hand, a slag with lower viscosity allows for a rapid heat transfer between the slag and the metal by convection.

Blast furnace slag contains CaO, SiO_2, Al_2O_3 and MgO as major constituents and MnO, FeO, CaO and TiO_2 as minor constituents. There exists complicated relationships between the viscosity and the composition of B.F. Slag. However, many investigators [34, 45] infer that variations of viscosity depend on the basicity of the slag expressed as CaO/SiO_2 ratio and also the MgO level in the slag. The higher is the MgO content the lower is the CaO/SiO_2 ratio for optimum viscosity. High Al_2O_3 containing B.F Slag (20-34% Al_2O_3) show erratic viscosity variations. This is because, at constant high Al_2O_3 content, higher CaO/SiO_2 ratio increase the Al/Si ratio. The former (high CaO/SiO_2) decreases the viscosity, whereas the latter (Al/Si) increases the viscosity.

Owing to these complicacies associated with viscosity variations and also the important role of viscosity in the BF process, an attempt is made in the present investigation to assess the effect of temperature on this important property as influenced by its composition and structural details. This knowledge is bound to enable the operator to make the compositional adjustments and to control the temperature to generate the slag with appropriate, optimum viscosity values which will result in the production of the metal of choice.

An inner cylinder rotating type Viscometer (VIS-403-HF) explained in P**ara 2.6** is used to measure the viscosity of synthetic slag prepared in the laboratory in agreement with compositional details of industrial BF slag. The viscosity of the slag is also calculated using a basic model (Iida Model) to throw light on the accuracy of measurement. The results are thoroughly analyzed to study the effect of the compositions, temperature and the structure of the slag sample on its viscosity.

Experimental Work

4.2 Selection of slag compositions for investigation

The composition of slag (**Table 4.1, Table 4.6, Table 4.8, and Table 4.10**) for viscosity measurements is carefully chosen keeping an eye to the compositional details of industrial BF slag. The slag is divided in 4 groups. The first group is concerned about variation of C/S ratio; the second group is concerned with variation of MgO content; the third group considers TiO_2 variation and in the fourth group simultaneous variation of C/S ratio & MgO is considered for a systematic study of viscosity. The respective groups are presented in details in the respective sections while considering the variation of C/S ratio, MgO content, TiO_2 content and simultaneous variation of C/S ratio & MgO.

In all the slag samples Al_2O_3, MnO, Na_2O, K_2O and Fe_2O_3 are kept constant at 20%, 0.1%, 1.1%, 0.5% and 1.0% respectively. In slag samples meant for assessing the effect of any one variable the percentage composition for the other two variables is kept at their respective mid-values within the stipulated range of compositions decided. For example, when C/S ratio is varied, MgO is kept at 8.0 wt. % and TiO_2 at 0.6 wt. %, the

respective mid values of the stipulated range of compositions for MgO and TiO_2 respectively.

Table 4.1
Chemical Compositions of slag selected for study of C/S variation

Sl. No	Al_2O_3 Wt.%	MnO Wt.%	K_2O Wt.%	Na_2O Wt.%	Fe_2O_3 Wt.%	TiO_2 Wt.%	MgO Wt.%	CaO Wt.%	SiO_2 Wt.%	CaO/SiO_2 (C/S)
1	20.0	0.1	0.5	1.1	1.0	0.6	8.0	32.54	36.16	0.9
2	20.0	0.1	0.5	1.1	1.0	0.6	8.0	33.47	35.23	0.95
3	20.0	0.1	0.5	1.1	1.0	0.6	8.0	34.35	34.35	1.0
4	20.0	0.1	0.5	1.1	1.0	0.6	8.0	35.19	33.51	1.05
5	20.0	0.1	0.5	1.1	1.0	0.6	8.0	35.99	32.71	1.1

4.3 Preparation of synthetic slag

Slag samples are prepared in the laboratory adopting the detailed procedure as presented in **Chapter-3.3.2**.

4.4 Equipment, its calibration and method used for viscosity measurement

The viscosity is measured by an inner cylinder rotating type high temperature Viscometer (VIS-403 HF) supplied by BAHR, Germany. The calibration of the Viscometer as well as the detailed test procedure adopted for the measurement of viscosity is given in Chapter**-3** in **Para 3.6.3** through **Para 3.6.4.2.**

VARIATION OF C/S RATIO

4.5 Effect of variation of C/S ratio on slag viscosity

The measured viscosity values with variation of the C/S ratio in the selected slag compositions from 0.9 to 1.1 in steps of 0.05, for slag nos. 1 to 5 are presented below in **Table 4.2**

Table 4.2
Viscosity values with varying C/S ratio

Slag No.	C/S ratio	Temperature K			
		1673	1723	1773	1823
		Viscosity in poise			
1	0.90	6.72	5.10	3.92	3.06
2	0.95	5.68	4.32	3.36	2.66
3	1.00	4.86	3.72	2.92	2.32
4	1.05	4.20	3.33	2.58	2.08
5	1.10	3.76	2.92	2.30	1.86

The variation of viscosity of these slag with temperature is also presented in **Figure 4.1**. Viscosity decreases with temperature increase for all the slag. As evident from the slopes of the individual plots, temperature has the greatest effect on lowering the viscosity for the slag with the lowest C/S ratio. The vice versa is also true, i.e. as the C/S ratio increases, the slope of the plot diminishes and temperature increase results in the lowering of the viscosity at a lower rate.

It is well known that two factors, namely temperature rise and the compositional details of the slag are together responsible for lowering the viscosity. Therefore, it is only natural that for a given drop in viscosity value, if the contribution of one of the factors is high, the contribution of the other factor will be low and vice versa. For BF type of slag CaO acts as a network modifier and is responsible for breaking of the silicate anionic network, which in turn is responsible for the lowering of viscosity. When C/S ratio is low the effect of CaO in modifying the structure is less and when it is high the reverse is true. Therefore, at lower values of the ratio, i.e. at lower CaO contents, temperature has a greater effect in lowering the viscosity and at a higher C/S ratio the effect of temperature in lowering the viscosity diminishes.

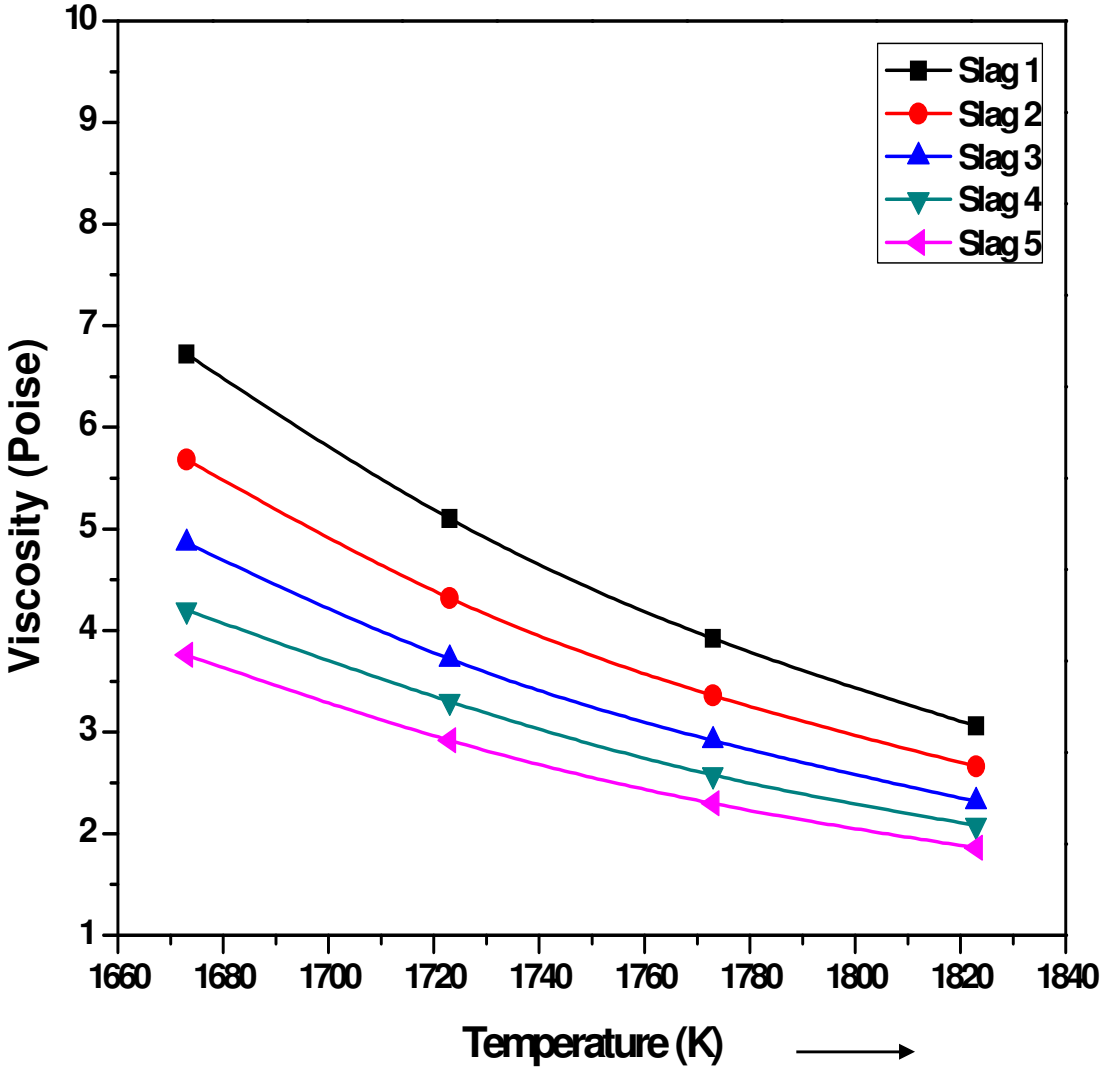

Figure. 4.1
Viscosity studies of Blast Furnace slag
Relationship between Viscosity and Temperature
(C/S ratio variation)

Table 4.3
Variation of viscosity (poise) with Mole % CaO

Slag No.	C/S ratio	Mole % CaO	Temperature K			
			1673	1723	1773	1823
			Viscosity in poise			
1	0.9	35.92	6.72	5.1	3.92	3.06
2	0.95	36.92	5.68	4.32	3.36	2.66
3	1.0	37.87	4.86	3.72	2.92	2.32
4	1.05	38.77	4.2	3.33	2.58	2.08
5	1.1	39.63	3.76	2.92	2.3	1.86

Table 4.4
Variation of Eμ (Kcal/Mole) with Mole % CaO

Slag No.	Wt. % CaO	Wt. % SiO_2	C/S ratio	Mole % CaO	Eμ in (KCal/Mole)
1	32.54	36.16	0.9	35.92	32.16
2	33.47	35.23	0.95	36.92	31.00
3	34.35	34.35	1.0	37.87	30.18
4	35.19	33.51	1.05	38.77	28.86
5	35.99	32.71	1.1	39.63	28.83

Figure 4.2 and **Table 4.3** shows the viscosity isotherms at different temperatures. The increase of the mole % CaO, i.e. the increase in C/S ratio, is seen to decrease the viscosity of the slag at all the temperatures at all levels of C/S ratio investigated. It is interesting to see that the plots gradually flatten out as the temperature increases and at a temperature of 1823°K it is almost a straight line indicating that ability of CaO to decrease the viscosity is low at high temperatures. The slope of the lines indicates that at high temperature the rate of drop of viscosity is lower compared to that at lower temperature for any given CaO mole %. This establishes that at relatively higher temperatures the lowering of viscosity with the increase in CaO mole % (i.e. increased C/S ratio) is more dictated by weakening of the cationic and anionic bonds. On the other hand the curved nature of the plots at relatively lower temperatures indicate a greater degree of depolymerisation of the anionic network with the increase in the CaO mole %. On the basis of the above, it can be informed that the effect of CaO in modifying the anionic silicate structure is more predominant at lower temperatures. Therefore, it is advisable to increase the C/S ratio of the slag in case the process is to run at relatively low temperatures.

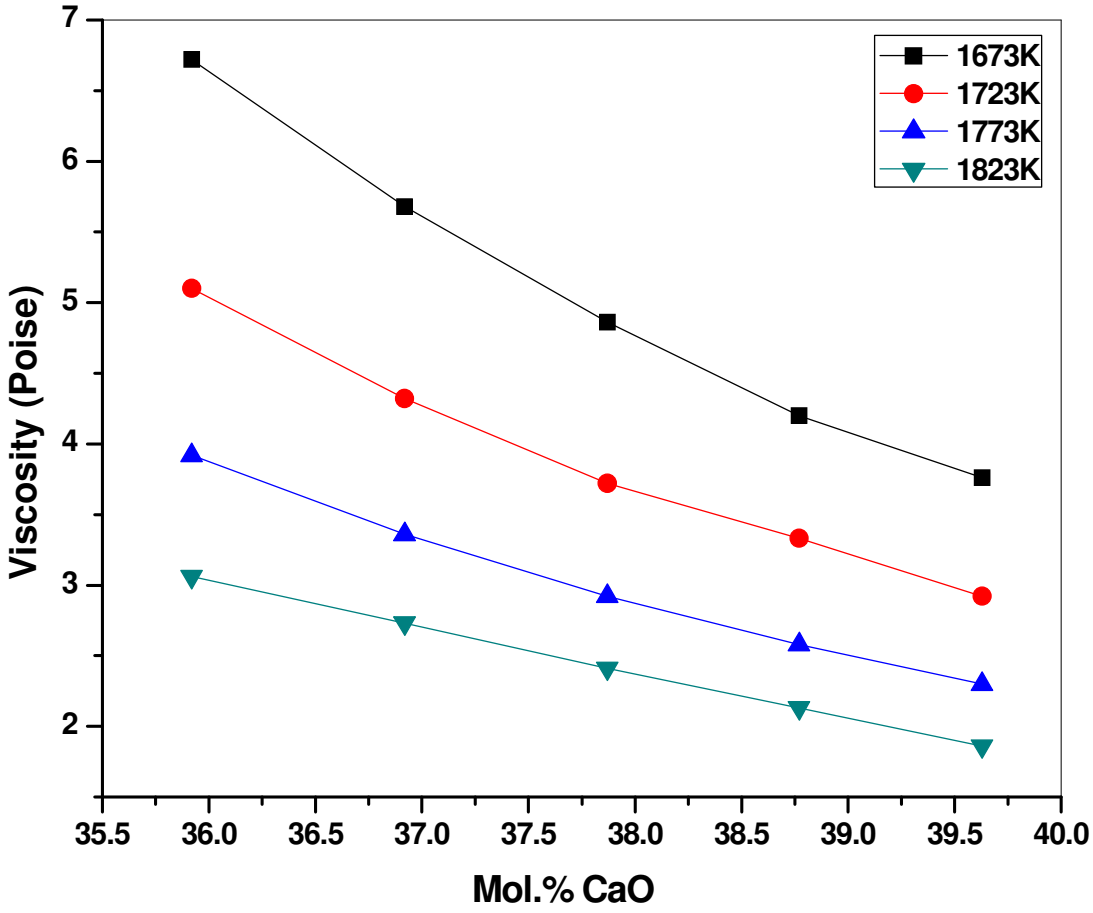

Figure 4.2

Viscosity studies of Blast Furnace Slag

Variation of C/S Ratio

Relationship between Viscosity and Mole % CaO

Figure 4.3 demonstrates the straight .line relationship between Eμ and 1/T (in absolute scale), establishing the fact that the viscosity of BF slag decreases with temperature and that it is in agreement with the Arrhenius Equation, $\mu = Ao\ _{Exp}(E\mu/RT)$. The slope of the plots gives the Eμ (Activation Energy of viscous flow) of the different slag. As evident from the plots Eμ for any slag does not change with temperature, the slope of any plot being constant. This fact demonstrates that the decrease of viscosity with increase in temperature is only a result of the weakening of the ionic bonds between the Ca^{++} cations and discrete silicate anions. The constant Eμ value further shows that the degree of polymerization is practically constant for any given composition of the slag at different temperatures. Thus, it can be inferred that the discrete anionic units do not break down to small units with the increase in temperature.

The Eμ values as calculated from the slopes of the plots in **Figure 4.3** are tabulated in **Table 4.4** against the mole % CaO of the different slag. **Figure 4.4** presents this data in the graphical form. As gathered from the graph, the Activation Energy of viscous flow (Eμ) of the BF slag, decreases with increase of the mole % CaO. This establishes the fact that higher and higher extents of CaO in the slag disintegrate the discrete anionic silicate network more and being more responsible for the breakdown of the structure into smaller and smaller anionic units, increasing the percentage of more de-polymerized units.

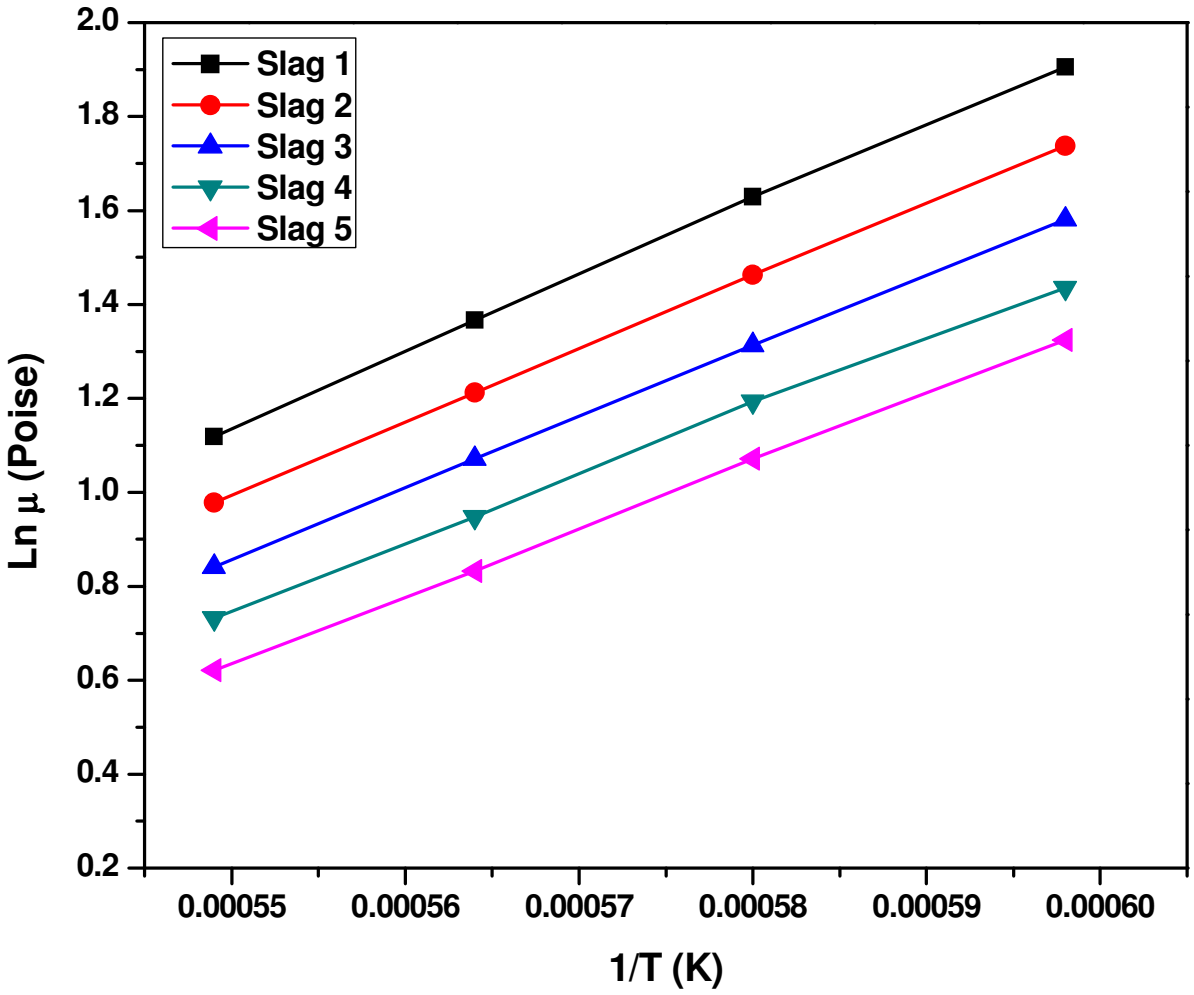

Figure 4.3
Viscosity studies of Blast Furnace Slag
Relationship between Viscosity and 1/T and Ln μ
(C/S ratio variation)

It is further gathered from the plot that the rate of decrease of Eμ is lower at higher mole percentages of CaO as compared to that of lower values as is evident from the lowering of the slope of the plot at higher CaO mole percentages. This can be attributed to the fact that smaller is the size of the anionic silicate flow units greater is the extent of requirement of oxygen contributed by the metal cations (Ca^{++}). Thus the progressive addition of CaO is less and less effective in reducing the flow unit size. Therefore, with the increase of CaO additions the size of the flow units and therefore, the Eμ value decrease only at a decreasing rate. The decrease rate of decreasing of Eμ may also be attributed to a small decrease of metal-oxygen attraction.

4.5.1 Comparison of measured viscosity values with calculated ones

Several models have been proposed by several researchers to calculate the BF slag viscosity. Some important models have been exhaustively discussed in **Chapter 1** of this thesis. It is proposed to calculate the viscosity of some of the slag investigated in the present work using one of the models and to compare the measured viscosity values of these slag with the calculated values. It is decided to choose the Iida model for this purpose as several workers [32, 36, 102] including Iida himself have commented that this model is more reliable than other models. Slag nos.1 to 5 are used to test the results vis-à-vis the Iida model.

Table 4.5 presents the calculated values using Iida model and the measured values of the viscosities of the respective slag. The calculation details for one of the slag at 1673°K is presented in **Annexure 3,** the Table also indicates the percentage deviation. It is evident from the table that the percentage deviation lies within 35.86% and 39.1% i.e. below 40%. This value thus is seen to be well below 62%, the average percentage deviation reported in the literature [83] for high Al_2O_3 slag (>15% Al_2O_3) between the measured viscosity and calculated viscosity values using Iida model.

Table 4.5
Comparison of calculated and measured viscosity values

Slag No.	CaO Wt. %	SiO2 Wt. %	C/S ratio	Measured viscosity in poise (at 1673K)	Calculated viscosity using Iida model in poise (at 1673K)	%age deviation
1	32.54	36.16	0.9	6.72	4.31	35.86
2	33.47	35.23	0.95	5.68	3.59	36.80
3	34.35	34.35	1.00	4.86	3.06	37.03
4	35.19	33.51	1.05	4.2	2.63	37.38
5	35.99	32.71	1.10	3.76	2.29	39.1

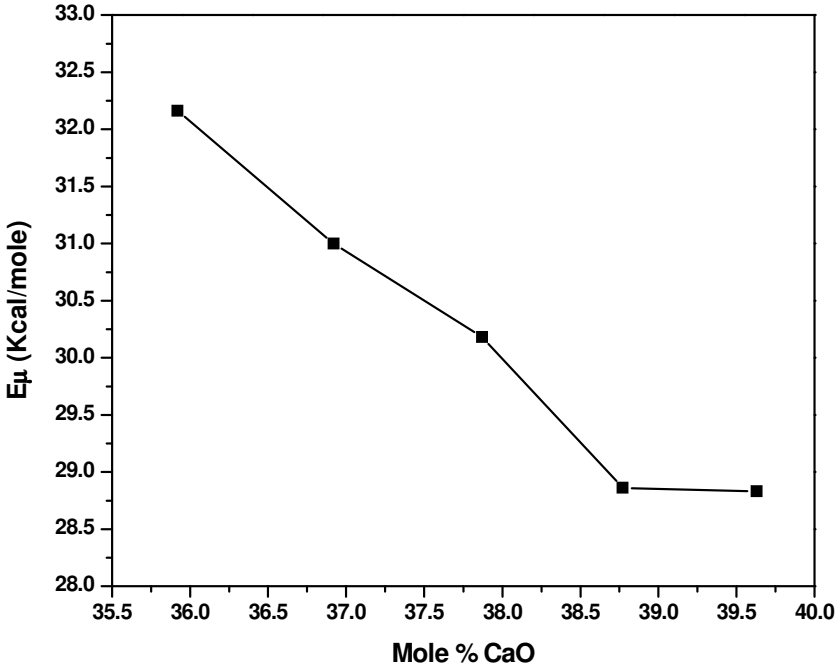

Figure 4.4
Viscosity studies of Blast Furnace Slag
Variation of C/S Ratio
Relationship between Eμ and mole % CaO

VARIATION OF MgO

4.6 Effect of variation of MgO content on slag viscosity

4.6.1 Trend of variation in viscosity

The 5 no. of slag presented in **Table 4.6** with MgO content varying from 4% to 12% are examined for viscosity variations.

Table 4.6
Chemical Compositions of slag selected for study of MgO variation

Sl. No	Al_2O_3 Wt.%	MnO Wt.%	K_2O Wt.%	Na_2O Wt.%	Fe_2O_3 Wt.%	TiO_2 Wt.%	CaO Wt.%	SiO_2 Wt.%	CaO/SiO_2 (C/S)	MgO Wt.%
6	20.0	0.1	0.5	1.1	1.0	0.6	36.35	36.35	1	4.0
7	20.0	0.1	0.5	1.1	1.0	0.6	35.35	35.35	1	6.0
8	20.0	0.1	0.5	1.1	1.0	0.6	34.35	34.35	1	8.0
9	20.0	0.1	0.5	1.1	1.0	0.6	33.35	33.35	1	10.0
10	20.0	0.1	0.5	1.1	1.0	0.6	32.35	32.35	1	12.0

The measured viscosities at different temperatures are presented in **Table.4.7**

Table 4.7
Viscosity data of slag with variation of MgO Content

Sl. No.	MgO %	Temperature			
		1673 K	1723 K	1773 K	1823 K
		Viscosity in poise			
6	4.0	6.76	5.05	3.91	3.07
7	6.0	5.74	4.35	3.41	2.63
8	8%	4.78	3.62	2.84	2.22
9	10%	4.32	3.31	2.56	2.03
10	12%	3.93	2.98	2.33	1.85

Figure 4.5 represents the variation of viscosity of BF slag at different temperatures for various MgO contents. As seen from the figure the BF slag viscosity decreases with increase of MgO content, an increase of temperature having a diminishing effect on decreasing of viscosity at higher MgO contents. This trend is similar to the trend found out for variation of viscosity with variation of C/S ratio. As explained earlier, since MgO is a network modifier, at lower MgO contents contribution of MgO in breaking down the silicate network is less. Here temperature has greater contributions for lowering the viscosity. At higher MgO contents the reverse occurs. It is further seen at lower MgO contents the rate of decrease of viscosity is higher compared to that of higher MgO contents, irrespective of the temperature variations. This is attributed to the fact that the MgO content in the excess of about 10 wt. % MgO does not enter the slag to participate in the stoichiometric slag structure. Rather, it forms a Magnesia-Alumina ($MgO\text{-}Al_2O_3$) spinel (melting point: 2015ºC) that crystallize at the relatively low process temperatures, thus decreasing the rate of lowering of viscosity [103].

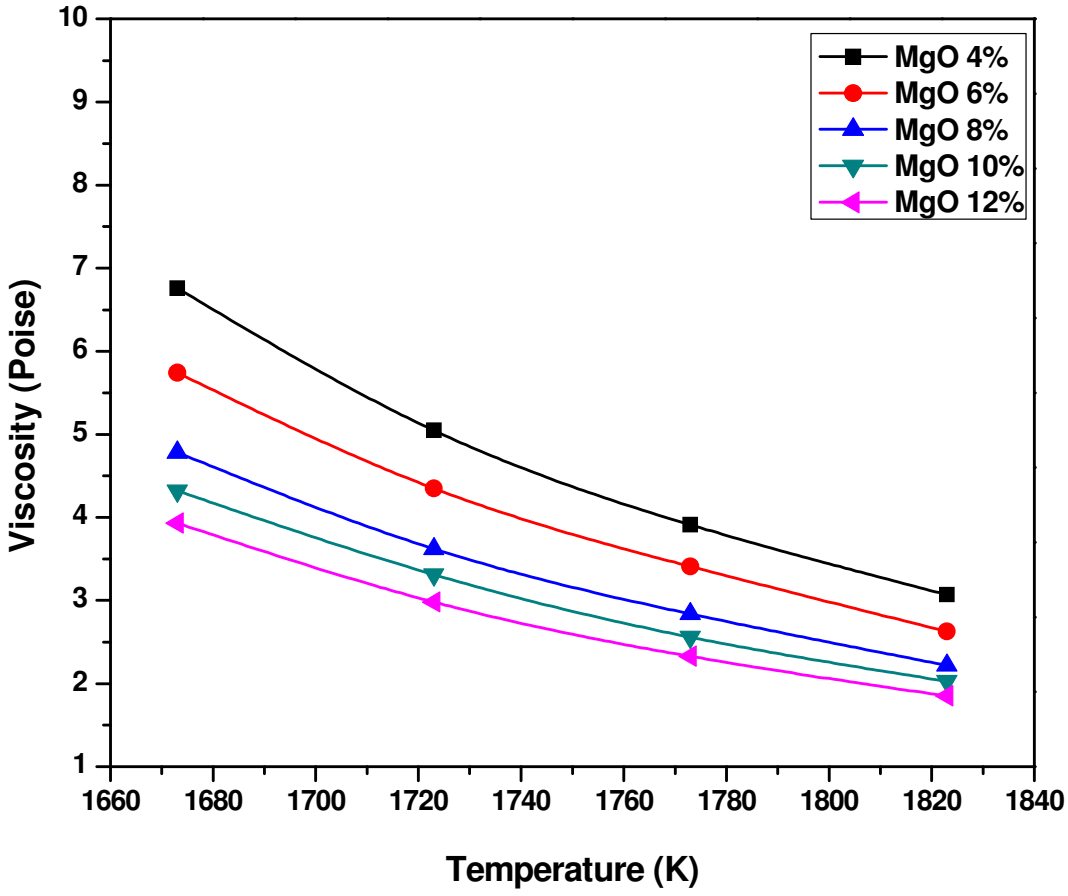

Figure. 4.5
Viscosity studies of Blast Furnace slag
Variation of MgO content
Relationship between Viscosity and Temperature (Variation in MgO content)

4.6.2 Variation in viscosity with MgO mole %

Coupled with the fact that MgO is more effective at decreasing the viscosity at lower temperature compared to that at higher temperatures, as established through **figure 4.5** and as is the case for C/S ratio variations, it can be judiciously concluded that CaO is replaceable by MgO on molar basis, so far as their effect on viscosity of BF slag is concerned. It is heartening to note that several workers [5, 21, 42, 47,104,105], are also of the same opinion. The lesser ability of MgO to bring lower the viscosity at higher mole percentages, further establishes that at higher contents of MgO, its ability to break down the silicate network into smaller flow units, decreases. This establishes the fact that progressive additions of metal oxides are less and less effective in reducing the flow unit size for smaller and smaller flow units require relatively higher oxygen. Further, it can be inferred that at higher MgO contents since the lowering of the viscosity is not due to any significant contribution from MgO content, it is due to a general slackening of the anionic silicate and cationic metal oxide bonds brought about by the increase of temperature and not due to the formation of smaller flow units.

Figure 4.6 exhibits two things;

1. Like C/S ratio, viscosity variation with change of MgO content also obeys the Arrhenius type of equations $\mu = A\mu_o Exp\ (E\mu/RT)$
2. $E\mu$, the activation energy decreases with increase of MgO content. Thus, with the increase of MgO content the energy requirement for the decrease of the bond strength for necessary viscous flow, decreases.

However, it must be clearly understood that the constant Eμ value of any specific MgO content establishes that the degree of polymerization/depolymerisation is practically constant at the specific MgO content irrespective of the temperature variations and that the decrease of viscosity with increasing temperature is only a result of slackening of the discrete anionic and the cationic bonds.

4.6.3 Variation Eμ, with mole % of MgO

The variation of Eμ, as calculated from the slope of the plots in **Figure 4.6** with mole % MgO is presented in **Figure 4.7.** The Eμ is seen to decrease sharply till about 13 mole % (8 wt. %) MgO after which it decreases with a relatively slower rate till about 15 mole % (10 wt. %) MgO. Further increase of MgO mole % brings about a very slow decrease of Eμ, the plot becoming almost parallel to the 'X' axis. This is in agreement with the findings of Athappan [40]. While experimenting with Indian B.F Slag with 20% Al_2O_3, Athappan [40] finds that viscosity decreases with MgO content till about 10 wt. % MgO after which further additions of MgO show no impact on viscosity. In the present case also MgO additions beyond 10 wt. % does not show any impact on the change of Eμ establishing that beyond 10 wt. % MgO further MgO additions do not help the formation of smaller flow units, i.e. the additions beyond 10 wt. % does not depolymerize the silicate network further. A careful comparison between the Eμ values with mole % CaO [**Figure 4.4**] establishes that these values are slightly higher with MgO variations. Thus the ability of MgO in breaking down the silicate network to the smaller flow unit is not as high as that of CaO. This is because of the Z/r^2 values (where 'Z' is the valency and 'r' is the radius of the cation). This value being higher than that of the Ca++ ion, their network's breaking ability is not as high as that of the calcium ions.

A term NBO/T, defined as the number of non-bridging oxygens per tetragonally coordinated atoms provides a measure for the degree of depolymerisation (**Para 1.2.2**) [106]. This term is calculated as per the formula given therein through **Equation 1.13** to **Equation 1.15**

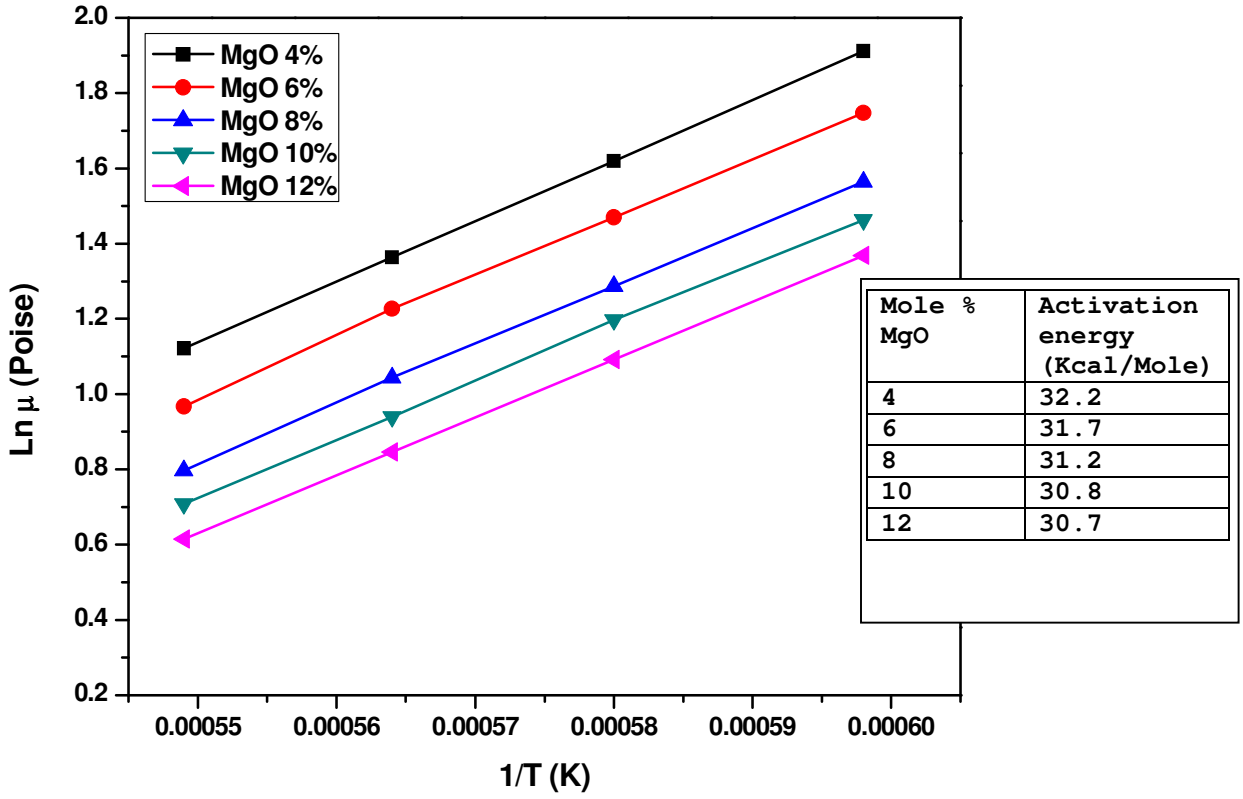

Mole % MgO	Activation energy (Kcal/Mole)
4	32.2
6	31.7
8	31.2
10	30.8
12	30.7

Figure 4.6
Viscosity studies of Blast Furnace Slag
Variation of MgO content
Relationship between Ln μ and 1/T

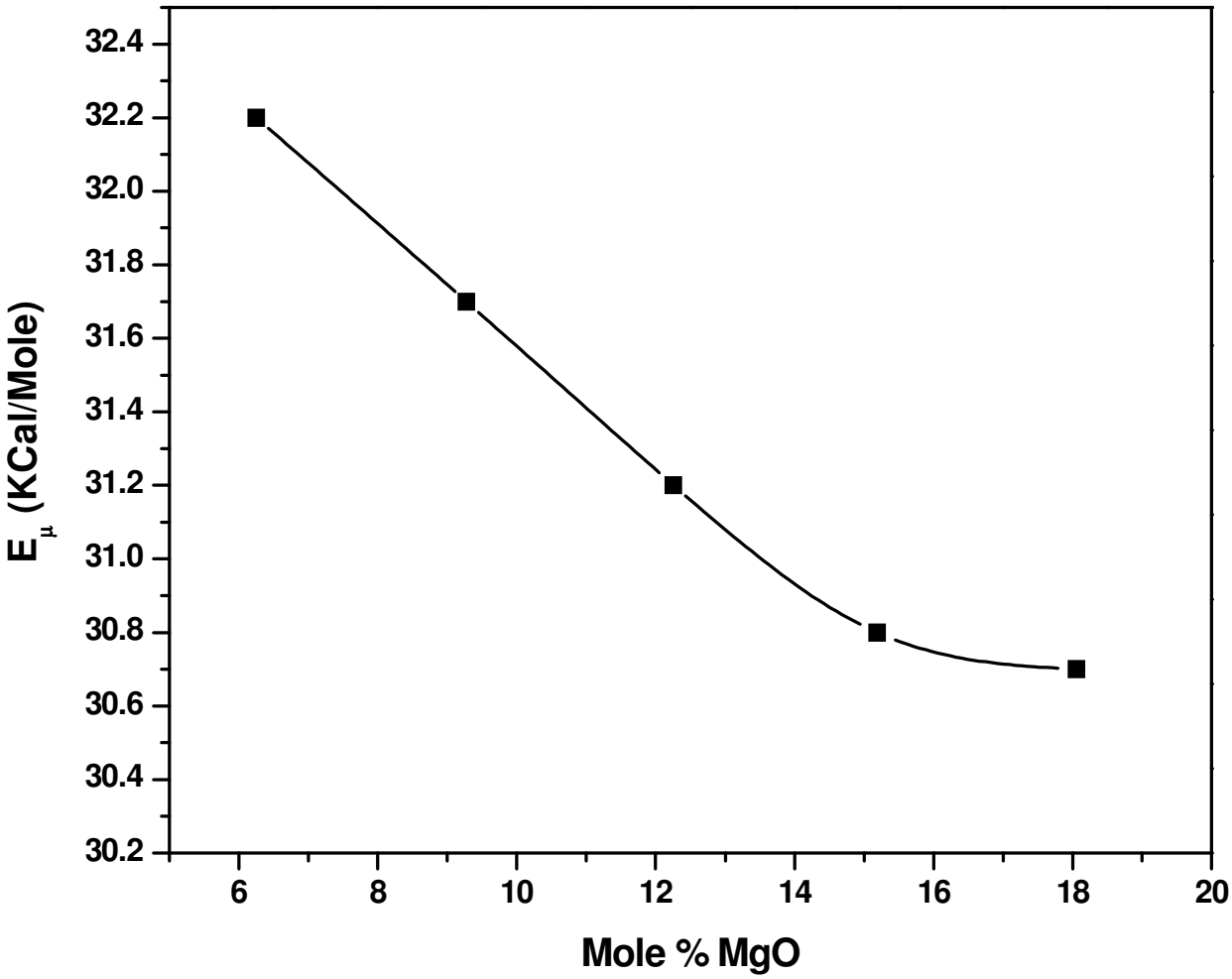

Figure 4.7
Viscosity studies of Blast Furnace Slag
Variation of MgO content
Relationship between Eμ & Mole % MgO

4.6.4 Relationship between Eμ and NBO/T

Figure 4.8 represents the plot for Log viscosity (Log μ) and NBO/T for all the 10 nos. of slag with C/S ratio and MgO content variations at a fixed temperature of 1673°K, to comment on the effect of degree of polymerization on the viscosity with both C/S and MgO variations .The points generated at the particular temperature establish that the viscosity is very much a function of degree of depolymerisation, Log μ confirming a decreasing trend with increased NBO/T values. An attempt is also made to show that the activation energy, Eμ changes with the degree of polymerization. Keeping this in mind the variation of Eμ with NBO/T is presented in **figure 4.9.** In this plot the points are seen to be somewhat scattered. It may be inferred that this trend is due to the fact that the ability of CaO & MgO in breaking down the anionic discrete silicate network are not the same owing to the differences between their Z/r^2 values as presented elsewhere.

It is opined [103] that, in general, MgO favors formation of eutectic phases rather than formation of Gehlenite (Calcium-Aluminum-Silicate, M.P-1590°C) which has the tendency to precipitate out at the eutectic temperatures increasing the slag viscosity. Thus the ability of MgO to bring down the slag viscosity in the MgO-CaO-SiO2-Al2O3 system, may be attributed to its ability to suppress the formation of di-calcium silicate over and above its ability to break down the silicate network into smaller flow units.

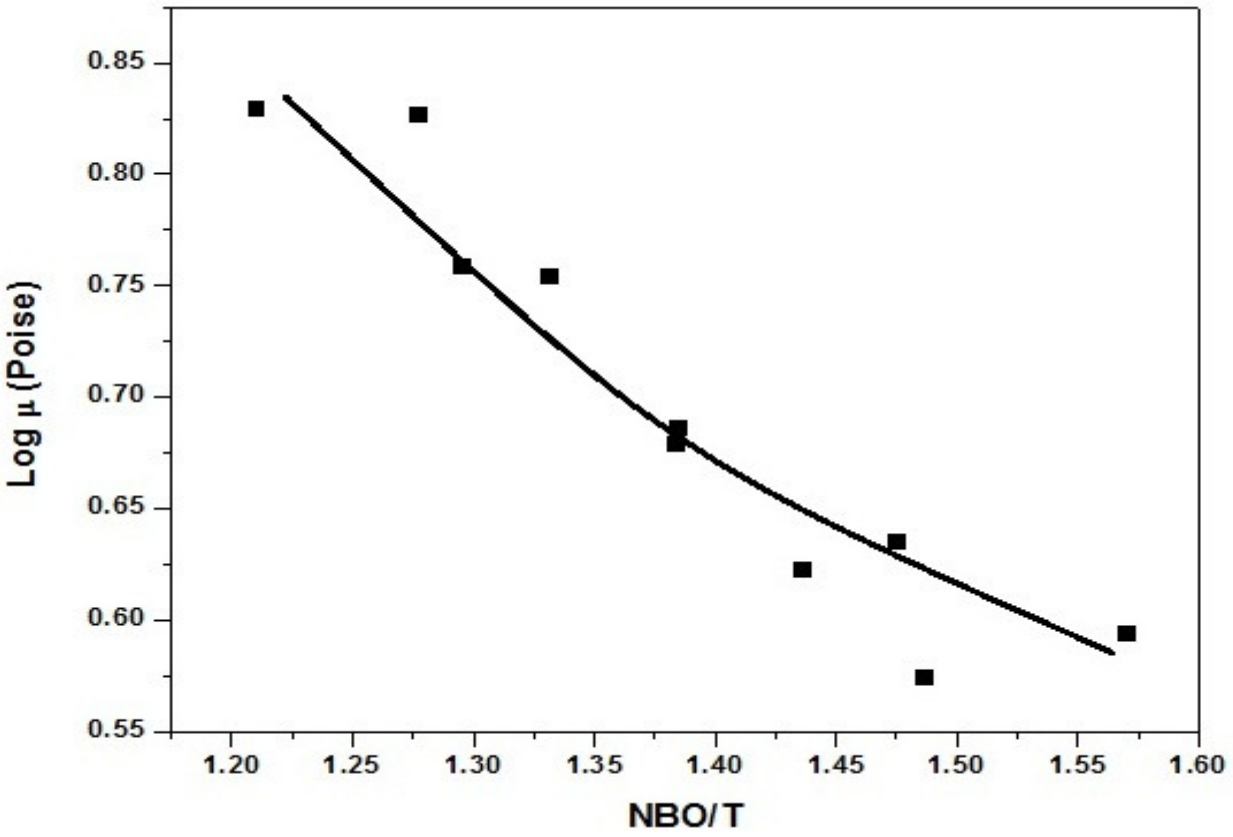

Figure 4.8
Viscosity studies of Blast Furnace Slag
Variation of MgO content
Relationship between Log μ vs. NBO/T (at 1673 K)

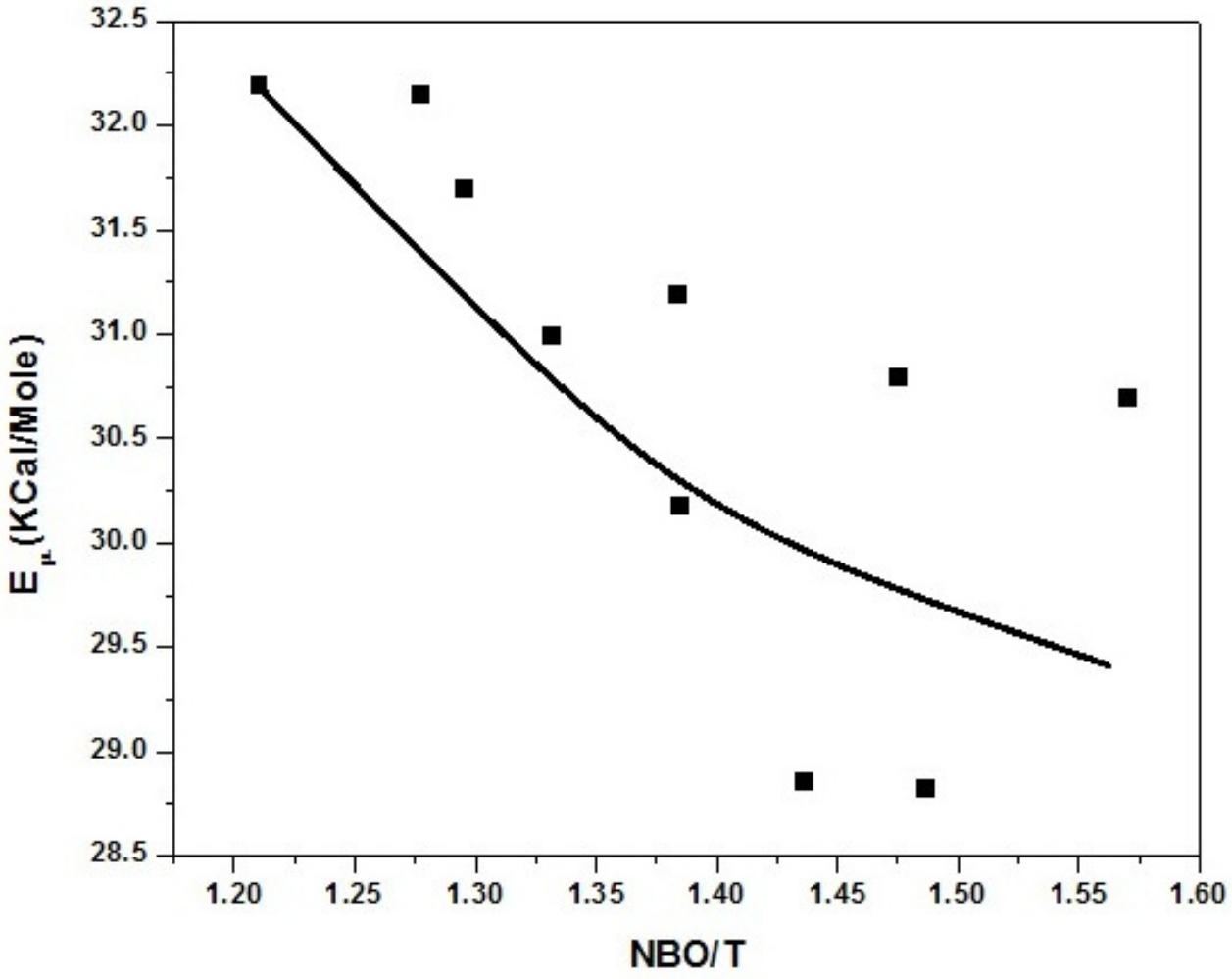

Figure 4.9
Viscosity studies of Blast Furnace Slag
Variation of MgO content
Relationship between Eμ and NBO/T

VARIATION OF TiO_2

4.7 Effect of Variation of TiO_2 on Viscosity.

Viscosity of Blast Furnace type of slag, generated from Titaniferrous ores having significant quantities of TiO_2, are known to be affected by its TiO_2 content to different extents depending on the amount of TiO_2 contained in the slag. Handfield and Charette [43] have reported that small amounts of TiO_2 additions decrease the slag viscosity, whereas high amounts of TiO_2 additions tend to increase the same. In the BF slag of $CaO\text{-}SiO_2\text{-}MgO\text{-}Al_2O_3$ type, TiO_2 additions up to 02 mass % is found to decrease slag viscosity under Argon gas [83] at different fixed extended Vee ratio $[(CaO+MgO)\ /(SiO_2+Al_2O_3)]$ of 0.46 and 0.83. Saito et al [91] report that TiO_2 additions of 10 and 20 mass % decrease the viscosity and activation energy of viscous flow of these slag. The present work, however, examines BF type slag generated from non-titaniferrous ores having insignificant quantities of TiO_2, to assess the effect of TiO_2 on the slag viscosity, when present in quantities as small as 0.2 wt. % to 1.0 wt. %. It is believed that such data are not available readily at hand. The slag examined have CaO/SiO_2 of unity with Al_2O_3 at 20 wt. % and MgO at 8 wt. %, with other usual components like Fe_2O_3, MnO, K_2O and Na_2O combinedly amounting to below 3 wt. %. The TiO_2 content is varied from 0.2 wt. % to 1.0 wt. % at steps of 0.2 wt. %. These slags presented in **Table 4.8** closely resemble their partners in the industry.

Table 4.8
Chemical Compositions of slag selected for study of TiO_2variation

Sl. No	Al_2O_3 Wt.%	MnO Wt.%	K_2O Wt.%	Na_2O Wt.%	Fe_2O_3 Wt.%	MgO Wt.%	CaO Wt.%	SiO_2 Wt.%	CaO/SiO_2 (C/S)	TiO_2 Wt.%
11	20.0	0.1	0.5	1.1	1.0	8.0	34.55	34.55	1	0.2
12	20.0	0.1	0.5	1.1	1.0	8.0	34.45	34.45	1	0.4
13	20.0	0.1	0.5	1.1	1.0	8.0	34.35	34.35	1	0.6
14	20.0	0.1	0.5	1.1	1.0	8.0	34.25	34.25	1	0.8
15	20.0	0.1	0.5	1.1	1.0	8.0	34.15	34.15	1	1.0

4.7.1 Variation of viscosity of slag containing TiO_2 with temperature

Figure 4.10 and **Table 4.9** present the variation of viscosity of these slag with temperature at different TiO_2 contents of the slag. The viscosity of the BF type slag decreases with temperature at all levels of TiO_2 contents investigated. Also the slag viscosity decreases with the increase of TiO_2 content at all temperatures though the decrease of viscosity at the insignificant variations of TiO_2 content of 0.2 wt. % is also insignificant, as evident from the plots. Further, from a minute observation of the slopes of the plots it will be evident that smaller quantities of TiO_2 at relatively low temperatures, are considerably more effective in decreasing the slag viscosities, with the slopes diminishing with higher percentages of TiO_2 at relatively higher temperatures. Some investigators [49,107] suggested TiO_2 to be a weak acidic oxide in a basic slag system, thus polymerizing the liquid slag silicate network structure being responsible for an increase in the resulting viscosity. However, the present work establishes something different. It is found that even with the small amounts of TiO_2 present in the slag, the additions decrease the slag viscosity. Thus, it can be inferred that even with its insignificant presence in the slag, TiO_2 behaves as a basic oxide and subsequently depolymerizes the silicate network structure. The present finding is in agreement with the findings of Park et al [93]. These workers found out from FTIR examinations, that 5 mass % TiO_2 significantly decreases the slag viscosity of $CaO\text{-}SiO_2\text{-}MgO\text{-}Al_2O_3$ type B F Slag compared to the TiO_2 free slag and that beyond 5 mass % TiO_2 meaningful changes in the viscosity is not observed. They also report that TiO_2 additions depolymerized the silicate network structure in the slag.

4.7.2 Relationship of viscosity with temperature in TiO_2 bearing slag

The straight line relationship between $Ln\mu$ and 1/T K (**Figure 4.11**) shows that viscosity variations of these slags obey the Arrhenius type of relations. Viscosity is found to decrease with the increase of temperature. $E\mu$, the activation energy of viscous flow, has been estimated from the slope of the plots and presented in **Table 4.10.**

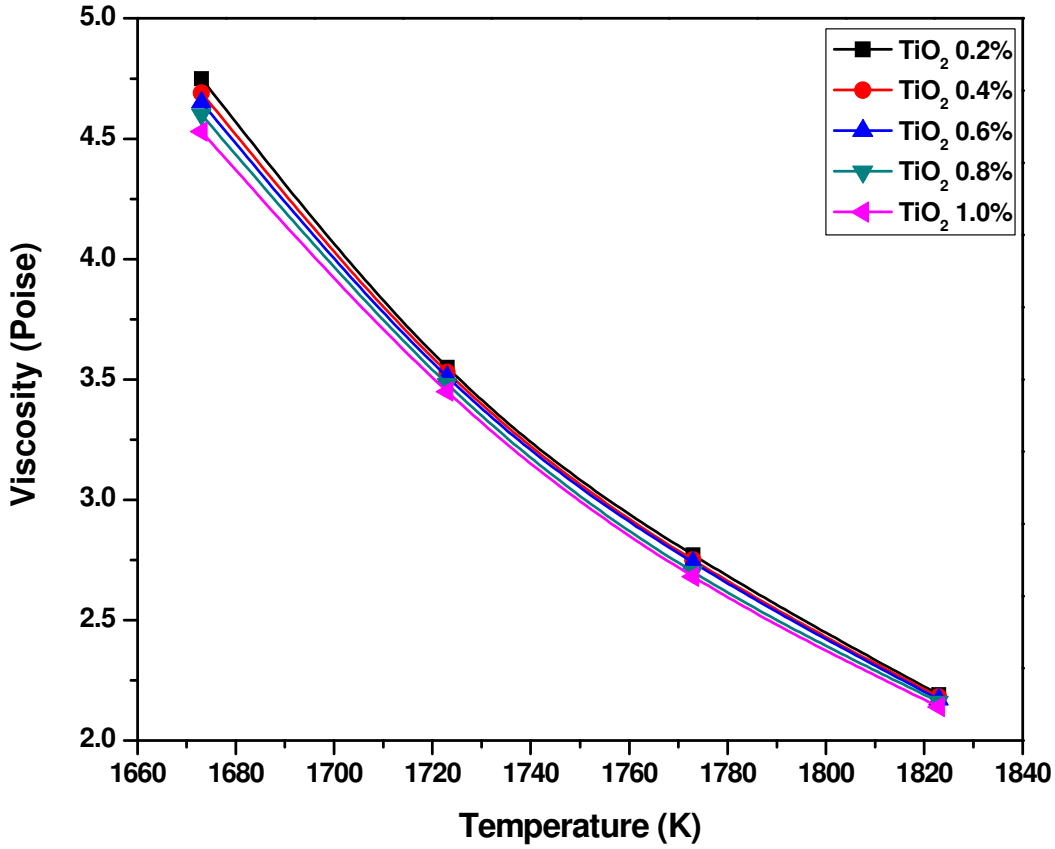

Figure 4.10
Viscosity studies of Blast Furnace Slag
Variation of TiO_2 Content
Relationship between Viscosity and Temperature

Eμ being constant for all the individual plots it is inferred that the lowering of the viscosity of the slag with increasing temperature is a result of the slackening of the discrete silicate anions and the TiO_2^+ cations and not due to any depolymerisation. It is further inferred that the degree of polymerization is practically constant for any composition of the slag at a given TiO_2 content at different temperatures. Thus, it is concluded that TiO_2 additions do not break down the discrete anionic units into smaller units as a consequence of the increase in the temperature. Any depolymerisation with the addition of TiO_2, therefore, is only a consequence of the ability of the basic TiO_2 to depolymerize the anionic silicate network by itself and not through any dictation by the rise in the temperature, thus TiO_2 in these slag though present in very small quantity behaves as a basic constituent oxide only.

Figure 4.12 presents the viscosity isotherms at different temperatures with TiO_2 additions. The plots are almost straight line plots with a slight downward slope indicating higher extents of dependence of viscosity on higher extents of TiO_2 contents. It is also seen that the slope is higher for the isotherms pertaining to lower temperatures compared to those at higher temperatures. Thus the effect of TiO_2 in decreasing the slag viscosity is more prominent at lower temperatures, i.e. increase of TiO_2 content is more effective in bringing down the slag viscosity at relatively low temperatures within the range of compositional variations investigated. However, due to the insignificant presence of TiO_2 in all the slag investigated, the trend is not very significant.

4.7.3 Variation of Activation energy of slag with change TiO_2 content

The activation energy of viscous flow for all the slag investigated, as calculated from the slopes of the plots in **Figure 4.11** are presented in **Figure 4.13** against mole % TiO_2. It is observed that the Eμ values show a significant high value below about 0.3 mole % TiO_2. The Eμ values continuously decrease above 0.3 mole % TiO_2 content. This suggests that TiO_2 contents at values greater than 0.3 mole % (0.4 wt. %) TiO_2 is capable of considerably breaking down the silicate network structure into small anionic flow units, bringing about considerable depolymerisation of the liquid slag network structure. This trend continues to about 0.775 (1.0 wt. %) mole % of TiO_2 the maximum extent of TiO_2 contents in the slag investigated in the present work.

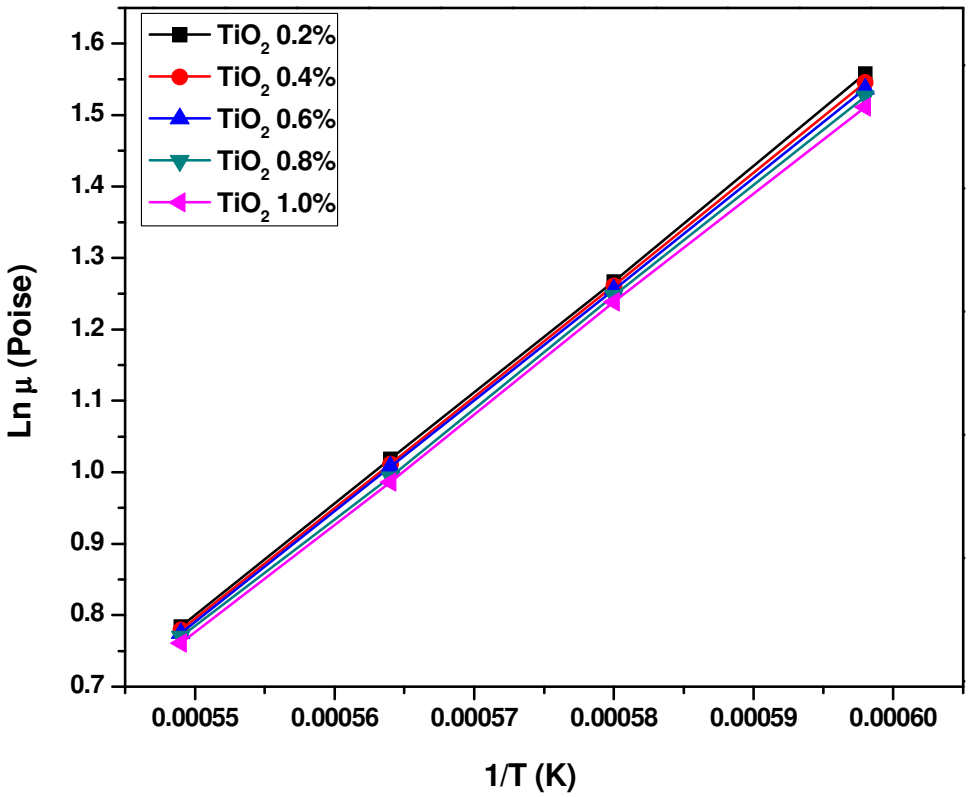

Figure 4.11
Viscosity studies of Blast Furnace Slag
Variation of TiO_2 Content
Relationship between Lnμ and 1/T

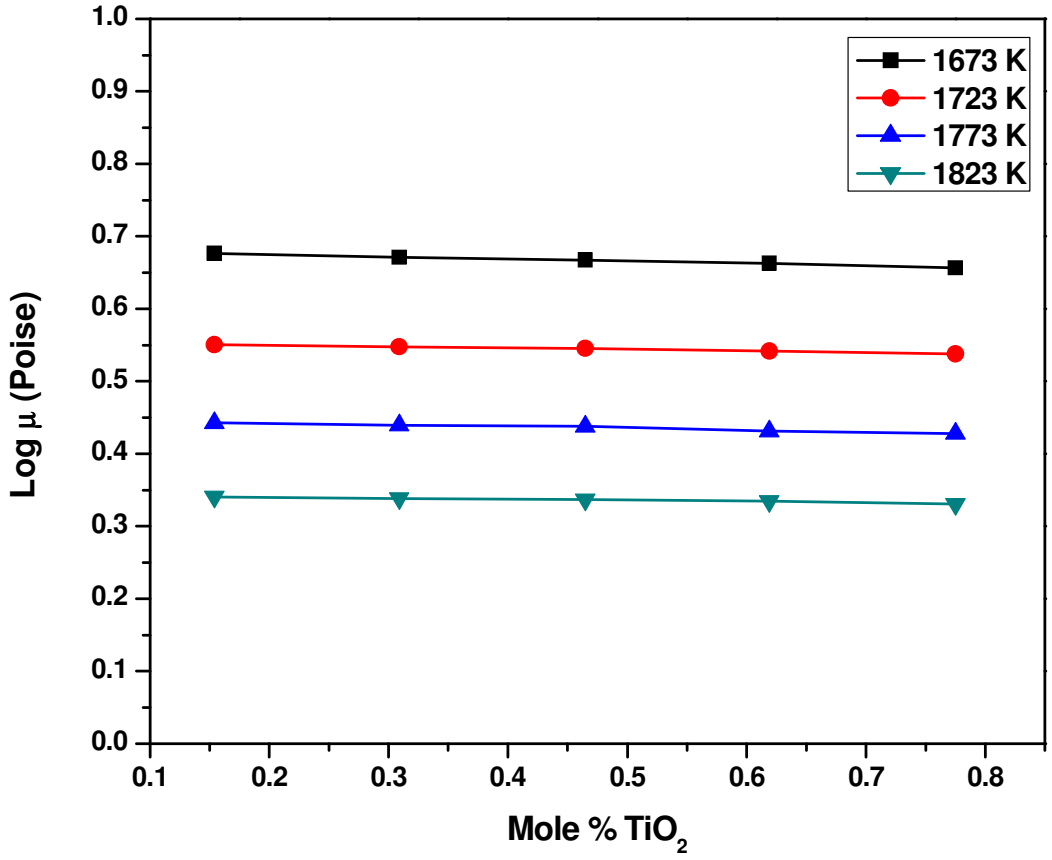

Figure 4.12
Viscosity studies of Blast Furnace Slag
Variation of TiO_2 Content
Relationship between Log μ and Mole % TiO_2

Out of curiosity an attempt is made to compare the effectiveness of C/S ratio and that of TiO_2 content of the slag in lowering its viscosity. It is seen that C/S ratio is more effective in decreasing the viscosity of the slag as compared to that of TiO_2, though both CaO and TiO_2 bring down the viscosity by a process of depolymerisation of the liquid silicate network structure.

Table 4.9

Measurement of viscosity of slag with varying TiO_2 at different temperatures

Slag No.		1673 K	1723 K	1773 K	1823 K
		Viscosity in poise			
11	TiO_2 0.2%	4.75	3.55	2.77	2.19
12	TiO_2 0.4%	4.69	3.53	2.75	2.18
13	TiO_2 0.6%	4.65	3.51	2.74	2.17
14	TiO_2 0.8%	4.6	3.48	2.7	2.16
15	TiO_2 1.0%	4.53	3.45	2.68	2.14

Table 4.10
Activation energy (Kcal) of slag with variation in TiO_2.

Wt.%	Mole%	Activation energy(Kcal/mole)
TiO2 0.2%	0.16	31.6
TiO2 0.4%	0.31	31.3
TiO2 0.6%	0.47	31.1
TiO2 0.8%	0.62	30.9
TiO2 1.0%	0.77	30.68

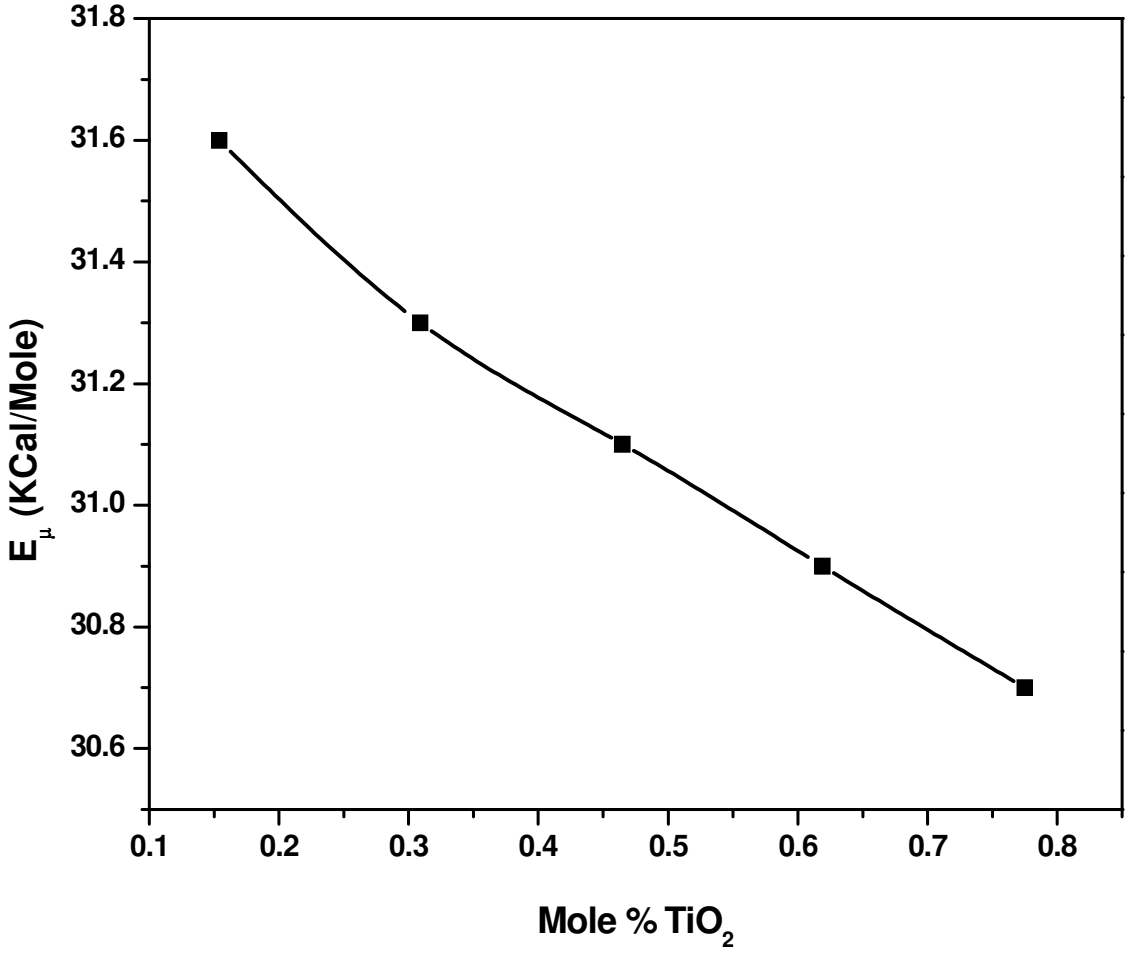

Figure 4.13
Viscosity studies of Blast Furnace Slag
Variation of TiO_2 Content
Relationship between Eμ and Mole % TiO_2

SIMULTANEOUS VARIATION OF C/S RATIO AND MgO CONTENT

4.8 Importance of Simultaneous variation of C/S ratio and MgO content

The slag viscosity has been always a function of its structure as dictated by the size, type and amounts of various irons present in the melt. Keeping this in mind an attempt has already been made to study the effect of two alkaline earth oxide additions, namely CaO and MgO separately on the Blast Furnace slag viscosity. It is decided to examine the effect of simultaneous variations of CaO/SiO_2 and MgO on the slag viscosity. CaO/SiO_2 ratio is varied from 0.9 to 1.1 in steps of 0.05 and MgO is varied from 4.0 wt. % to 12 wt. % in steps of 2.0 wt. %. The variations are so arranged that both the variables are simultaneously increased/decreased such that when the CaO/SiO_2 ratio attains its minimum value of 0.9 MgO also attains its minimum value of 4.0 wt. % in the slag. Similarly, when one of the variables reaches its maximum value, say 1.1 as in the case of C/S ratio, the other reaches also its max value, 12 wt. % in the case of MgO. From an estimation of viscosity and activation energy of viscous flow, Eμ, the possible structure of the melt has been suggested. The compositional details of the slag investigated are presented in **Table 4.11** Besides CaO/SiO_2 ratio and MgO contents all other constituents are allotted fixed values as indicated in the table, with Al_2O_3 is being 20 wt. % in all the slag.

Table 4.11
Chemical Compositions of slag selected for study of Simultaneous variation of C/S Ratio and MgO for viscosity measurement

Sl. No.	Al_2O_3 Wt.%	MnO Wt.%	K_2O Wt.%	Na_2O Wt.%	Fe_2O_3 Wt.%	TiO_2 Wt.%	CaO Wt.%	SiO_2 Wt.%	CaO/SiO_2 (C/S)	MgO Wt.%
16	20.0	0.1	0.5	1.1	1.0	0.6	26.86	29.84	0.9	4.0
17	20.0	0.1	0.5	1.1	1.0	0.6	26.65	28.05	0.95	6.0
18	20.0	0.1	0.5	1.1	1.0	0.6	26.35	26.35	1.0	8.0
19	20.0	0.1	0.5	1.1	1.0	0.6	25.97	24.73	1.05	10.0
20	20.0	0.1	0.5	1.1	1.0	0.6	25.51	23.19	1.1	12.0

4.8.1 Variation of Viscosity after varying C/S and MgO simultaneously

As evident from **Table 4.12** and **Figure 4.14** the viscosity of these slags decreases continuously with the increase of the C/S ratio and the MgO wt. %, the change being more gradual at higher values of these variables at relatively higher temperatures.

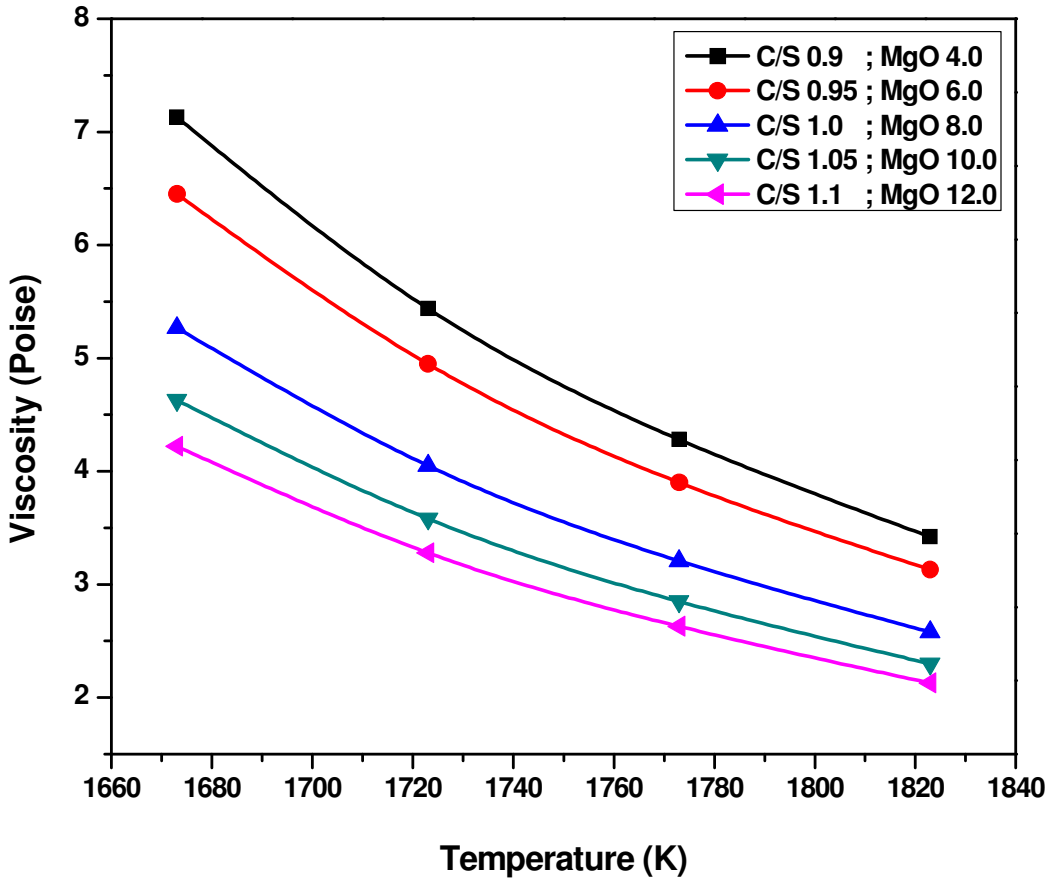

Figure 4.14
Viscosity studies of Blast Furnace Slag
Simultaneous Variation of C/S ratio & MgO Content
Relationship between Viscosity and Temperature

Table 4.12
Viscosity of slag with simultaneous variation with C/S ratio & MgO%

Slag No.	Composition	1673 K	1723 K	1773 K	1823 K
		Viscosity in Poise			
16	C/S 0.9 ; MgO 4.0	7.13	5.44	4.28	3.42
17	C/S 0.95 ; MgO 6.0	6.45	4.95	3.9	3.13
18	C/S 1.0 ; MgO 8.0	5.27	4.05	3.21	2.58
19	C/S 1.05 ; MgO 10.0	4.63	3.58	2.85	2.3
20	C/S 1.1 ; MgO 12.0	4.22	3.28	2.63	2.13

It is further observed that when C/S ratio varies between 0.9 and 0.95 combinedly with MgO variations from 4.0 wt. % to 6.0 wt. %, the viscosity of the resultant slag decrease abruptly, i.e. at a much faster rate, with temperature. It is mandatory to closely monitor the temperature, during industrial operations, for such slag. Such slag, if the temperature is allowed to fall below a certain threshold value, become very viscous, affecting the slag metal reactions/exchanges as well as the slag metal separations. This problem is not likely to be encountered when C/S ratio is above 1.0 together with MgO above 6.0 wt. % in the slag. This is because, as evident from the viscosity vs. temperature plots, the viscosity for these slag decreases more gradually with increase of temperature, within the range of variations investigated.

A careful observation of the plots in **Figure No.4.14** reveals that below C/S ratio 1.0 and MgO wt. % 8.0, the viscosity values and trend of their variation are almost similar. This is also true for slag compositions above C/S ratio of 1.0 and MgO content of 8.0 wt. % where the viscosity values and the trend of their variations with temperature tend to follow similar trends. On the basis of the above, it can be safely concluded that both the viscosity and the trend of its variations in composition and temperature, attained an average value when the C/S ratio is 1.0 and MgO is 8 wt. %. In other words slag no. 18, with C/S ratio of 1.0 and MgO content of 8.0 wt. % can be considered to be the representative one of this group of slag examined to assess the effect of simultaneous variations of the combination of the two alkali earth oxides, namely CaO and MgO respectively.

4.8.2 Relationship between viscosity and temperature

The straight line relationship between lnμ and 1/T (k) as shown in **Figure 4.15** confirms that viscosity obeys the Arrhenius type of equations. The slopes of the plots give the activation energy of viscous flow. The activation energy of viscous flow Eμ, so obtained, are tabulated in **Table 4.13** for each of the slag. It is seen from the plots that Eμ decrease with the temperature increase and that Eμ also decreases as the C/S ratio and MgO contents are increased.

Table 4.13
Activation Energy (Kcal) of slag with simultaneous variation with C/S ratio & MgO% from graph (fig 6.20)

slag	B_2: {(CaO+MgO)/SiO_2}	B_3 {(CaO+MgO)/SiO_2 +Al_2O_3}	Activation Energy(Kcal/mole)
C/S 0.9 ; MgO 4.0	1.01	0.675	30
C/S 0.95 ; MgO 6.0	1.12	0.725	29.5
C/S 1.0 ; MgO 8.0	1.23	0.776	28.9
C/S 1.05 ; MgO 10.0	1.34	0.840	28.5
C/S 1.1 ; MgO 12.0	1.48	0.910	28.13

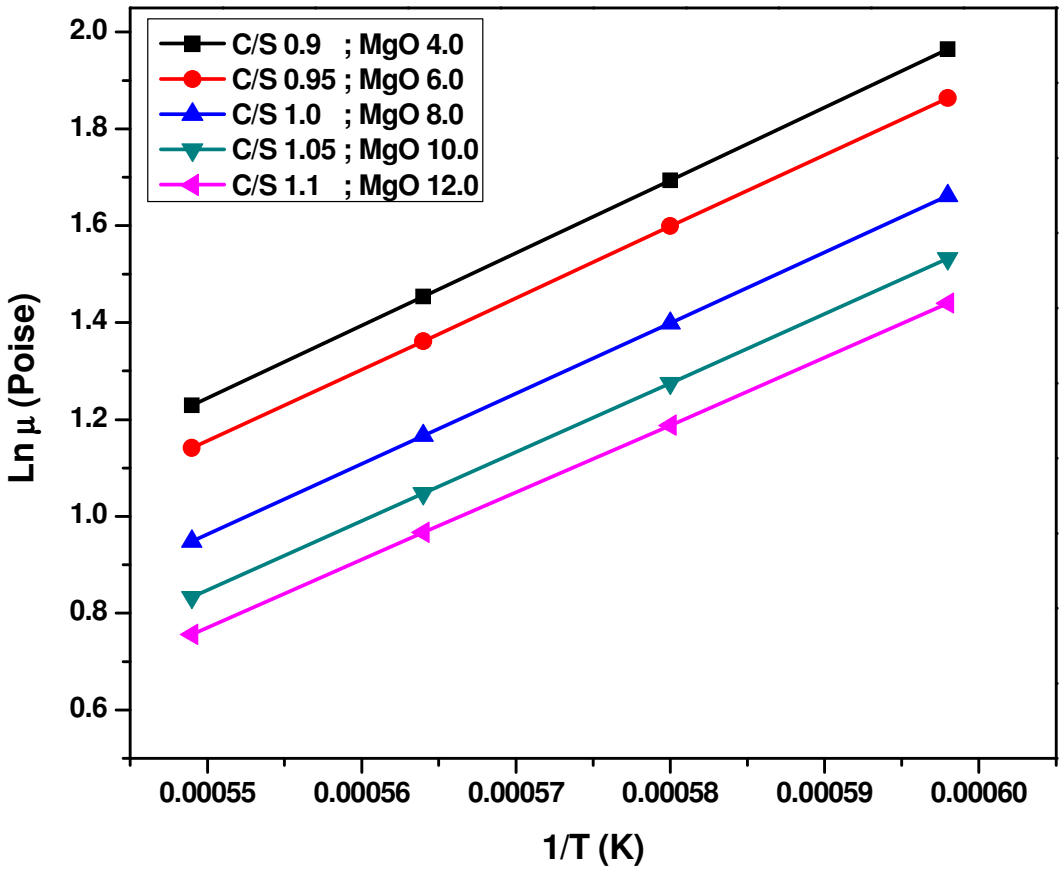

Figure 4.15
Viscosity studies of Blast Furnace Slag
Simultaneous Variation of C/S ratio & MgO Content
Relationship between Ln μ and 1/T

This establishes that the degree of depolymerisation increases, i.e. smaller flow units are produced to a greater extent by a process of depolymerisation, with the increasing amounts of CaO and MgO additions, as a result of the breaking of the discrete anionic silicate structure. However, for any given composition, even with the variation of temperature, the slope of the line showing relationship between lnμ and I/T (k) is maintained. Thus the degree of polymerization/depolymerisation is practically constant for a given composition of the slag at various temperatures. The decrease of Eμ with temperature is attributed only to the slackening of the cationic Ca^{++}, Mg^{++} and the discrete anionic silicate bonds. The decreasing trend of Eμ with increasing C/S ratio, i.e. increasing CaO contents as well as increasing MgO contents, indicate the lower extents of energy requirements to break the bond for necessary viscous flow with increasing amounts of CaO and MgO additions. It may be pointed out here that cations like Al^{3+}, SiO^{4+}, Ti^{4+}, etc. having a higher value of ion oxygen interaction parameter 'I' {'I' for Al^{3+}, Si^{4+} and Ti^{4+} are high, (I > 1.16)} have higher ability to hold the oxygen ions together tightly in a particular type of packing. These ions are thus network formers. However, cations like Mg^{++}, Ca^{++} have a low ion oxygen attraction ('I' < 0.7). Their ability to hold oxygen ions together is low. Thus, they are supposed to be network breakers. This demonstrates that the presence of higher amounts of CaO and/or MgO in the slag would facilitate depolymerisation requiring lower extents of energy to break the bond.

4.8.3 Variation in viscosity at different basicities.

Figure No.4.16 and **Figure No.4.17** show the viscosity isotherms at different basicity B_2 ($\frac{CaO+MgO}{SiO2}$) and B_3 ($\frac{CaO+MgO}{SiO2+Al2O3}$) respectively. Both the plots establish similar tends of viscosity variations, at all temperature with B_2 as well as B_3. Viscosity continuously decreases with increase of B_2 and B_3 at all temperatures. However, in case of B_2, viscosity at all temperatures, decreases rather faster till B_2 attains a value of about 1.25 beyond which the decrease of viscosity with B_2 is gradual. In case of B_3 this value is approximately 0.775.

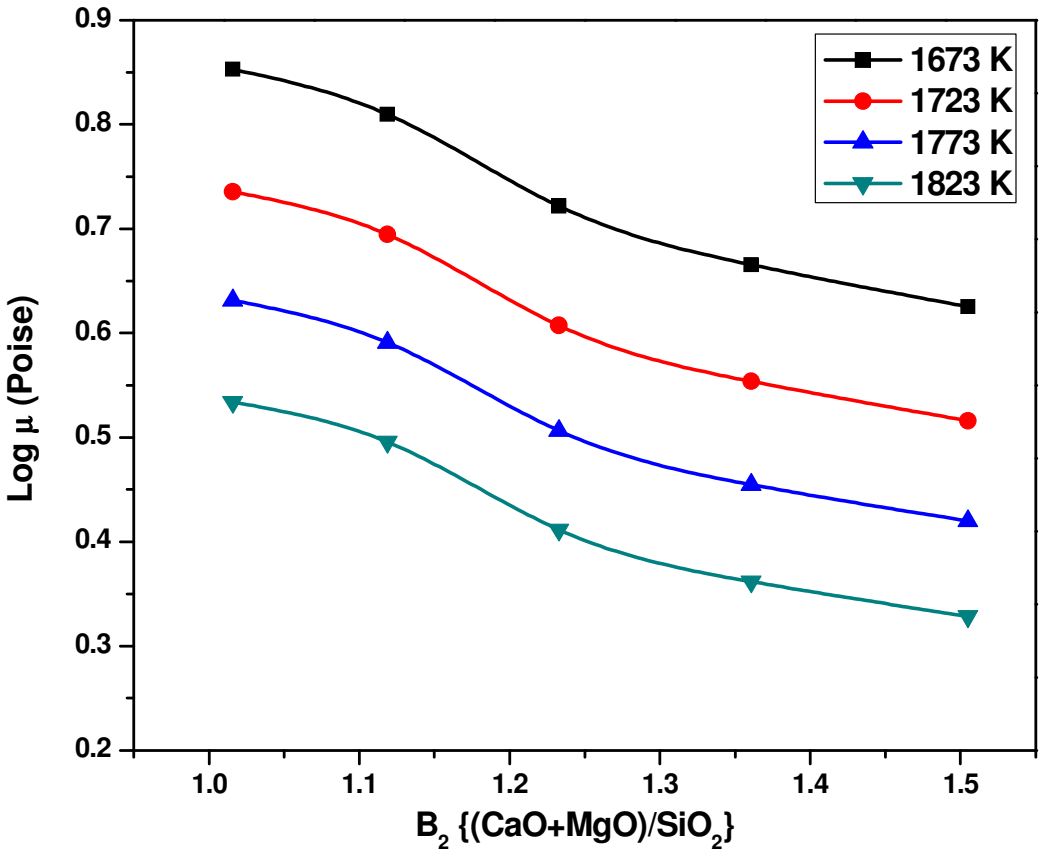

Figure 4.16

Viscosity studies of Blast Furnace Slag

Simultaneous Variation of C/S ratio & MgO Content

Relationship between Log μ and B_2 {(CaO+MgO)/SiO_2}

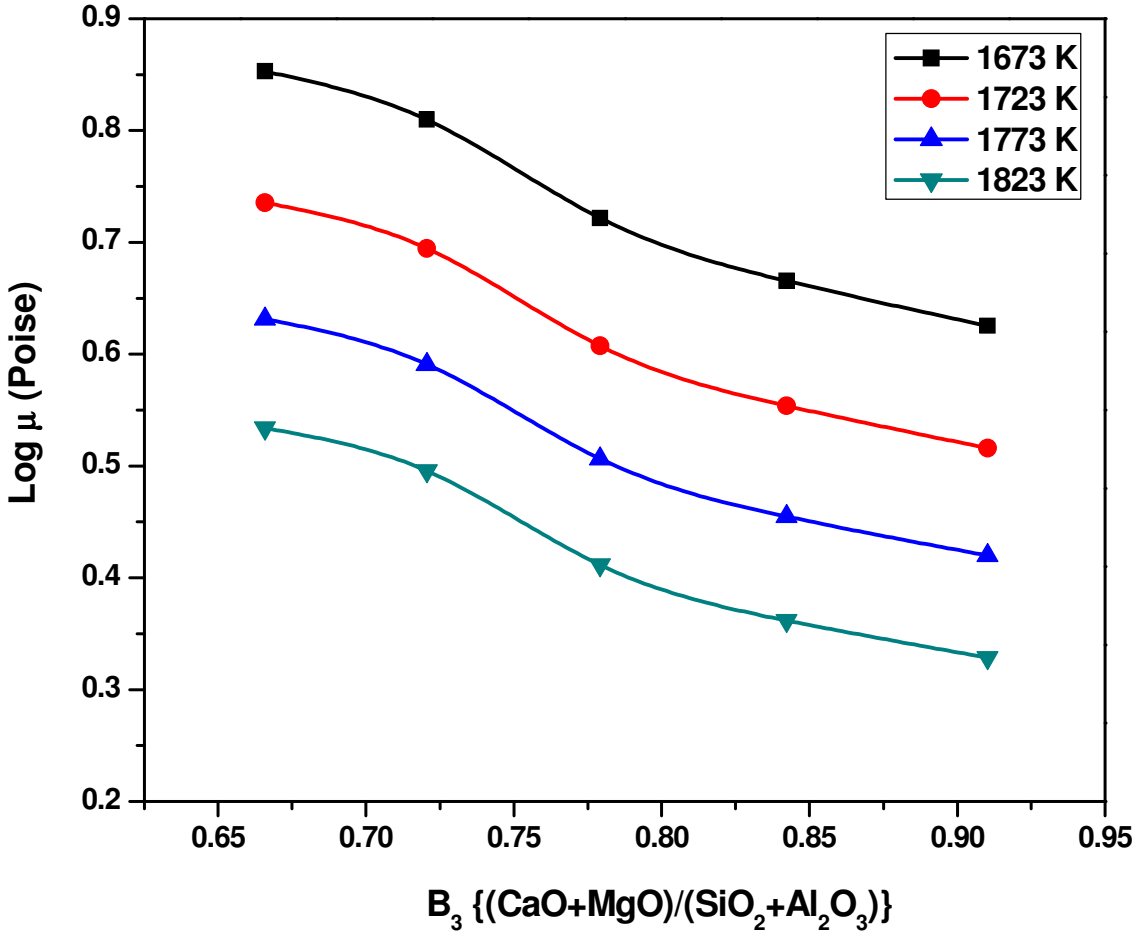

Figure 4.17

Viscosity studies of Blast Furnace Slag

Simultaneous Variation of C/S ratio & MgO Content

Relationship between Log μ andB_3 {(CaO+MgO)/SiO2+Al_2O_3}

As stated elsewhere in this thesis, since smaller and smaller flow units require relatively higher oxygen to be contributed by the alkali earth oxides CaO and MgO, the progressive addition of these oxides is less and less effective in reducing the flow unit size. Therefore, after the initial breakdown of the silicate network at a faster rate as a consequence of the addition of the oxide flux resulting in the faster rate of decrease of viscosity, further additions of the oxides bring about the reduction of the size of the flow units at a sluggish rate only. This explains the reduced rate of decrease in the viscosity at higher basicities of the slag presented by B_2 and B_3.

Figure No.4.18 and **Figure No.4.19** show the change of activation energy of viscous flow with basicities B_2 and B_3 respectively. The $E\mu$ values continuously decrease with either B_2 or B_3. However, the rate of decrease is lower at a higher basicity value.

We know that the progressive addition of the oxide flux is less and less effective in reducing the silicate flow unit size, thereby causing a slower rate of decrease of the associated negative charges. Thus the number of ionic bonds, which has to be broken or distorted to enable the flow units to move with respect to each other become less. This leads to the decrease of the activation energy of viscous flow, $E\mu$, at a slower rate only.

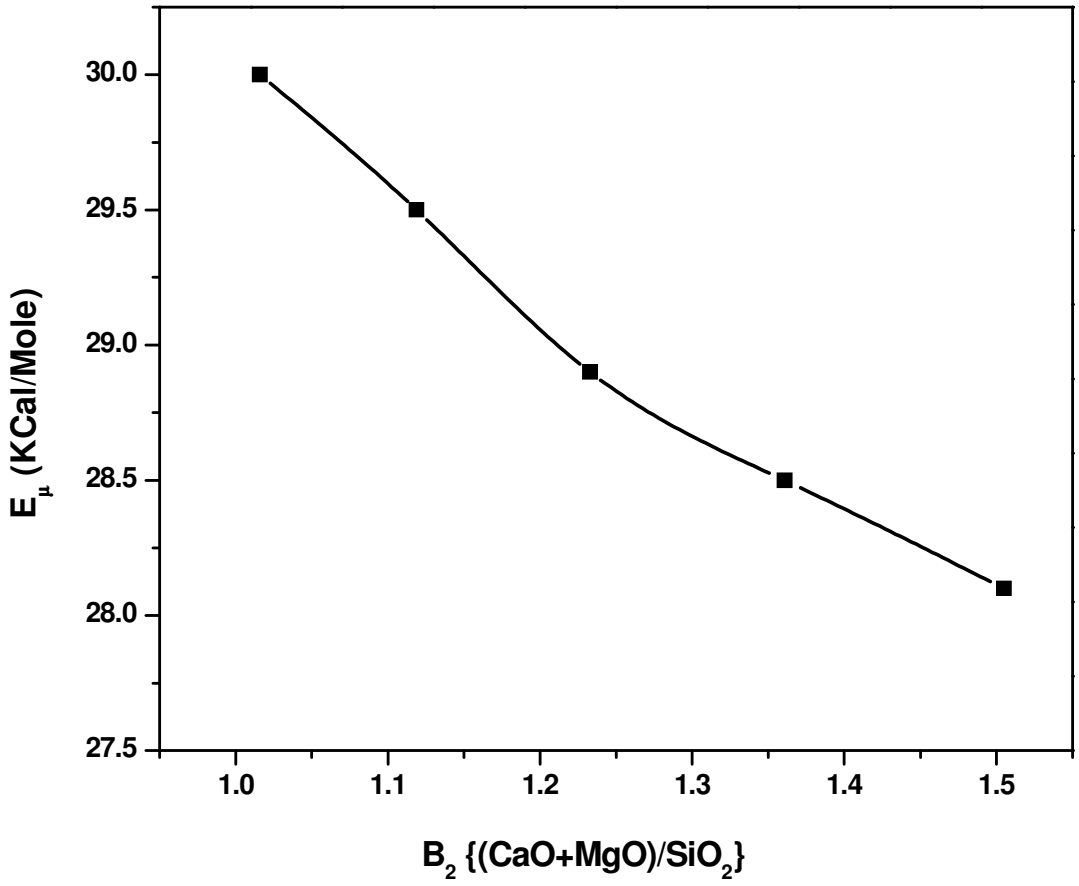

Figure 4.18

Viscosity studies of Blast Furnace Slag

Simultaneous Variation of C/S ratio & MgO Content

Relationship between Eμ and B_2 {(CaO+MgO)/SiO_2}

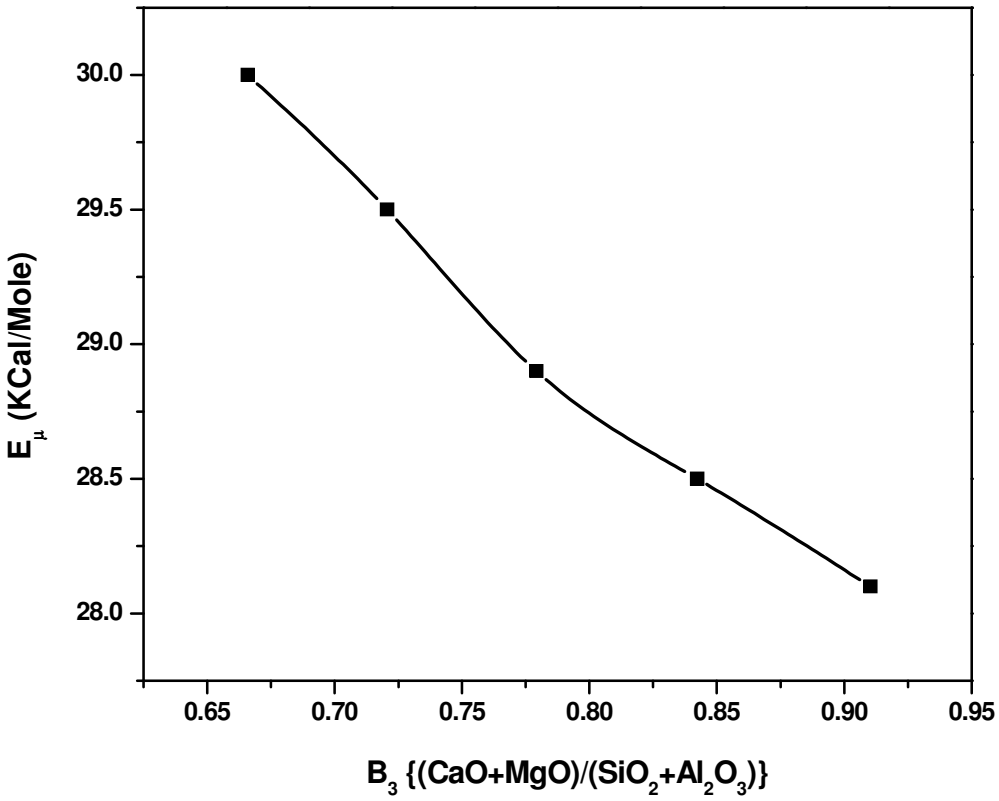

Figure 4.19

Viscosity studies of Blast Furnace Slag

Simultaneous Variation of C/S ratio & MgO Content

Relationship between Eμ and B_3 {(CaO+MgO)/SiO2+Al_2O_3}

Chapter 5

CONCLUSION

5.1 Conclusion

The author concludes the followings from a systematic analysis of the experimental finding pertaining to viscosity data of high alumina Blast Furnace slag as influenced by its major constituents.

a. Flow Characteristic of Blast Furnace Slag

1. *The empirical equations developed using the factorial-design-technique, can be used to predict the flow-characteristics of Blast Furnace slag fairly accurately, within the range of compositions investigated.*
2. *The significant variables, viz: C/S ratio, MgO content and TiO_2 content of the Blast Furnace slag are combinedly involved in influencing the characteristic temperatures of the slag. Any attempt at assessing the effect of any one of the variables, independent of the other two, will not be justified.*
3. *The combination of high C/S ratio and high MgO content at all levels (high/low) of TiO_2 content, within the range of compositions investigated, aids to the process of iron-making in the Blast Furnace route in way of assisting the generation of a short slag.*

b. Viscosity of Blast Furnace

1. *There exists an inverse function between the rise of temperature and increase of the C/S ratio in bringing down the slag viscosity, temperature increase being more effective in bringing down the slag viscosity at lower C/S ratio.*
2. *Similar observation holds good for MgO variation, though, in general, the ability of MgO to depolymerize the discrete silicate network is lower than that of CaO.*
3. *The degree of depolymerization, as presented by NBO/T, is responsible for lowering of both the viscosity of the slag as well as the activation energy of viscous flow $E\mu$.*
4. *Higher MgO contents (above 10 wt. % MgO) don't participate in stoichiometric slag structure.*
5. *Even with its insignificant presence in the slag, TiO_2 behaves as a basic oxide in the slag compositions investigated and lowers the slag viscosity.*

6. *Ability of TiO_2 to depolymerize the liquid silicate network structure is lower than that of CaO, though both CaO and TiO_2 bring down the slag viscosity behaving as a basic constituent oxide.*
7. *It is mandatory to monitor temperature more carefully during industrial practices while operating with slag having a C/S ratio below 0.95 combined with MgO contents of less than 6 wt. %.*

----------xoxox----------

ANNEXURES

Annexure-1

Details of Viscometer used in the experiment (Para 2.6)

Application area: To measure the viscosity of slag
Measuring principle: Searle- measuring principle with rotation of bob/crucible
Maximum measuring temperature: 1680°C
Temperature accuracy: +/- 3°C
Viscosity measurement method: Comparison methods with known Glass samples
Working atmosphere: Air, inert gas, Vacuum (Optional)
Viscometer Operation Mode: Vertical type
Viscosity Measurement Range: 10 - $10^{4,5}$ dPas, Statically : 10 - $10^{7,5}$ dPas,
Heating principle: Induction heating
Heating coil: Water/air cooled copper coil
Generator frequency: 250 KHZ
Input power: 2 KW
Input voltage: 230V 50HZ Single ph/400V 50HZ 3ph
Max input current: 16A
Temperature control: Micro controller
Heating/Cooling rate: 5°C-100°C/Min
Measuring head control: By motor
Speed range: 10-800RPM
Torque Range: 0 - 50 mNm
Accuracy of torque and rotational speed: ± 1 %
Measuring Head Connection to rotor: Through Coupling holder, & Flexible coupling & to the drive shaft and coupling piece.
Rotar position indicator: Through position scale of measuring head
All mechanical parts: Water cooled, with spring bellows coupling, working under inert gas
Water pressure and floe rate: 3litres/min at 2 Bar (with flow monitor)
Gas pressure: 10L/hr. at 1 bar (supplied with mass flow controller)
Sample holder:
Crucible Material: Pt Rh80/20
Crucible Diameter: 23 mm
Crucible Height: 55 mm
Bob Material: PtRh70/30
Bob Diameter: 9 mm
Bob height: 20 mm
Bob holder / platform: Recrystallized Al2O3 (This is with built in thermocouple Type B for measuring temperature. Thermocouple should be terminated at Pedestal with a suitable plug).
Bob immersion depth: Adjustable through software
Alignment of Rotor & crucible: With adjusting screw
Temperature recording: Both for S and B type with amplifier and digital display
Temperature linearity: +/- 10°C
Visual Inspection of Viscometer during operation: Through glass window

Annexure -2

Factorial analysis -Para 3.3
The abbreviations are given in text.

Table 1
Response Test

Factors	Levels	Response (R)		
RMC		ST	HT	FT
R1M1T1	+ + +	1518	1668	1681
R1M1T2	+ + -	1539	1673	1703
R1M2T1	+ - +	1499	1681	1718
R1M2T2	+ - -	1534	1691	1726
R2M1T1	- + +	1487	1623	1628
R2M1T2	- + -	1503	1653	1675
R2M2T1	- - +	1451	1583	1623
R2M2T2	- - -	1488	1625	1665

Table 2

Variance Analysis for ST, HT and FT

Source of Variance	Degree of Freedom	Sum of Squares			Fischer Ratio		
		ST	HT	FT	ST	HT	FT
R	1	3240.125	6555.125	7021.125	529	1070.224	693.4444
M	1	703.125	171.125	253.125	114.7959	27.93878	25
T	1	1485.125	946.125	1770.125	242.4694	154.4694	174.8272
R-M	1	91.125	1225.125	703.125	14.87755	200.0204	69.44444
M-T	1	153.125	36.125	45.125	25	5.897959	4.45679
R-T	1	1.125	406.125	435.125	0.183673	66.30612	42.97531
Residual	1	6.125	6.125	10.125	1	1	1

Calculation of variance for ST:

Correction factor (CF) = $(\Sigma R)^2/8$ = 18057045.13

Total variance = $(\Sigma R)^2$ – CF = 5679.875

Variance due to R = $[(\Sigma R_1)^2 + (\Sigma R_2)^2]/2$ – CF = 3240.125

Variance due to M = $[(\Sigma M_1)^2 + (\Sigma M_2)^2]/2$ – CF = 703.125

Variance due to T = $[(\Sigma T_1)^2 + (\Sigma T_2)^2]/2$ – CF = 1485.125

Interaction variance due to R and M =

$[(\Sigma R_1M_1)^2 + (\Sigma R_1M_2)^2 + (\Sigma R_2M_2)^2 + (\Sigma R_2M_1)^2]/2$ – Variance due to R – Variance due to M – CF = 91.125

Interaction variance due to M and T =

$[(\Sigma M_1T_1)^2 + (\Sigma M_1T_2)^2 + (\Sigma M_2T_2)^2 + (\Sigma M_2T_1)^2]/2$ – Variance due to M – Variance due to T – CF = 153.125

Interaction variance due to T and R =

$[(\Sigma T_1R_1)^2 + (\Sigma T_1R_2)^2 + (\Sigma T_2R_2)^2 + (\Sigma T_2R_1)^2]/2$ – Variance due to T – Variance due to R – CF = 1.125

Residual variance = Total variance – Sum of above six variances = 6.125

Variance ratio or Fischer ratio (F) = Variance/Residual variance

Table 3

Relative Significance

Specification	R	M	T
ST [ai]	+20.125	+9.375	-13.625
HT [ai]	+28.625	+4.625	-10.875
FT [ai]	+29.625	-5.625	-14.875

Calculation of relative significance for ST:

ST [ai] = [$\Sigma Response_+/4 - \Sigma Response_-/4$]/2

R_S (Softening Temperature) = $a_0+a_1R+a_2M+a_3T$

R_H (Hemispherical Temperature) = $b_0+b_1R+b_2M+b_3T+b_4(M-R)$

R_F (Flow Temperature) = $c_0+c_1R+c_2M+c_3T$

a_0, b_0 and c_0 are the average response values of ST, HT and FT respectively.

(a_1, b_1, c_1), (a_2, b_2, c_2) and (a_3, b_3, c_3) are the respective [ai] values of R,M,T respectively.

b_4 is the average of eight readings of HT response with signs of product M and R.

$R_S = 1502.375 + 20.125R + 9.375M – 13.625T$

$R_H = 1649.625 + 28.625R + 4.625M – 10.875T – 12.375 (M-R)$

$R_F = 1677.375 + 29.625R – 5.625M – 14.875T$

Annexure 3

Calculation of viscosity for slag no.1 at 1673°K using Iida Model- (Para 4.5.1)

According to the model – $\eta\ (p_a\text{-}s) = A\eta o_{\ exp}\ (E/Bi)$

Where 'η' is the viscosity in P_a-s

A – The pre exponential term = $1.745 - (1.962 \times 10^{-3} \times T) + (7 \times 10^{-7} \times T^2)$

'T' being the temperature in the absolute scale

E – Activation Energy=$11.11-3.65*10^{-3}*T$, (At 1673K,E=5.003).

So, For 1673K, A = 0.422 and E = 5.003

η_{oi} = Hypothetical Viscosity for each of the individual slag constituents

η_{oi} is calculated by the formula : $\dfrac{1.8\times10^{-7}(M_i.T_{mi})½.\exp(H_i/RT)}{(V_{mi}\ )^{2/3}\ \exp(H_i/RT_m)}$

Where - Tmi = melting temperature of the individual constituents in absolute scale

R = Gas constituent

$H_i = 5.1\ (T_{mi})^{1.2}$, is the melting enthalpy of individual component

V_{mi} = Molar volume of the individual component

Mi = Formula weight of component 'i' = $(M_{wi} \times 10^{-3})$

The further required data for slag no.1 are given below:

Table 1

Constituents	Wt. % 'W'	Molenlar Wt MW	No. of Moles Ni = w/Mw	Mole Fraction 'Xi' Ni/∑Ni
Al_2O_3	20	101.96	0.196	0.121
MnO	0.1	70.94	0.001	0.0008
K_2O	0.5	94.2	0.005	0.003
Na_2O	1.1	61.98	0.017	0.011
Fe_2O_3	1.0	159.69	0.006	0.003
TiO_2	0.6	79.87	0.007	0.005
MgO	8.0	40.3	0.198	0.123
CaO	32.54	56.08	0.580	0.359
SiO_2	36.16	60.08	0.602	0.372

Where ∑Ni = 1.615013 (as calculated) is the total number of moles of all the components of slag no.1

On the basis of the above the following are found out for each of the slag constituents

Slag constituents	T_{mi}	Mi	V_{mi}	$(V_{mi}^{2/3})$	Hi
Al_2O_3	2313	0.0196	33.58×10^{-6}	0.001	55536.81
MnO	2053	0.07094	16.97×10^{-6}	0.0006	48132.33
K_2O	980	0.0942	40.96×10^{-6}	0.001	19817.16
Na_2O	1193	0.06198	27.25×10^{-6}	0.0009	25092.2
Fe_2O_3	1838	0.15969	37.66×10^{-6}	0.001	42148.76
TiO_2	2108	0.0798	21.88×10^{-6}	0.0007	49683.81
MgO	3073	0.0403	16.16×10^{-6}	0.0006	78098.96
CaO	2873	0.05608	23.49×10^{-6}	0.0008	72039.87
SiO_2	2001	0.06008	27.29×10^{-6}	0.0009	46673.1

Now ηo = Hypothetical viscosity of the slag

$= \sum \eta_{oi} \times X_i$

η_o for slag no.1 is calculated to be 0.016

B_i = Basicity index for slag with given composition at all the temperature

$B_i = [\{(L_iW_i) / \{(L_iW_i)A] = 1.205748$ for slag 1 (calculated)

Where αi – specific coefficient

Wi – Wt % of component

'A' and 'B' represent acidic and basic oxides

Here Acid oxides are (SiO_2, TiO_2)

Basic oxides are (CaO, MgO, Na_2O, K_2O, MnO)

Amphotenic oxides are (Al_2O_3, Fe_2O_3)

$\therefore \eta = 0.422 \times 0.016 \exp\left(\frac{5.003}{1.205748}\right) = 0.431(P_a\text{-}S)$ for slag 1 at 1673K

$\mathcal{L}_i$ values for the different constituents in slag 1 are

Al_2O_3	MnO	K_2O	Na_2O	Fe_2O_3	TiO_2	MgO	CaO	SiO_2
0.1	1.03	1.37	1.94	0.08	0.36	1.57	1.53	1.48

-----oxoxoxoxo-------

Annexture 4

Photo graphs of Equipments used

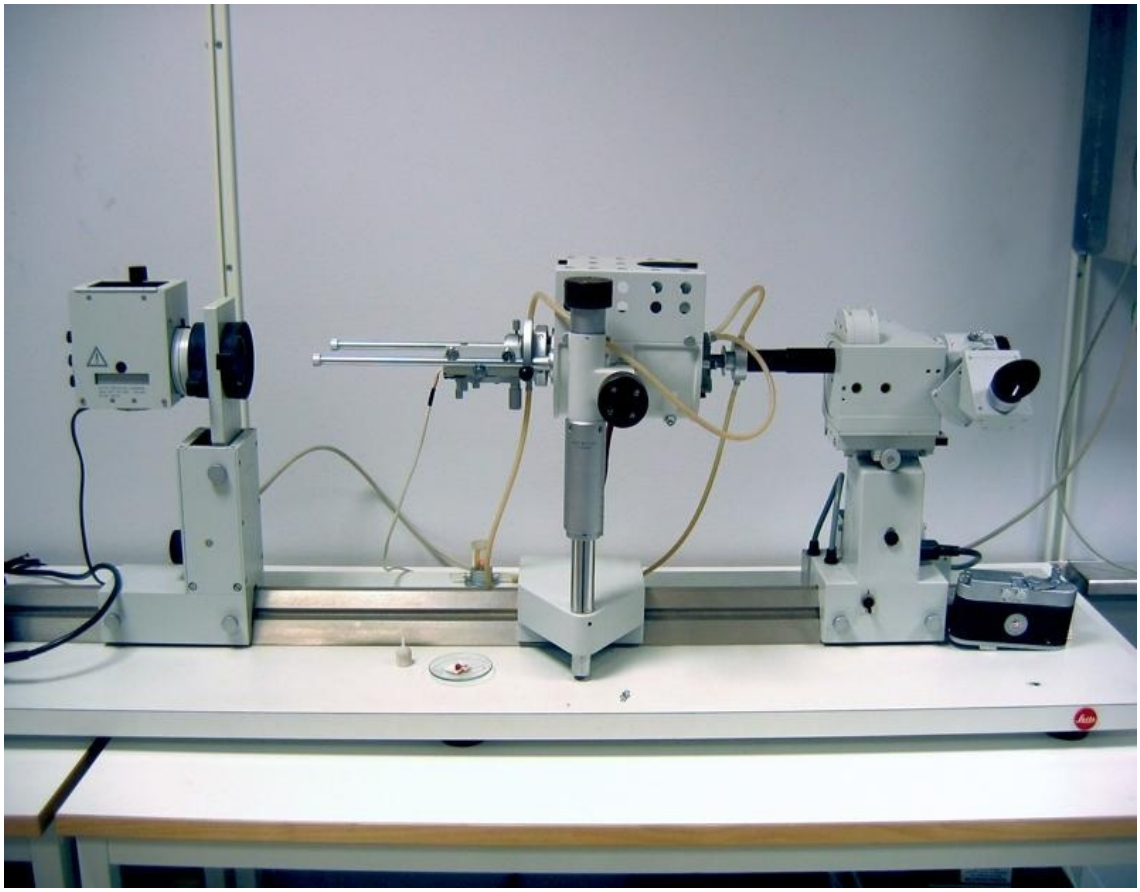

Photo graph 1
High temperature microscope (Para-2.5.2)

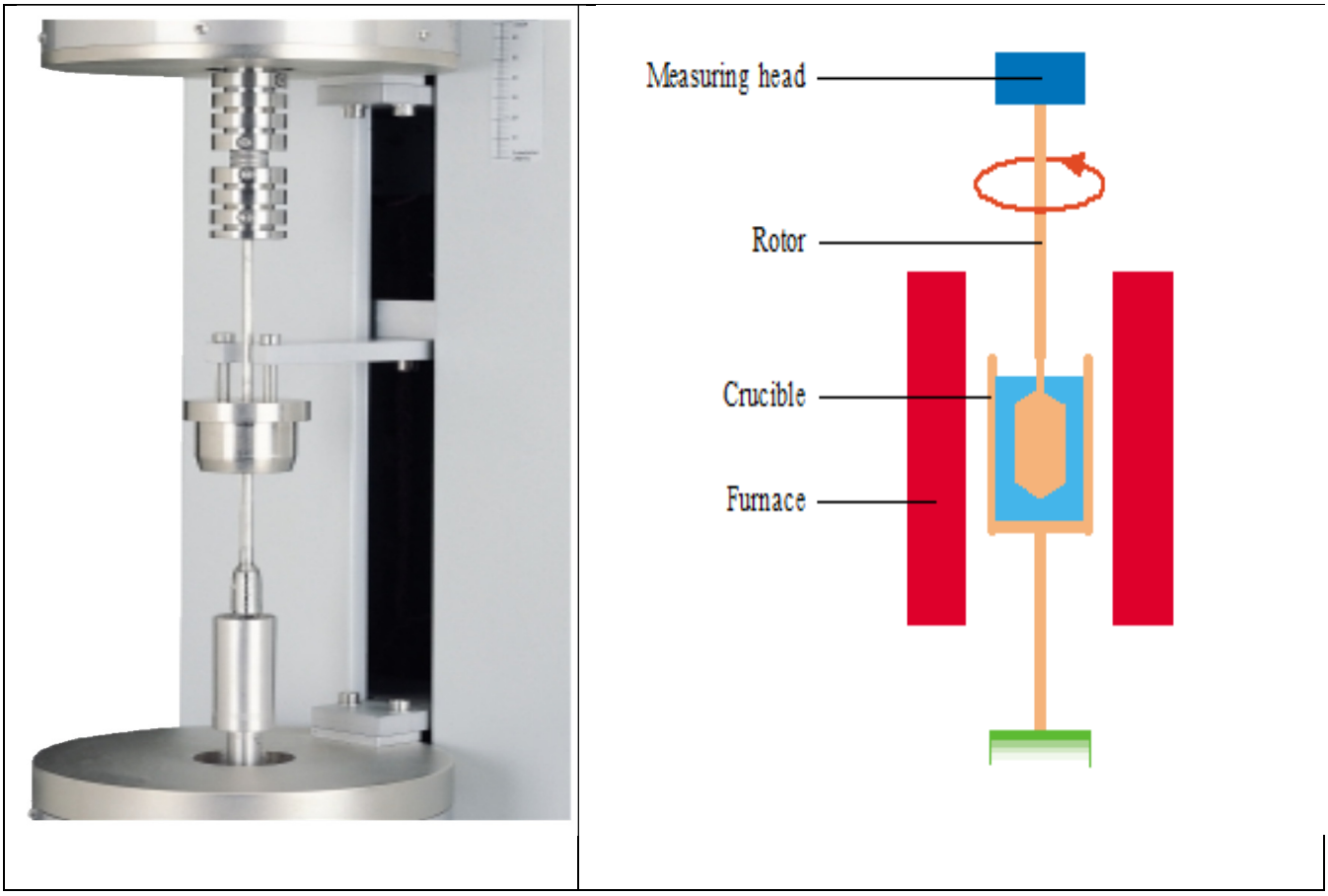

Photograph 2
High temperature Viscometer VIS 403
(Para 2.6)

Photograph 3

Planetary ball mill

(Para 2.9.1)

Photograph- 4
Raising Hearth furnace
(Para 2.9.2)

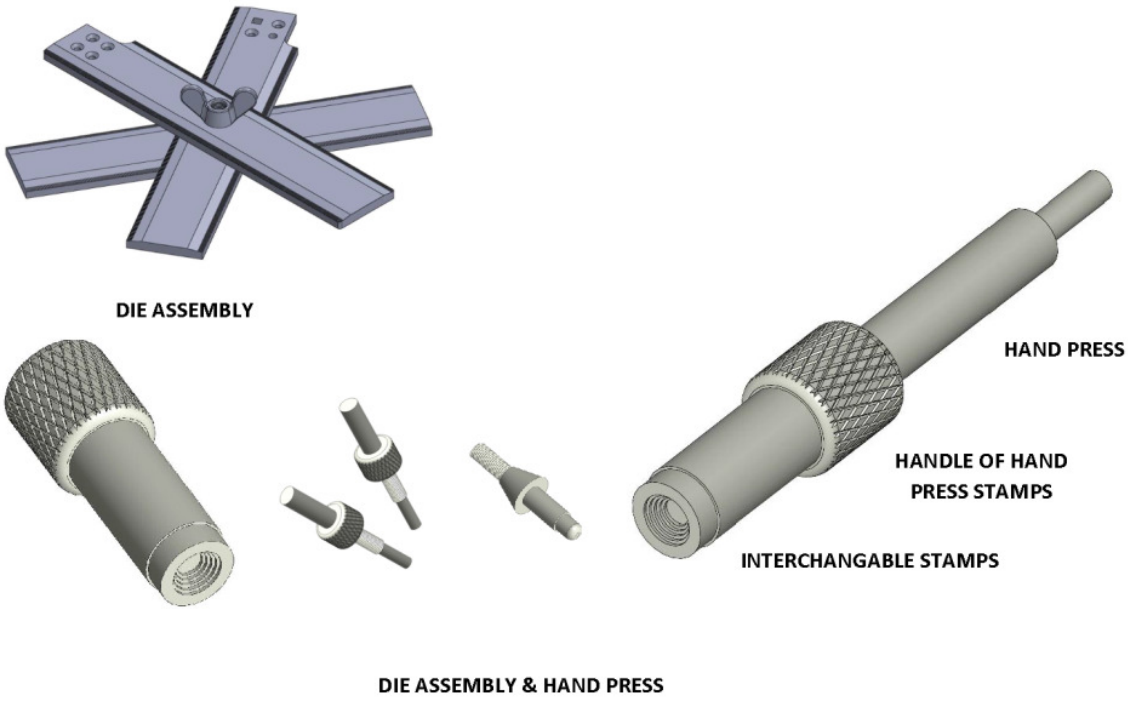

Phtograph-5
Die Assembly and Hand Press
(Para 2.9.3)

BIBLIOGRAPHY

REFERENCE LIST

1	Mysen, B.O., Earth Science Rev.(1990),vol. 27,pp.281
2	Kang, T.W., Gupta, S., Saha-Chaudhury, N. and Sahajwalla, V., ISIJ International(2005),44(11),pp.1526-1535
3	Mackenzie, J D, Trans. Faraday Soc.(1957),vol.53,pp.1488-1498
4	Weyl, W.A., J.Soc.Glass. Tech.(1951),vol. 35,pp.401
5	Machin, J S and Yee, T B, J.Am.Cer.Soc.(1948),vol.31,pp.200-204.
6	Moore, H., and McMillan, P.W., J.Soc.Glass.(1956),vol. 40,pp. 193
7	Tiwari J N,Sarkar AK,Mishra, B,Mohanty,UK,ICE, Vol2,EMR-3,10th May 2013,pp 152-162
8	Behera, R. C., Mohanty, U.K and Mohanty, A K, 1990, vol.9, pp. 57-75
9	Bockris, J.OM and Lowe, D.C., Royal Soc.(1954),vol. 226, pp.423-435
10	Sunahara,K., Nakano,K., Hoshi,M., Inada,T., Komatsu,S. and Yamamoto,T., ISIJ International(2008), vol.48(4),pp.420-429
11	Toop, G.W., M.A.Sc. Thesis, University of British Colombia(1960), pp.4
12	Lee, Y S, Kim, J R, Yi, S H and Min, D J., VII international conference on molten slags, fluxes and salts, The South African Institute of Mining and Metallurgy, (2004)
13	Masson, C.R., Proc. Royal Soc.(London-1965),vol.287(A), pp.201.
14	Gaskel, D R, Can. Metallurgical Wquarterly(1981),vol. 1(20), pp.3-19
15	Whiteway, S.G., Smith, I.B., and Masson, C.R Can.J.Chem.(1970),vol. 48,pp.33
16	Lin, P L and Pelton, A D., Metall. Trans.(1979),vol.10(B),pp.667
17	Paul, M., Principles of Chem. Thermodynamics, New York(1951), pp.146.
18	Bockris,J.O., Mackenzie,J.D. and Kitchener,J.A., Trans. Faraday Soc.(1953),vol.51(12),pp.1734-1748
19	Zhang,G.H. and Chou,K.C., Journal of Mining and Metallurgy(2012),vol.48(1),pp.1-10
20	Behera, R.C. and Mohanty,U.K., ISIJ International(2001),vol.41(8),pp.827-833
21	Machin, J.S., Yee, T B and Hanna, D.L., J.Am.Cer.Soc.(1952),vol.35,pp.322-325
22	Ditz, H. and Schulz, G.W, Glass Tech. Ber.(1969),vol. 42, pp.89
23	Dash,S, Mohanty,N, Mohanty,U.K. and Sarkar,S, Open Journal of Met,2(2012),pp.42.
24	Kucharski,M, Stubina, N M and Togury, J.M., Can. Met. Quarterly(1989), 28(1), pp.7-11
25	Waseda, Y., Shiraishi, Y. and Togur I J.M., Trans.Japan.Inst.Metals(1980),vol. 21,pp.51
26	Dietzel, A., Z.Electrochem(1942),vol. 48, pp. 9-23
27	Morinaga, K., Suginohara, Y., and Yanagase T., J.Japan. Inst. Met.(1976),vol. 40,pp.480 and 775.

28	Seki, K., and Oeters, F., Trans. ISII(1984),vol. 24,pp.254
29	Lee, Y S, Min, D J, Jung, S M and Yis, H., ISIJ International(2004)), vol.44,pp.1283-1290
30	Toop, G.W. and Semis, C.S., Can.Met. Quarterly, 1(1962), pp.129-151
31	Toop,G.W. and Samis,C.S., Transactions of Metallurgical Soc. Of AIME(1962),vol.224,pp.878-887
32	Mills, K.C., Yuan,L. and Jones,R.T., 611(2011), pp.649-658
33	Mills,Ken, Short course presented as part of South African Pyrometallurgy 2011
34	Gupta, V K and Seshadri, V, Trans. Ind. Inst. Met.(1993),vol. 26, pp.55-64.
35	Ghosh,D., Krishnamurthy,V.A. and Sankaranarayanan,S.R., Journal of Mining & Metallurgy(2010),vol.46(1),pp.41-49
36	Kondratiev A ,Zhao B,Raghunath S Hayes PC ,Jak E, EMC 2007 page 1-21.
37	Seetharaman, S. and Sichen, D., ISIJ(1997),vol. 37, pp.109-118.
38	Kawai,Y., The research institute of mineral dressing and metallurgy, Oct 8,1952
39	Nogueira,P.F. and Fruehan,R.J., Metallurgical and Materials Trans.B(2004),vol.35B,pp.829-838
40	Athappan, R., RDCIS, SAIL, Ranchi, Dec (1985)
41	Jia, Shyan Shiau and Shih-Hsien, Liu, China Steel Tech Report(2008),vol. 21, pp.21-28
42	Yakusev Romashin, V.M., and Amfiteatrov, V.A., steel in USSR(1977),vol. 7, pp.617-618
43	Handfield, G., Charette, G G, Canadian Metallurgical Quarterly(1971), vol.10, pp.235-243
44	Kawahara, M., Morinaga, K J and Yanagase T., Can. Mett. Quarterly(1983),vol. 22 pp.143-147
45	Singh, N., Muthykrishnan, V., and Rajozinski, T., MML Tech. Journal(1970),vol. 12, pp.12-21.
46	Poe, B.T. and McMillan, P.F., Journal of the Am. Cer. Soc.(1994),vol. 77(7), pp.1832-1838
47	Turkdogan, E.T., and Bills, P.M, Am. Cer.Bull.(1960),vol. 39,pp.682-687
48	Muller, J., and Erwee, M, Southern African Institute of Mining and Metallurgy(2011), pp.309-326.
49	Mikhailov and Belyakova, Ural Met.(1939),vol.6,pp.7-9
50	Semik, I.P., Bull Acad. Sci. USSR(1941),vol. 4, pp.55-56.
51	Migas,P., Korolczuk-Hejnak,M., Karbowniczek,M. and Ledzki,A., Technical Transactions, Chemistry(2013)
52	Togobitskaya, D.N., Mozharenko, N.M., Bel'kova, A.I. and Stepanenko,D.A., Metallurgical and Mining Industry(2010), 2(4),pp.249-253
53	Shiau,Jia-Shyan, Ho,Chung-Ken and Liu,Shih-Hsien, AISTech(2010) Proceedings,vol.1
54	Kaushik,P. and Fruehan,R.J., Ironmaking & Steelmaking(2006), vol.33(6),pp.507-519

55	German Industrial standards 51730
56	Teng,L, Matsushita,T and Seetharaman, S., Association of Metallurgical Engineers of Serbia,pp.267-274
57	Chuang,H-C., Hwang,W-S. and Liu,S-H., Materials Trans.(2009),vol.50(6),pp.1448-1456
58	Roscoe, R., British Journal of Applied Physics(1952),vol.3
59	Hagemann,R., Pettsold,L. and Sheller,P.R., Metallurgical and Mining Industry(2010), vol.2(4), pp.262-266
60	Nakamoto,M., Tanaka,T., Lee,J. and Usui,T., ISIJ International(2004),vol.44(12),pp.2100-2104
61	Ayala R.E, Casassa E.Z and Parfitt G.D, Powder Technology.51(1987),3
62	Zuo Guangqing, ISIJ International(2000), vol.40(12),pp.1195-1202
63	Clinby, G, Ironmaking steelmaking, 13(1986),1
64	Labib,H.M., Monaghan,B.J., Longbottom,R. and Chew,S.J., High Temperature Processing Symposium(2011), pp.65-67
65	Fukutake,T and Rajkumar, V, Trans. ISIJ, Vol.22(5),1982,May, pp.355-364
66	Hussalage, WM, Dynamic Distribution : Sulphur transfer and flow in a high temperature packed coke bed "Doctoral Thesis, Delf University NL 2004"
67	WU Andrew ,Hayes P.C. and Lee HG, ISIJ International,Vol.38 (1998),No.3,PP 213-219
68	Mehrdad Massoudi & Ping Wang, Energies, 2013, 6, 807-838
69	H D Weymann: Kollioid Z Polymer, 1962, Vol 181, p 131-137
70	Kondratiev A, Jak, E. and Hayes,P C., JOM,2002
71	Mohanty,U.K, Ph.D Dissertation RE College, Rourkela, 1988
72	Raitar -Transaction of British Ceramic Society ,40,157,1941
73	Ritwik Ph.D Thesis, May 2012
74	Mills KC, NPL report DMM (A) 30 ,Teddington ,Middlsex UK 1991
75	Meckenzie JD, Viscometry -------- Page no 331-333
76	Sinha ,BC, Saha, M.R., and Roy, S.K, Talanta, 26, 827-831 (1979). 8
77	Sen, R Transaction of Indian Ceramic Society, Vol.XXXIV (5), Sep-Oct 1975, Page 94-98.
78	ASTM (573-70), 1976, Chemical analysis of fire clay and high alumina refractories.
79	Sahu, P, Central Glass Ceramic Research Institute Bull, 37 (1-4), 17-22, 1990.
80	Sinha B.C. CG&CRI, Bulletin 22 (40, P.172, 1975.
81	Vogel A.I. - A test book of quantitative in organic analysis, 3rd Edition, Pub. by the English Language Book Society, London, P.29, 1975
82	Dusseldorf, "Slag Atlas" – 2nd Ed., 167, publisher : Verlag Stahleisen(1995), ISBN: 3514004579
83	Shankar,A., "Studies on high alumina blast furnace slags", Doctoral Thesis, School of Industrial Engineering and Management, Department of Material Science and Engineering, Royal Institute of Technology,Sweden,2007
84	Kekkonen,M., Oghbasilasie,H. and Louhenkilpi,S.,

	Science+Technology(2012), Research Report, Aalto University
85	Gupta, SS and Chatterjee,A., "Iron making and steel making theory & practice", SBA publication(1995)
86	Kim,J.R., Lee,S.Y., Min,D.J., Jung,S.M. and Sang H.Y., ISIJ International(2004),vol.44(8),pp.1291-1297
87	Sahoo,S.K., Tiwari,J.N., and Mohanty,U.K. "Metallurgical and Materials Trasc B, Published online(2013),pp.269
88	Mohanty U.K., Behera R.C., ISIJ Int., 2003, 43 (12), 1875
89	Hopkins D.W, Phys. Chem. of Metal Extn., Garner and Miller, London, 1954
90	Biswas,A.K, "Principles of Blast Furnace Ironmaking", SBA Publication, Kolkata(1999)
91	Saito,N, Hori, N, K,Nakashima and K.Mori, "Metallurgical and Materials Transc.B,34B(2003),pp.509
92	Park,J.H, Min,D.J., Song,H.S., "Metallurgical and Materials Trasc B,35B(2004),pp.269
93	Park,H., Park,J.Y., Kim,G.H. and Sohn,I., "Steel Research International,83(2) (2012),pp.150
94	Kim.H, Kim,W.H., Sohn,I and Min,D.J., "Steel Research International, 81(4) (2010),pp.261
95	Waseda ,Y, Togury J.M, Canadian Metallurgical Transactions, 1977, 8(b), 563
96	Shankar, A, Gornerup, M, Lahiri, A.K, Seetharaman, S, Met. Mat. Trans. B, 2007, 38B, 911.
97	Phase diagram for Ceramist 1969, compiled at Natural Bureau of Standards, American Ceramic Society, Fig.No.2647, Fig.No.2648
98	Abdul-Wahab,S.A., and Abdo,J, "Appl. Therm Eng.,27(2007),pp.413
99	Greenwood ,P.E, Nikulin M.S, A Guide to Chi Squared Testing, Wiley, New York, 1996.
100	Gupta, V.K, Seshadri, V, Silver Jubilee Symposium, Process Metallurgy, Indian Institute of Metals, 1972, 203.
101	Gupta, V.K, Seshadr,i V, Trans. IIM, 1973, 26, 55.
102	Forsbaka,L, Holappa,L., Iida,T., Kits,Y. and Toda,Y., Scandinevian Journal of Metallurgy, vol.32,2003,pp.273-280.
103	Panigrahy,S.C., Verstraetin,P and Dileneijins,I, Metallurgical Transactions B,Vol-15B,March 1984-23
104	Bockris,J.OM.,Tomlinson,J.W., and White,J.L., Trans. Faraday Soc..,52,299-310(1950)
105	Machine,J.S. and Yee,B., Journal of American Soc., 37,177-186,(1954)
106	Mills,K.C., ISII International,33,1,148-155 (1993)
107	A.Ohno, H.U.Ross, Can. Met.Q, 1963,2,259

Papers Published

and

Papers communicated.

Papers published

1. Sahoo,S.K., Tiwari,J.N., and Mohanty,U.K. “Metallurgical and Materials Trasc B, Published online(2013),pp.269

2. Structural Aspects of Blast Furnace slag, Tiwari J N, Sarkar AK, Mishra B, Mohanty,UK , ICE, Vol-2,EMR-3,10th May 2013,pp 152-162

Papers communicated

1. Prediction of flow characteristic of Al_2O_3-CaO-MgO-SiO2-TiO2 type Blast Furnace slag and its evaluation. J N Tiwari et.al Canadian Metallurgist Quarterly.
2. Viscosity of High Alumina Blast Furnace Slag as Influenced by its Major Constituents. J.N.Tiwari et.al